

Ion-Selective Electrochemical Sensors

By Isaac Trachtenberg and Charles T. Baker, Texas Instruments Incorporated, Dallas, Texas, for Office of Saline Water, Chung-ming Wong, Director; W. Sherman Gillam, Assistant Director, Research; Sidney Johnson, Chief, Applied Science Division; Raymond H. Horowitz, Project Monitor

Contract No. 14-01-0001-1737

UNITED STATES DEPARTMENT OF THE INTERIOR • Walter J. Hickel, Secretary
Carl L. Klein, Assistant Secretary for Water Quality and Research

As the Nation's principal conservation agency, the Department of the Interior has basic responsibilities for water, fish, wildlife, mineral, land, park, and recreational resources. Indian Territorial affairs are other major concerns of America's "Department of Natural Resources".

The Department works to assure the wisest choice in managing all our resources so each will make its full contribution to a better United States—now and in the future.

FOREWORD

This is one of a continuing series of reports designed to present accounts of progress in saline water conversion and the economics of its application. Such data are expected to contribute to the long-range development of economical processes applicable to low-cost demineralization of sea and other saline water.

Except for minor editing, the data herein are as contained in a report submitted by the contractor. The data and conclusions given in the report are essentially those of the contractor and are not necessarily endorsed by the Department of the Interior.

INTERMEDIATE REPORT
FOR
ION-SELECTIVE ELECTROCHEMICAL SENSORS

TABLE OF CONTENTS

<u>SECTION</u>		<u>PAGE</u>
I	INTRODUCTION	1
II	SENSOR MATERIAL PREPARATION AND ANALYSIS	3
III	RESISTIVITY OF SENSOR MATERIAL	26
IV	SENSOR EVALUATION AND DISCUSSION	36
	A. Fe ⁺³ Sensors	38
	B. Mn ⁺² Sensors	67
	C. Ca ⁺² Sensors	74
	D. Mg ⁺² Sensors	74
	E. Na ⁺ , K ⁺ , Ag ⁺ , Cl ⁻ , and I ⁻ Sensors	74
	F. Cd ⁺² Sensors	83
	G. SO ₄ ⁼ Sensors	86
	H. Ge ₂₉ S ₇₁ Sensors	86
	I. Conclusion of Sensor Evaluation	88
V	SUMMARY AND RECOMMENDATIONS	89

APPENDIX A

CONVERSION OF MOLES/LITER
TO PARTS PER MILLION
FOR VARIOUS IONS

APPENDIX B

NON-OXIDE GLASSES DOPED WITH IRON OR MANGANESE

INTERMEDIATE REPORT
FOR
ION-SELECTIVE ELECTROCHEMICAL SENSORS

LIST OF ILLUSTRATIONS

<u>FIGURE</u>		<u>PAGE</u>
1	1% BaCl ₂ -1173 (80X)	6
2	1 Mole % CdSe (160X)	7
3	1 Mole % Mn (Metal) (160X)	7
4	Crystalline Clusters in 2.39% Fe-Doped 1173 Glass	13
5	Crystalline Clusters in 1.62% Fe-Doped 1173 Glass	14
6	A. 1.5 Mole % FeTe-1173 Glass (160X). B. 1.5 Mole % FeSe-1173 Glass (160X). C. 1.5 Mole % FeSe ₂ -1173 Glass (160X)	16
7	ESR Spectra	17
8	A. Voltammogram of 2.39 Mole % Fe ⁰ -1173 Glass Electrode in 0.1 M KNO ₃ at pH = 2. B. Voltammogram of 2.39 Mole % Fe ⁰ -1173 Glass Electrode in 0.1 M Fe(NO ₃) ₃ at pH = 2	19
9	Current-Time Behavior for 2.0 Mole % MnSe-1173 Glass	27
10	Effect of Mn ⁰ and Fe ⁰ Concentrations on the Specific Resistivities of Doped 1173 Glass	31
11	Effect of Temperature on the Resistivity of 1.0 Mole % MnCl ₂ -1173 Glass	32
12	Effect of Temperature on the Resistivity of 5 Mole % MnSe-1173 and 10 Mole % CdSe-1173 Glasses	34
13	Sensor Configurations	37
14	Effect of [Fe ⁺³] on the Potential of a 5.0 Mole % FeSe ₂ -1173 Glass Electrode	39
15	Potential Response of a 1.5 Mole % FeTe-1173 Glass Electrode to Fe ⁺³ and Fe ⁺² in 0.1 M KNO ₃ at pH = 2.0	41
16	Potential Response of a 1.5 Mole % FeSe-1173 Glass Electrode to Fe ⁺³ and Fe ⁺² in 0.1 M KNO ₃ at pH = 2.0	42
17	Potential Response of a 1.5 Mole % FeSe ₂ -1173 Glass Electrode to Fe ⁺³ and Fe ⁺² in 0.1 M KNO ₃ at pH = 2.0	43

TABLE OF CONTENTS
(Continued)

LIST OF ILLUSTRATIONS
(Continued)

<u>FIGURE</u>		<u>PAGE</u>
18	Effect of $[Fe^{+3}]$ and $[Fe^{+2}]$ Concentrations and Measurement Sequence on the Potential of an FeSe-Epoxy Electrode	44
19	Effect of $[Fe^{+3}]$ and $[Fe^{+2}]$ Concentrations and Measurement Sequence on the Potential of an FeSe ₂ -Epoxy Electrode	45
20	Effect of $[Fe^{+3}]$ and $[Fe^{+2}]$ Concentrations and Measurement Sequence on the Potential of an FeTe-Epoxy Electrode	46
21	Effect of pH on the Potential of FeTe-, FeSe ₂ -, and FeSe Epoxy Electrodes	47
22	Effect of $[Fe^{+3}]$ and $[Fe^{+2}]$ Concentrations and Measurement Sequence on the Potential of a 0.8 Mole % Fe ⁰ -1173 Glass Electrode	48
23	Effect of $[Fe^{+3}]$ and $[Fe^{+2}]$ Concentrations and Measurement Sequence on the Potential of a 1.62 Mole % Fe ⁰ -1173 Glass Electrode	49
24	Effect of $[Fe^{+3}]$ and $[Fe^{+2}]$ Concentrations and Measurement Sequence on the Potential of a 2.0 Mole % Fe ⁰ -1173 Glass Electrode	50
25	Effect of $[Fe^{+3}]$ and $[Fe^{+2}]$ Concentrations and Measurement Sequence on the Potential of a 2.39 Mole % Fe ⁰ -1173 Glass Electrode	51
26	Effect of pH on the Potential of Fe ⁰ -1173 Glass Electrodes	53
27	Effect of pH on the Potential of Fe ⁰ -1173 Glass Electrodes	54
28	Effect of Varying the Fe ³⁺ Concentration without Removing the 2.39 Mole % Fe ⁰ -1173 Glass Electrode from the Test Solution	55
29	2.39 Mole % Fe ⁰ -1173 Glass Electrode Response Times for Changing $[Fe^{+3}]$	56
30	Potential Response of Electrode and Membrane of 2.0 Mole % Fe ⁰ -1173 Glass to Fe ³⁺ Concentration	58

TABLE OF CONTENTS

(Continued)

LIST OF ILLUSTRATIONS

(Continued)

<u>FIGURE</u>		<u>PAGE</u>
31	Potential Response of 2.0 Mole % Fe ⁰ -1173 Glass Membrane to Fe ⁺³ in 0.1 M KNO ₃ at pH = 2.0	59
32	Potential Response of a 1.62 Mole % Fe ⁰ -1173 Glass Electrode to Fe ⁺³	60
33	Effect of Contaminant Concentration on the Potential of a 2.0 Mole % Fe ⁰ -1173 Glass Electrode	61
34	Effect of Cl ⁻ and SO ₄ ⁼ Concentration on the Electrode Potential of a 2.0 Mole % Fe ⁰ -1173 Glass Electrode when Fe ⁺³ is not Present in Solution	63
35	Response of 2.0 Mole % Fe ⁰ -1173 Glass Electrode to Fe ⁺³ Concentration in an Excess Cl ⁻ Medium	64
36	Potential Response of 1.62 Mole % Fe ⁰ -1173 and 2.0 Mole % Fe ⁰ -1173 Glass Electrodes to Cu ⁺² in Cl ⁻ and NO ₃ ⁻ Media	66
37	Potential Response of 1.5 Mole % Co ⁰ -1173 and 1.5 Mole % Ni ⁰ -1173 Glass Electrodes to Fe ⁺³	68
38	Potential Response of a 1.5% Ni ⁰ -1173 Glass Electrode to Cu ⁺² in NO ₃ ⁻ and Cl ⁻ Media	69
39	Potential Response of a 1.5 Mole % Co ⁰ -1173 Glass Electrode to Cu ⁺² in NO ₃ ⁻ and Cl ⁻ Media	70
40	Voltammogram of Pt in 10 ⁻² M Mn ⁺³ , 10 ⁻¹ M Mn ⁺² , 0.4 M Na ₄ P ₂ O ₇ , and 2 M H ₂ SO ₄	72
41	Potential Response of a 4.0 Mole % Mn ⁰ -1173 Glass Electrode to Electrochemically Generated Mn ⁺³ in 0.1 M MnSO ₄ , 0.4 M Na ₄ P ₂ O ₇ , and 2 M H ₂ SO ₄	73
42	Electron Microprobe Profile Analysis of the Diffusion of Mn ⁰ into n-type Si (ρ = 0.007 Ω-cm - phosphorus doped)	75
43	Profile Analysis of the Diffusion of Mn ⁰ into p-type Si (ρ = 0.0015 Ω-cm - boron doped)	76
44	Effect of [Ag ⁺] on the Potential of the 1.0 Mole % KCl-1173 Glass Electrode	78
45	Effect of [Ag ⁺] on the Potential of the 2 Mole % KI ¹³¹ -1173 Glass Electrode	79

TABLE OF CONTENTS

(Continued)

LIST OF ILLUSTRATIONS

(Continued)

<u>FIGURE</u>		<u>PAGE</u>
46	Effect of pH on the Potential of a 2.0 Mole % KI-1173 Glass Electrode	80
47	Effect of $[I^-]$ on the Potential of a 2.0 Mole % KI ¹³¹ -1173 Glass Electrode	81
48	Effect of $[Ag^+]$ and $[Cl^-]$ on the Potential of a 2.0 Mole % AgCl-1173 Glass Electrode	82
49	Potential Response of a 2.0 Mole % Ag ₂ Se-1173 Glass Electrode to Ag^+ and Cl^- in 0.1 M KNO_3 at pH = 5.4	84
50	Effect of $[Cd^{+2}]$ and Measurement Sequence on Membrane and Electrode Potentials for 10 Mole % CdSe-1173 Glass . .	85
51	Potential Response of 0.5 Mole % Ba ⁰ -0.5 Mole % Ni ⁰ -1173 and 1.5 Mole % Ni ⁰ -1173 Glass Electrodes to $S_2O_8^{=}$ in 0.1 M KNO_3 (pH = 3.65).	87

LIST OF TABLES

<u>TABLE</u>		<u>PAGE</u>
I	Summary of Doped 1173 Glass Samples Prepared	9
II	Samples of Doped Chalcogenide Glasses	22
III	Specific Resistivities of Undoped and Doped Sensor Material Samples	29

INTERMEDIATE REPORT
FOR
ION-SELECTIVE ELECTROCHEMICAL SENSORS

I. INTRODUCTION

Ion-selective electrochemical sensors should provide a means for rapidly determining and continuously monitoring the concentration of electroactive species in aqueous solutions, particularly saline and brackish waters. This is the broad goal of the research program sponsored by the Office of Saline Water under Contract No. 14-01-0001-1737 with Texas Instruments Incorporated. Specifically, the program goal is to develop inexpensive, chemically durable, and highly selective electrochemical sensors which will give rapid and specific response to Ca^{+2} , Mg^{+2} , Mn^{+2} , Fe^{+3} , Na^{+} , K^{+} , and SO_4^{-2} in saline and brackish water. The approach taken in this program is to use nonoxide materials which, when fabricated into sensors, will give the desired response to the specific ions of interest.

Ion-selective electrochemical sensors can be combined with other sensors to build up process control systems. These systems will permit better control and automation of such processes as reverse osmosis demineralization of brackish waters. Ion-selective electrochemical sensors will provide accurate monitoring of the concentration of individual ionic species in solution on a continuous and real-time basis. The efficiency of the various subsystem elements (pretreatment section, chemical addition, membranes, etc.) can be easily determined and optimized for the current operating conditions. The quality of incoming and product water could be easily established. In addition, such process control systems can signal changes in raw materials and in environmental and operating conditions. These signals will allow corrective actions to be initiated before the operation has degraded to the point at which it must be shut down. However, if the changes have been too drastic and cannot be corrected within a reasonable period of time so that continued operation at these levels would result in permanent damage to the systems, the process control system would actually shut the process down to prevent serious damage to expensive components such as the membranes. Inclusion of ion-selective electrochemical sensors in process control systems will provide critical information needed to improve operations at a lower total operating cost.

The general plan of the research program on ion-selective electrochemical sensors can be divided into three major parts: sensor material preparation and analysis, resistivity of sensor material, and evaluation of sensor specific ion response and selectivity. Resistivity measurements were used as a screening technique prior to sensor fabrication. If the resistivity was above a certain

value, the material was not evaluated as a sensor. Materials which exhibited resistivity values below the maximum were fabricated into sensors. Depending on the type of conductivity (ionic or electronic), the material was fabricated either as a membrane sensor, which requires two reference electrodes and one reference solution, or as an electrode sensor, requiring only one reference electrode to complete the electrochemical cell.

II. SENSOR MATERIAL PREPARATION AND ANALYSIS

Sensor material preparation efforts were concerned principally with doping of nonoxide chalcogenide glasses to produce materials which, when fabricated into sensors (membrane or electrode), exhibited specific ion response and selectivity. Several preparations were made using conventional semiconductor materials such as n- and p-type silicon. Many attempts were made to prepare doped samples, but only those preparations which yielded materials suitable for resistivity measurements and sensor fabrication will be described in this section.

The host material used in most of the experimental work was a chalcogenide glass composed of 60 mole % selenium, 28 mole % germanium, and 12 mole % antimony. This glass composition will be referred to as 1173 glass. It was chosen because of its chemical inertness, mechanical durability, and ease of preparation. In addition, Texas Instruments has had a great deal of experience with this glass system in previous investigations, and materials preparation and evaluation technologies are well developed.

The properties of the undoped glass include:

Strain point (viscosity = $10^{14.6}$ poise)	240°C
Anneal point (viscosity = $10^{13.4}$ poise)	259°C
Softening point (viscosity = $10^{7.6}$ poise)	370°C
Thermal expansion coefficient	$15.0 \times 10^{-6}/^{\circ}\text{C}$
Knoop hardness (50 g load)	150
Density	4.67 g/cc
Resistant to air at 250°C	
Resistant to acids and solvents	
Soluble in strong alkalies	

Samples were prepared for this study by either (1) compounding the glass from the elements, with direct addition of the ionic salts in question, and reaction of all constituents at one time; or (2) doping prereacted 1173 glass by adding appropriate amounts of the salts, with subsequent reaction to take them into solution.

A standard compounding procedure was used. High purity elements (5-9's or better Se, Ge, and Sb, and reagent grade or better salts) were weighed and sealed in an evacuated quartz ampoule. The ampoule was placed in a rocking

furnace and heated slowly to 900°-1000°C. The melt was allowed to mix and/or react for 16 to 24 hours, then air-quenched to solid and annealed for 2 to 3 hours at 275°C to remove strains. Samples were identified as glass or crystalline by visual examination and by optical microscopy, and on the basis of their ability to transmit infrared radiation. Particular importance was placed on determining whether or not a crystalline phase was present, and if so, its type, amount, size, and distribution. Samples exhibiting a crystalline phase were not necessarily excluded from further investigation if the crystals were very finely divided and homogeneously dispersed in the glass matrix, as was the case in many of the samples prepared. Homogeneous distribution is easily accomplished by solution and subsequent dissolution and crystallization, in situ, of the ionic salt. Virtually all samples showing the desired response were of this glass-crystal composite nature.

It was determined early in the program that there was no observable difference in the properties of glasses prepared by compounding from pre-reacted 1173 glass and those of the same doped glass prepared from the elements. All samples prepared for this program were therefore made by doping prereacted 1173 glass. This eliminates some variability in the compounding steps, since the base glass can be prepared in a large batch (1500 grams) and then used in small amounts for each doping experiment (usually 15-gram samples). This procedure assures uniformity of composition and a very high, constant purity level. Prereacted 1173 glass is virtually free of cationic impurities (~ 10 ppm total) and has a low oxygen content (< 20 ppm).

One of the major steps in going from the glass to an electrode or membrane is to determine the success of the doping process. Visual examination yields information about the vitreous nature of the sample, its ruggedness, and rejection of the salt. Resistivity measurements also indicate some success or total failure in the doping of a given sample. To date, all samples have had at least the analyses mentioned above. When problems were encountered or anticipated, other tools of analysis were utilized.

The primary objective in doping these glasses has been to fabricate homogeneous (on a macro-scale), mechanically sound material doped as heavily as possible with some form of the desired ion. This is done by taking the dopant into solution in the glass and then quenching the glass to solidification. The dopants used thus far have been principally metals, salts, or other compounds containing the element for which electrochemical response is desired.

When added in small amounts (usually less than 2 mole %), some of these dopants remain in solution when the glass is quenched. In other cases (different dopants or higher doping levels), the material comes out of solution

upon cooling and crystallizes, in situ, homogeneously. ("Homogeneous" in this case means uniform size and distribution of the crystalline phase throughout the ingot.) The desired electrochemical response has been seen in both types of material, but the characteristics of the glass-crystal composite material are generally better. This composite material is often physically stronger and usually has a lower bulk electrical resistivity. Both characteristics are desirable for the proposed use.

The crystalline phases formed in this manner vary in size, shape, and, of course, chemical composition for the various dopants used. The dopant may crystallize out in exactly the same elemental or compound form in which it was added, or it may combine with one of the elements which make up the glass and crystallize out in the form of some different compound. In addition, the crystallites have been found to be of varied shapes and sizes. In some cases they are roughly spherical, cubical, or star-shaped (see Figure 1); but more often they are dendritic or interlocking needle-type crystals (see Figures 2 and 3). The size of these dispersed crystals may vary from a few hundred angstroms (KI-doped glass) to nearly a millimeter (AgCl-doped glass). It is not yet known which set of characteristics (i.e., the chemical form, concentration, size, and shape) is necessary in this dispersed phase for the composite to have optimum response characteristics. The crystalline phase is being analyzed in several of the more successful glasses now. It is hoped that the information obtained will provide knowledge of what chemical form the dispersed phase should have and thus also dictate the type of dopant necessary to arrive at this condition.

In all samples prepared thus far the aim has been to dope the glass as heavily as possible. However, as the doping level is increased, a limit is generally reached where the composite becomes highly inhomogeneous (on a macro-scale). That is, some type of bulk segregation occurs. In many cases physical segregation occurs, and the resulting ingot is made up of large areas of very metallic material combined with large areas of crystallite-free glassy material. These samples, of course, are unusable for the small electrode configuration desired. In other cases, excess dopant is rejected in gaseous form from the glass when it is cooled. The resulting ingot is full of bubbles, voids, and blowholes and is not usable. Both of these conditions can be alleviated somewhat by altering the preparation procedures. For example, because smaller ingots can be quenched more rapidly, up to 5% Mn (metal) can be incorporated in a 15-gram ingot, but 3% Mn shows segregation in a 30-gram ingot. In addition, gaseous rejection can be reduced by maintaining a higher temperature at the top of the ampoule during quench. This increases the vapor pressure of the dopant above that of the melt and forces the dopant to stay in the glass.

The optimum shape and size for the dispersed phase is not yet known. However, it is believed at this time that the crystals should be very small



Figure 1 1% BaCl₂-1173 (80X). Light area is glass.

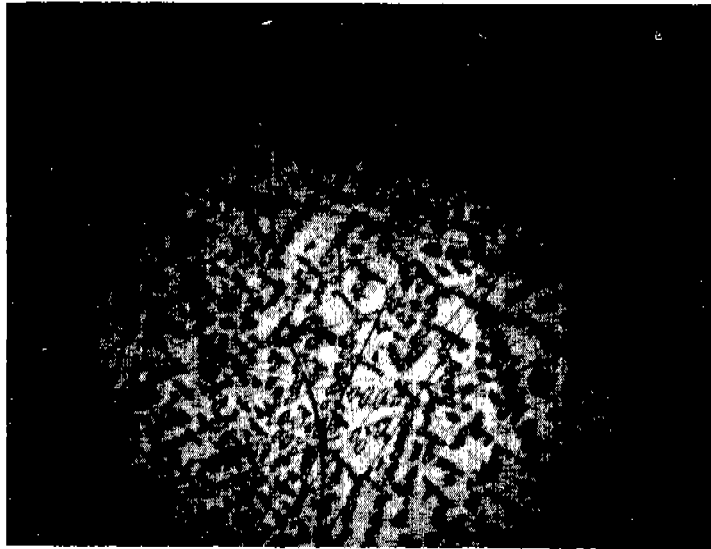


Figure 2 1 Mole % CdSe (160X). Light area is glass.

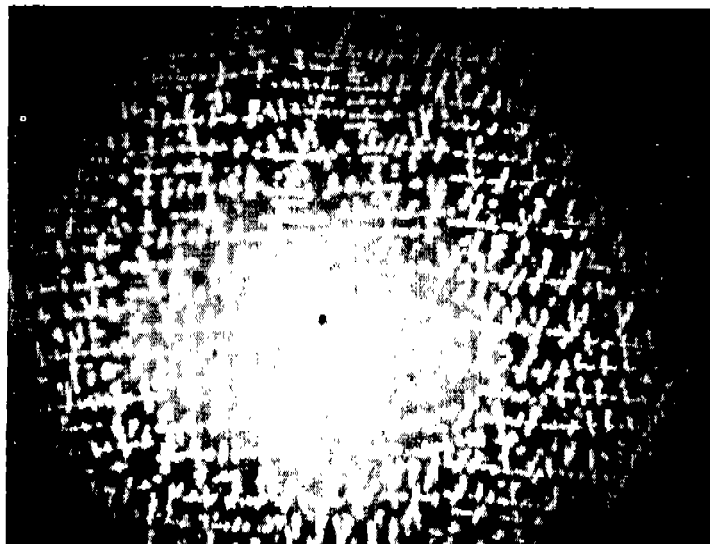


Figure 3 1 Mole % Mn (Metal) (160X). Dark area is glass.

and of a shape that provides a very large amount of active surface area, such as the needle or dendrite type of crystal. Unfortunately, little can be done to alter the characteristic habit of any particular crystalline phase. However, crystal size can be controlled somewhat by adding nucleating agents and altering the quench cycle. A post-quench heat treatment may also be used.

Table I is a summary of samples using 1173 glass as the host material. Additional descriptive comments concerning many of these samples are presented in the text which follows.

During preparation of a 0.5 mole % CaCl_2 -1173 glass, it was noted that a portion of the CaCl_2 appeared to be rejected. Autoradiograms of another sample doped with $\text{Ca}^{45}\text{Cl}_2$ confirmed the rejection and showed that much of the Ca that remained in the glass was present in clusters. These aggregates of Ca were not homogeneously spread through the sample, but increased in concentration from the bottom of the glass ingot to the top. These results indicated that the largest concentration of CaCl_2 obtainable in 1173 glass by this doping process was 0.1 mole %. Effects of BaCl_2 on the 1173 glass were even more adverse. Even a 0.1 mole % BaCl_2 -1173 glass sample crumbled so badly it could not be tested. Attainment of a Ca- or Ba-doped 1173 glass electrode by this doping process seems highly improbable.

Visual examination indicated the 2 and 4 mole % KI-1173 glasses and the 1.0 mole % KCl-1173 glass were good, but that the 4 mole % KI-1173 glass was easily broken. Isotopic analysis of a 2 mole % KI^{131} -1173 glass showed that I^{131} was homogeneously dispersed throughout the glass and that the doping process was quantitative. Emission spectrographic analysis showed the doping process was also quantitative with respect to K.

Emission spectrographic analysis has also been used to determine Mn in 1.0 mole % MnCl_2 -1173. This semiquantitative technique indicates the concentration level of Mn is close to the amount used in the doping process. The electron microprobe further substantiates the results of the emission spectrographic analysis and gives similar results for the Cl. However, electron microprobe analysis indicated some nonuniformities in the glass.

Examination of the MnSe- and CdSe-1173 glasses under an optical microscope showed that crystals were dispersed throughout the glass. A Debye-Scherrer powder pattern did not identify the crystals in the CdSe-1173 glass as simple CdSe.

Much effort was expended in improving the Fe-doped glasses to obtain sound mechanical structure and better reproducibility. This was considered

TABLE I

Summary of Doped 1173 Glass Samples Prepared
(Glass 60 mole % Se, 28 mole % Ge, 12 mole % Sb)

<u>Sample No.</u>	<u>Dopant</u>	<u>Mole %</u>	<u>Comments</u>
1	BaCl ₂	0.5	Large crystals (star-shaped).
2	BaCl ₂	1.0	Large crystals (star-shaped). 0.01 - 0.1 mm; poor distribution; not many crystals.
3	BaCl ₂	0.1	No crystals.
4	CdSe	2	No crystals -- some voids.
5	CdSe	10	Many large, interlocking, needle-type crystals. No estimate of crystal size.
6	CaCl ₂	0.1	Bubbles - rejection of CaCl ₂ (not homogeneous when hot).
7	CaCl ₂	1.0	Bubbles - voids (not homogeneous when hot).
8	KI	2	Many very fine crystals; very homogeneous.
9	KI	4	Many very fine crystals; very homogeneous.
10	KCl	1.0	No crystals.
11	AgCl	2	Very large crystals; some rejection.
12	MnCl ₂	1.0	Very many bubbles; some crystal structure.
13	MnSe	2	No crystals.
14	MnSe	10	Very many fairly large crystals.
15	MnSe	5	Interlocking, needle-type crystals.
16	Mn (metal)	1	No crystals; mechanically sound.
17	Mn (metal)	2	No crystals; mechanically sound.
18	Mn (metal)	3	Segregation; not homogeneous.
19	Mn (metal)	5	Fine dendritic crystalline dispersion; fairly uniform and homogeneous, but many voids and bubbles.
20	Fe (metal)	1	No crystals; mechanically sound.
21	Fe (metal)	2	A few crystalline inclusions; otherwise homogeneous and mechanically sound.
22	Fe (metal)	3	Segregation; not homogeneous.
23	FeSe ₂	5	Dendritic-type crystals; homogeneous, well dispersed, mechanically sound.
24	Fe (metal)	1.62	A few large crystalline clusters ~ 0.5 mm in size.
25	Fe (metal)	1.62	Very few clusters, ~ 0.1 mm; otherwise good.

TABLE I
(Continued)

<u>Sample No.</u>	<u>Dopant</u>	<u>Mole %</u>	<u>Comments</u>
26	Fe (metal)	2.0	A few clusters.
27	Fe (metal)	2.39	Many clusters.
28	Fe (metal)	3.0	1020°C - 72 hours. Uniform dendritic crystalline dispersion.
29	Mn (metal)	1.62	No crystals; mechanically sound.
30	Mn (metal)	3.0	Fine dendritic crystalline dispersion, very uniform and homogeneous.
31	Mn (metal)	4.0	Fine dendritic crystalline dispersion, very uniform and homogeneous.
32	Fe (metal)	1.62	1050°C - 48 hours. High temperature and longer time to eliminate clusters. Still a few small ones detected.
33	Mn (metal)	2.0	1000°C - 48 hours. Fine, dendritic crystalline dispersion, similar to patterns found at higher Mn concentrations, but smaller crystallites.
34	Na (metal)	1.0	Good glass.
35	Na (metal)	1.5	Good glass.
36	CaSe	3.0	Good glass.
37	CaSe	5.0	Good glass.
38	Mg (metal)	1.5	Exploded (Mg attacked quartz?)
39	Mg (metal)	3.0	Coated quartz with graphite; ampoules still cracked.
40	MgSe	1.5	1000°C - 12 hours. Very poor; hydrolyzed readily; crumbled.
41	FeSe	1.5	Good glass, but second immiscible glassy phase present.
42	FeSe ₂	1.5	Good glass, but second immiscible glassy phase present.
43	FeTe	1.5	Good glass, but second immiscible glassy phase present.
44	Ag ₂ Se	2.0	Small dendritic crystals dispersed in the glass.
45	Na (metal)	5.0	No crystals, but glass is not mechanically strong.
46	Ni (metal)	1.5	1050°C - 15 hours. Good glass, but has long, needle-like crystals dispersed throughout the ingot.
47	Co (metal)	1.5	650°C - 17 hours. Good glass, but has crystals or unreacted Co ⁰ dispersed in it.
48	CaF ₂	1.5	1050°C - 20 hours. Glassy material, but fragile.
49	Ca (metal)	1.0	1050°C - 15 hours. Glassy material, but fragile.
50	Ba (metal)	0.5	1020°C - 3 hours. Fragile glass with crystals in it.

TABLE I
(Continued)

<u>Sample No.</u>	<u>Dopant</u>	<u>Mole %</u>	<u>Comments</u>
51	MnO ₂	2.0	1034°C - 20 hours. Good glass, but has small grainy crystals dispersed in the sample.
52	MnSe	10	1100°C - 71 hours. Devitrified glass. Ingot broke into chunks. Dendritic crystalline dispersion.
53	MnSe Mn ⁺ O ₂	2.0 2.0 ⁺	1100°C - 44 hours. Devitrified glass. Small grainy crystals dispersed in sample. Material is very fragile.
54	Fe (metal)	2.0	1000°C - 50 hours. Annealing started at 420°C. Very fine whisker-like crystals dispersed throughout the glass.
55	Ba + Ni (metals)	0.5 0.5 ⁺	1000°C - 22 hours. Crystals dispersed in glass.

important, since the Fe-doped glasses have shown selective response. The problems with this material have resulted principally from the existence of large crystalline clusters in the glass (Figures 4 and 5). These clusters are thought to be agglomerates of partially reacted iron which did not go into solution in the glass, and experiments tend to support this contention. The clusters have been present in all ingots containing more than 0.8 mole % Fe. It has been established that the number and size of these clusters can be reduced by reacting the glass at higher temperatures for longer periods of time. However, at or above concentrations of approximately 2.5 mole % Fe, some of these inhomogeneities are always present, regardless of time or temperature of reaction (within practical limits). It is not presently known whether any crystalline structure other than the clusters exists in these glasses. Nothing else is observed with an optical microscope. Also, the fracture characteristics are glasslike, and it is believed that the Fe that goes into the glass is still in solution in it. Electron microscopy will be used to verify this.

The structure of the Mn glasses was discussed briefly in the Fifth Quarterly Report for this contract, and a photomicrograph of the 1.0 mole % Mn (metal) glass was included to show the typical crystalline dispersion produced. These crystals are not present in specimens that have less than approximately 2 mole % Mn. The resistivity-composition curve also shows the effect of these crystals. Glasses containing less than approximately 2 mole % Mn have no crystals and show only a gradual decrease in resistivity of about one and one-half orders of magnitude compared to the undoped glass. It is assumed that this effect occurred because the Mn was completely dissolved in the glass and did not come out of solution during cooling. However, at compositions greater than approximately 2 mole %, crystals which are believed to be MnSe begin to appear, and a corresponding sharp change of slope of the resistivity curve is present. There are probably two effects operable at this point. The first is just the appearance of the separated low-resistivity crystalline phase. A far greater effect, however, should be brought about at higher doping levels when the number and size of crystals are such that crystal-to-crystal contact takes place.

Several Fe- and Mn-doped 1173 glasses were prepared to establish the exact shapes of the resistivity versus dopant concentration curves. These data are necessary to determine the mechanism by which the resistivity is lowered. As previously discussed, there is a considerable decrease in resistivity before the sudden drop to 100 ohm-cm or less occurs at about 2% Fe and 3% Mn.

The possibility of using the Mössbauer effect to determine how the Fe is incorporated into the glass has been investigated. Tests showed that the absorption of the 14 kV radiation by the Se in the glass (x-ray absorption edge 12.65 kV) is too large to allow Mössbauer transmission spectroscopy. If

5581-10

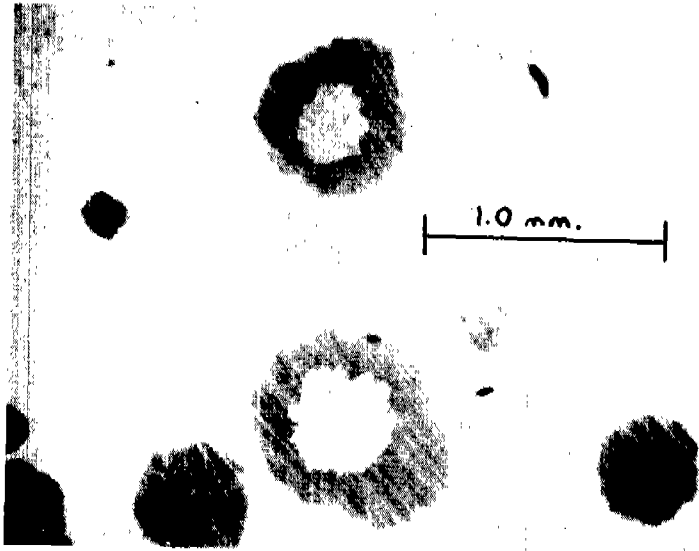


Figure 4 Crystalline Clusters in 2.39% Fe-Doped 1173 Glass.
21 hours at 975°C. (32X)

5581-9

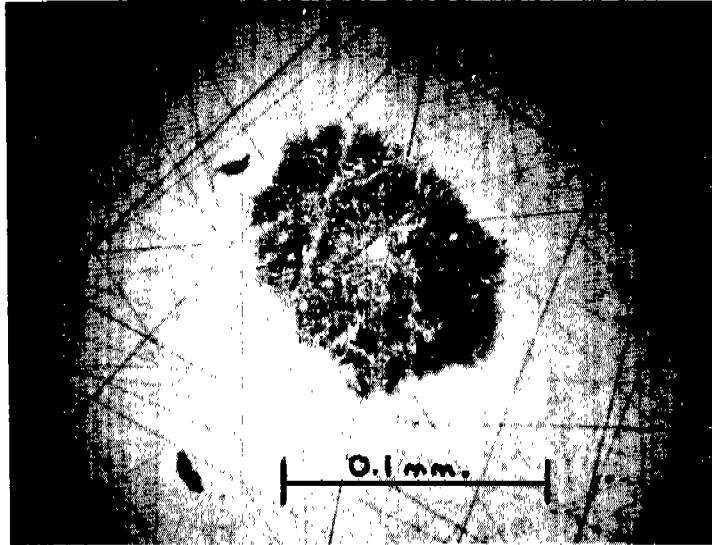


Figure 5 Crystalline Clusters in 1.62% Fe-Doped 1173 Glass.
25 hours at 1000°C. (350X)

the non-resonance scattering from the glass does not increase the background too much, one might be able to do the measurement in scattering geometry. Another possibility for determining the iron environment is, of course, magnetic susceptibility measurements.

The FeTe, FeSe, and FeSe₂-doped 1173 glasses were prepared in the same manner as the elemental Fe⁰-doped 1173 glasses. Figure 6 shows photographs of the three glass samples at 160X magnification. All three samples have what appears to be a second immiscible glassy phase, but this can probably be corrected by increasing the time in the rocking furnace and/or by increasing the furnace temperature to 1050°C.

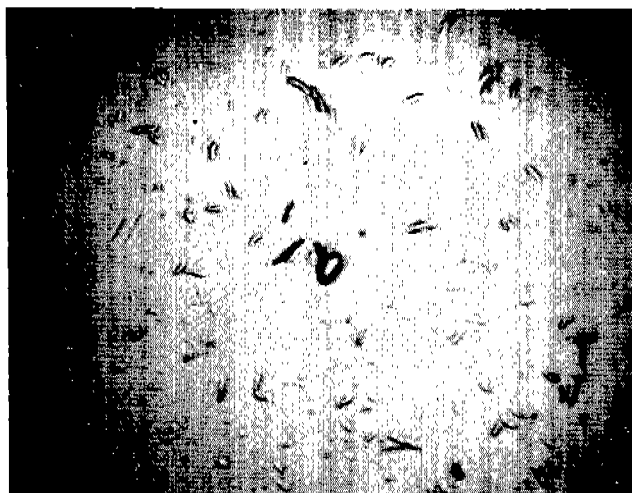
Fe in various oxidation states (Fe⁺² and Fe⁺³) was added to 1173 glass to determine the effect on the electrochemical behavior of the final Fe-doped sample. Essentially, the question was whether or not the oxidation state of the Fe in the glass is independent of the oxidation state of the Fe prior to its introduction into the glass.

Qualitative analyses for the oxidation state(s) of Fe in 1173 were made on a 1.62 mole % Fe⁰-1173 glass sample. The sample was dissolved in 10% KOH, acidified with H₂SO₄, and filtered. The filtrate was tested for the presence of Fe⁺³ and Fe⁺². Spot tests with K₄Fe(CN)₆ and KSCN indicated that Fe⁺³ was present, and the presence of Fe⁺² was confirmed by a positive spot test with ferroin.

Electron spin resonance (ESR) spectra (Figure 7) of undoped 1173, 0.05 mole % Fe⁰-1173, and 0.8 mole % Fe⁰-1173 confirm that Fe⁺³ is present in the Fe-doped 1173 glasses. For both undoped and doped samples a peak corresponding to a spin coupling constant of $g = 2$ is observed. This is attributed to free electrons associated with defects in the glass. For the Fe-doped samples, however, a peak at $g = 8$ is present. The $g = 8$ peak is believed to be Fe⁺³ in a tetrahedral structure which is influenced by a mixture of axial and rhombic fields.

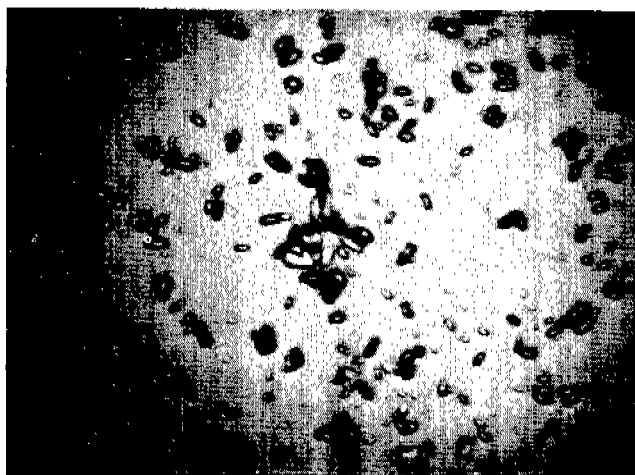
An attempt to confirm the presence of Fe⁺² in 0.05 mole % Fe⁰-1173 was made by exposing the sample to light from a high pressure Hg-vapor lamp while it was in the ESR cavity. In some semiconductor glasses light is known to induce a reaction similar to a disproportionation reaction ($2 \text{Fe}^{+2} \rightarrow \text{Fe}^{+3} + \text{Fe}^{+1}$). The Fe⁺³ generated from such a reaction would then appear at the $g = 8$ peak of the ESR spectrum. The results were negative, however, and it cannot be conclusively stated from this experiment whether or not Fe⁺² is present.

A

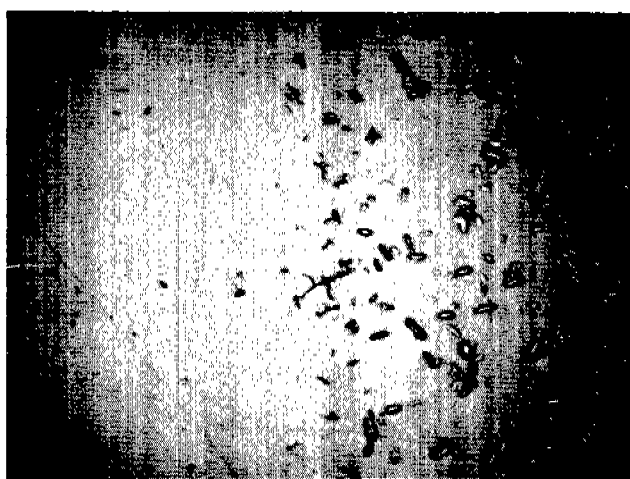


1.5% FeTe
1.5% FeSe
1.5 FeSe₂
160 X

B

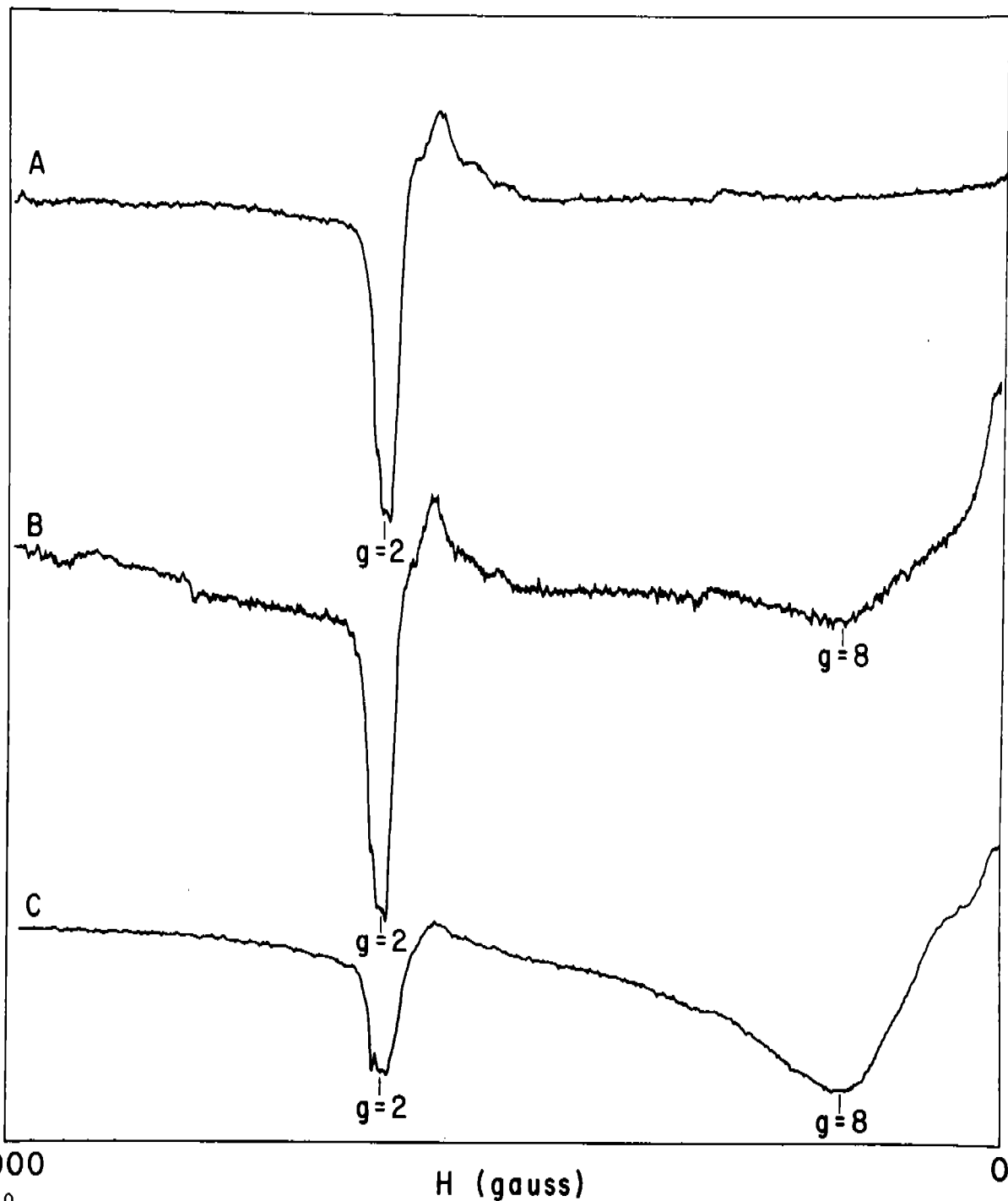


C



5820-12

Figure 6 A. 1.5 Mole % FeTe-1173 Glass (160X). B. 1.5 Mole % FeSe-1173 Glass (160X). C. 1.5 Mole % FeSe₂-1173 Glass (160X).

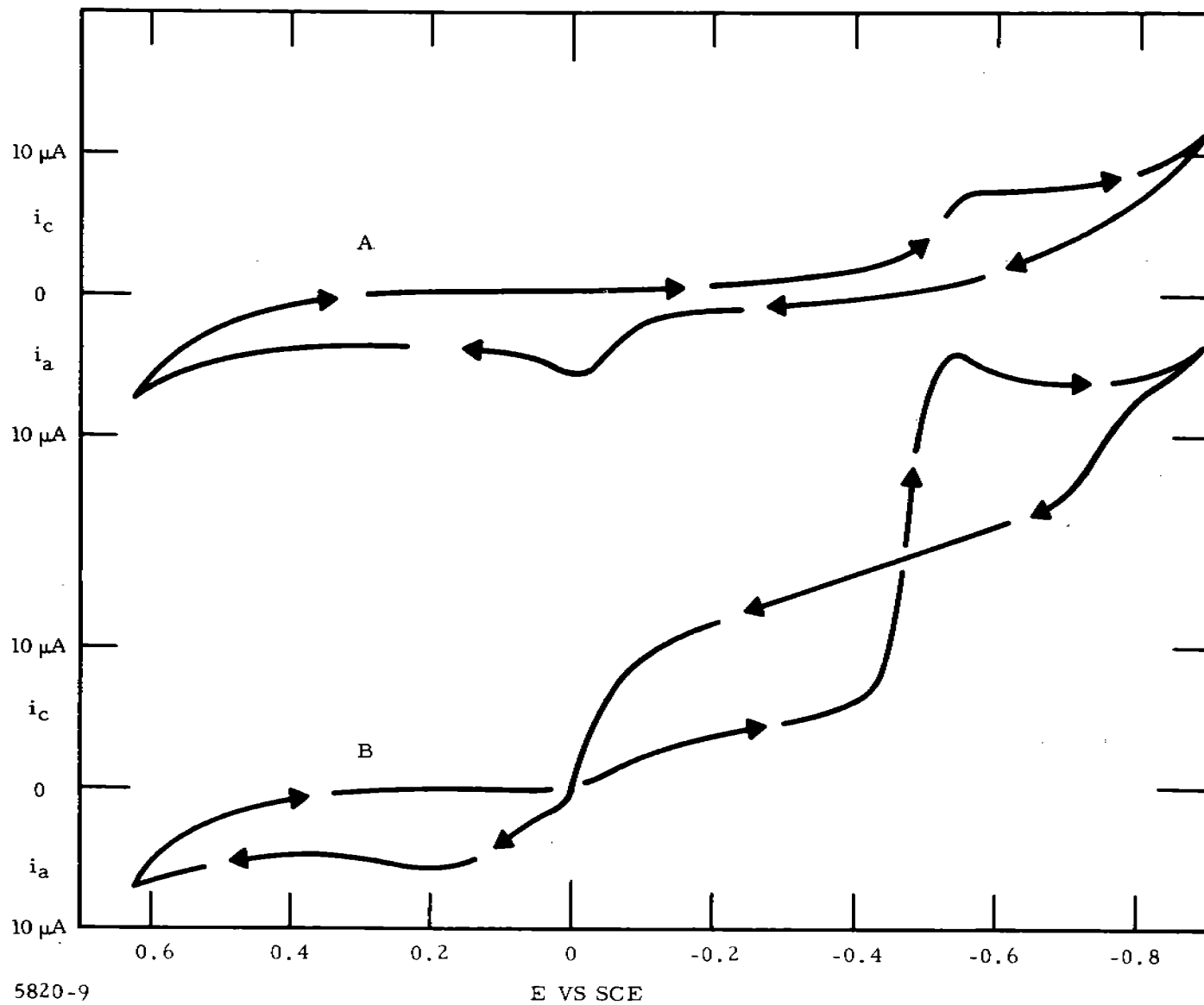


5820-10

Figure 7 ESR Spectra. A. Undoped 1173 glass.
 B. 0.05 mole % Fe^0 -1173 glass.
 C. 0.8 mole % Fe^0 -1173 glass.

In the more concentrated Fe^0 -doped 1173 glasses (2.39 and 2.5 mole % Fe^0), small clusters (a second phase) are present. Since these samples have a low resistance, it was possible to study the electrochemical behavior of the 2.39 mole % Fe^0 -1173 glass electrode by cyclic voltammetry and controlled potential electrolysis techniques. Cyclic voltammograms of the 2.39 mole % Fe^0 -1173 glass electrode in 0.1 M KNO_3 (pH = 2) and in 0.1 M $\text{Fe}(\text{NO}_3)_3$ (pH = 2) are shown in Figure 8. With this technique the potential of the electrode is related to a triangular (or sawtooth) waveform and is controlled by a potentiostat. The resulting current-voltage curves were obtained at a voltage sweep rate of ~ 0.03 V/sec. The voltage is swept from 0 V vs SCE (saturated calomel reference electrode) to more cathodic (negative) potentials. At -0.9 V the direction of the voltage sweep is reversed and the anodic excursion goes to +0.6 V, where the voltage sweep is reversed again. The voltage sweep cycle is complete when the voltage sweeps negatively from 0.6 V to 0 V. The cathodic peak at -0.55 V in 0.1 M KNO_3 is due to the reduction of Fe in the cluster phase of the glass. Because of the shape of the peak and the height of the peak current, the anodic peak at ~ 0.0 V is assumed to be the reverse of the process that occurs at -0.55 V. When the same voltammogram is run in 0.1 M $\text{Fe}(\text{NO}_3)_3$, the cathodic peak at -0.55 V increases. It is notable that on the anodic half-cycle the cathodic current does not decrease to zero until 0.0 V. Also, the original anodic peak at ~ 0.0 V is seen as a shoulder on a new anodic peak at +0.2 V. It was concluded that the increase in cathodic current is due to reduction of Fe^{+3} in solution to Fe^{+2} and that this process would have occurred initially at ~ 0.0 V if there had been no barrier to inhibit the passing of cathodic current. At -0.55 V, the reduction of the Fe in the cluster phase removes the barrier and the two cathodic processes can occur simultaneously. On the anodic excursion (from -0.9 V to +0.6 V), cathodic current is allowed to flow until the potential is in the neighborhood of 0.0 V, where the barrier (or passivating film) is formed again. The anodic peak at 0.2 V is believed to be the oxidation of Fe^{+2} formed by the cathodic reduction of (Fe^{+3}) solution during the cathodic half-cycle.

In an attempt to confirm the identity of the cathodic and anodic processes occurring at the 2.39 mole % Fe^0 -1173 glass electrode, controlled potential electrolysis experiments were carried out in 0.1 M KNO_3 with ferroin or KSCN present. With ferroin present in solution, an orange streaming from the cluster phase was noted at reduction potentials negative to -0.5 V and oxidation potentials positive to +0.1 V. In the former case, the cathodic process would be $\text{Fe}^{+3} + e \rightarrow \text{Fe}^{+2}$, with the Fe^{+3} initially tied up as a passivating film of ferric selenide or ferric oxide. In the latter case, the anodic process would be $\text{Fe}^0 \rightarrow \text{Fe}^{+2} + 2e^-$. In solutions with KSCN present, the red color of $\text{Fe}(\text{SCN})_2^+$ streaming from the cluster occurs at oxidation potentials positive to +0.3 V. Therefore, reduction of Fe^{+3} to Fe^{+2} is occurring at the cathodic peak at -0.55 V. It is also possible that some of the Fe^{+2} is reduced further to Fe^0 . The anodic peak at ~ 0.0 V appears to be due to the



5820-9

Figure 8 A. Voltammogram of 2.39 Mole % Fe^0 -1173 Glass Electrode in 0.1 M KNO_3 at $\text{pH} = 2$.
 B. Voltammogram of 2.39 Mole % Fe^0 -1173 Glass Electrode in $0.1 \text{ M Fe(NO}_3)_3$ at $\text{pH} = 2$.

oxidation of elemental Fe^0 to Fe^{+2} , with oxidation to Fe^{+3} occurring at slightly more positive potentials.

On the basis of the electrochemical experiments, it is concluded that probably all the oxidation states of Fe (Fe^0 , Fe^{+2} , and Fe^{+3}) are present in the cluster phase of 2.39 mole % Fe^0 -1173 glass.

Investigation of 2.5 mole % Fe^0 -1173 with the electron microprobe showed that the cluster phase contained 2.29 wt % Fe, and the normal glassy phase contained 1.94 wt % Fe. Electron microscope scanning revealed no detectable quantity of crystallites in either phase.

From results obtained to date on Fe^0 -doped 1173 glasses with less than 2 mole % Fe, Fe^{+2} and Fe^{+3} appear to be present, but the concentration of each state has not been determined. Magnetic susceptibility measurements may be helpful in elucidating the concentrations of the two oxidation states.

Additional physical, chemical, and spectral data on Fe- and Mn-doped 1173 are presented in Appendix B. Although these studies were not a part of this contract, they are included in the appendix in an attempt to report as much information as possible about the materials tested in sensor fabrication.

1173 glasses doped with 2.0 mole % Ag_2Se and 1.0, 1.5, and 5.0 mole % Na^0 were prepared from commercially available Ag_2Se and elemental Na^0 . Dendritic crystallites about 0.02 mm long were distributed over the surface of the 2.0 mole % Ag_2Se -1173 glass. Photomicrographs of the Na^0 -doped samples showed no significant crystalline structure.

Mn in the +4, +2, and combination of +2 and +4 oxidation states was introduced into 1173 glass in an attempt to arrive at a state in which an exchange current or ion exchange involving the Mn^{+2} might be set up at the electrode-solution interface. Although various oxidation states have been introduced into the glass, it is possible that the final oxidation state of Mn in the glass is the same regardless of its initial value.

The same approach was used for doping 1173 glass with Ca and Ba. Both Ca^0 and Ca^{+2} (CaF_2) and Ba^0 and Ba^{+2} (BaO) were used. The Ca-doped 1173 glass samples are designed to be sensors for Ca^{+2} , while it is hoped the Ba-doped 1173 sample will be sensitive to $\text{SO}_4^{=}$.

Samples of 1173 glass doped with Ni^0 and Co^0 were prepared because of the properties that they have in common with Fe^0 . The importance of these samples in the elucidation of the potential mechanism for the Fe^{+3} sensitive sensors will be discussed later.

The 2.0% Fe^0 -1173 glass sample prepared most recently did not have the clusters that were present on previous 2.0% Fe -1173 samples, but it did have very fine, whisker-like crystals throughout the ingot. The difference is due to the increased temperature for the start of the annealing process. The air-quenched glass was placed in the annealing furnace which was at 420°C (above the softening point of 370°C), the furnace was turned off, and the sample was slow-cooled to less than 100°C (four-hour process).

Mn metal was evaporated onto slices of undoped and 5% MnSe -1173 glass. The samples were then sealed into evacuated ampoules and placed in a furnace at 250 - 260°C . One group of samples of undoped 1173 glass was heated for 24 hours at 260°C . Slight warping occurred. Microprobe analysis indicated that the Mn diffused only 6 to 7 μm beyond the Mn-glass interface. A second series was then placed in ampoules, supported to prevent warpage, and maintained at 260°C for 92 hours. An additional run was made at 255°C for 284 hours. Some of these samples had Mn evaporated on both sides of the glass. A final series of Mn-evaporated samples was prepared with 5 mole % MnSe -1173 glass as the substrate. This diffusion was carried out at 255°C for 429 hours.

Resistivity measurements of doped 1173 glass indicated that all these materials were essentially electronic conductors. The ionic contributions to the total conductivity of the samples were usually less than 1%. Because of the reported high ionic conductivity of Cd-containing GeS_2 glass,¹ this glass was selected for additional sensor material preparation. A summary of the samples of doped chalcogenide glass other than 1173 glass are presented in Table II.

Samples of Mn-doped GeSe_2 glass were prepared in an attempt to get a usable electrode for Mn. Since it is difficult to quench GeSe_2 rapidly enough to form a glass with the large diameter samples required for the electrode measurements, some excess Se was added to move well down into the easy glass-forming region; the actual composition was $\text{Ge}_{28}\text{Se}_{72}$. The Mn-containing glass was unstable in water, forming a dark red powder, and so appears unsuitable for electrodes. Glass of the same composition, but without Mn, was quite stable in water.

1. E. R. Plumat, J. Am. Ceram. Soc. 51, 499 (1968).

TABLE II

Samples of Doped Chalcogenide Glasses

<u>Sample No.</u>	<u>Dopant and Host</u>	<u>Mole % Dopant</u>	<u>Comments</u>
1	Ge ₂₈ Se ₇₂	--	1020°C - 24 hours. Good glass.
2	Ge ₂₀ Se ₇₅ Mn _{0.5}	--	1000°C - 72 hours. Poor glass, black, no luster, porous, dark red regions.
3	GeS ₂ + 5% S	--	900°C - 28 hours. Inhomogeneous ingot - amber glassy region, white leafy crystalline region, and dark gray crystalline region.
4	GeS ₂ + 15% S	--	900°C - 23 hours. Ingot composed of amber glassy material and yellow crystalline material.
5	GeS ₂ + 25% S (Ge ₂₉ S ₇₁)	--	900°C - 20 hours. Amber glass - shattered when ingot was removed from ampoule.
6	Na (metal) + GeS ₂ + 5% S	3	900°C - 20 hours. Outer rim of ingot was glassy, but center was crystalline.
7	Pb + Na (metals) + Ge ₂₉ S ₇₁	7 (as Na ₂ S) 5 (as PbS)	900°C - 5 hours. Good glass with crystallites dispersed in it. Mechanically very strong.
8	Pb (elemental) + Ge ₂₉ S ₇₁	2.3	1000°C - 68 hours. No annealing. Very strong polycrystalline material.
9	Fe (metal) + Ge ₂₉ S ₇₁	2.0	1050°C - 24 hours. No annealing. Very strong polycrystalline material.
10	Mn (elemental) + Ge ₂₉ S ₇₁	1.0	1050°C - 20 hours. No annealing. Green opaque glass. Very strong.
11	Ni (metal) + Ge ₂₉ S ₇₁	1.0	1000°C - 44 hours. Annealed from 300°C. Polycrystalline with some glassy phase. Very strong.

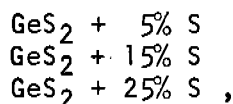
TABLE II
(Continued)

<u>Sample No.</u>	<u>Dopant and Host</u>	<u>Mole % Dopant</u>	<u>Comments</u>
12	Co (metal) + Ge ₂₉ S ₇₁	1.0	1000°C - 21 hours. Two separate glassy phases plus unreacted or crystalline phase. Very strong. No annealing.
13	Fe (metal) + Ag ₂₀ Ge ₃₀ Se ₅₀	2.0	1000°C - 47 hours. Annealed at 360°C. Fine crystals dispersed throughout the glass.

Measurements were made to confirm the ionic conductivity of Cd-doped GeS_2 . A sample doped with 5% Cd was checked with the falling sample conductivity apparatus during compounding, and it was found that the melt consisted of two phases at temperatures below about 1060°C ; thus, it appears unlikely that the work reported by Plumat on this material could have been based on a uniform sample. Because the ampoule broke during the measurements at high temperature, no electrical measurements on the solid were made.

In general, attempts to prepare GeS_2 in sealed quartz ampoules (which is necessary to avoid contamination with oxygen) have ended in explosion, even when the ampoule is heated very slowly. To avoid this difficulty, a two-zone furnace for compounding the GeS_2 was constructed.

The following GeS_2 glasses were prepared:



where the % S is the amount of S in excess of the stoichiometric amount required for compounding GeS_2 . Only the $\text{GeS}_2 + 25\% \text{ S}$ ($\text{Ge}_{29}\text{S}_{71}$) has been obtained as a completely glassy ingot. The other two samples contained crystallized areas. The $\text{Ge}_{29}\text{S}_{71}$ is mechanically very strong and is stable in deionized H_2O .

A two-step process was used to compound the glass. First, compounds of Ge and S were formed in a two-zone furnace under conditions that would prevent the S vapor pressure from causing an explosion of the sealed ampoule (S-side 400°C , Ge-side 900°C). Then the ampoule was placed in a rocking furnace, heated to 900°C for 20 to 30 hours, and air-quenched. A microquartz collar or sleeve was used to keep the upper part of the ampoule hot and the S vapor pressure high so that S would not boil out of the ingot as it set up in the quenching process.

$\text{Ge}_{29}\text{S}_{71}$ has been doped with elemental Pb^0 and Na^0 to give a glass with the following composition: 69 mole % GeS_2 , 5 mole % PbS , 7 mole % Na_2S , and 19 mole % S. Crystallites approximately 0.06 mm in diameter were dispersed in the glass and have not been identified. The glass was mechanically strong, but chemically unstable in aqueous solutions, apparently because of its high Na content. In spite of its poor chemical stability, the sample was evaluated as a sensor for Pb^{+2} and Na^+ .

The $\text{Ge}_{29}\text{S}_{71}$ glass has been doped with Pb^0 , Fe^0 , Mn^0 , Ni^0 , and Co^0 . The resulting materials were mechanically very strong (much stronger than 1173). Only the Mn-doped $\text{Ge}_{29}\text{S}_{71}$ was a glass. The other samples were either polycrystalline or polycrystalline with some glassy phase present. The very high resistivities of the $\text{Ge}_{29}\text{S}_{71}$ samples constitute a major problem.

The 2.0 % Fe^0 - $\text{As}_{20}\text{Ge}_{30}\text{Se}_{50}$ glass sample was prepared by the same procedure used with the doped 1173 sample except for the higher annealing temperature (360°C).

In general, it was demonstrated that a large number of doped chalcogenide glasses could be prepared by the procedures outlined in this section. Many of the samples exhibited mechanical, chemical, and electrical properties which justified their construction into sensors of either the electrode or the membrane configuration. Evaluation of these sensors is reported in Section IV.

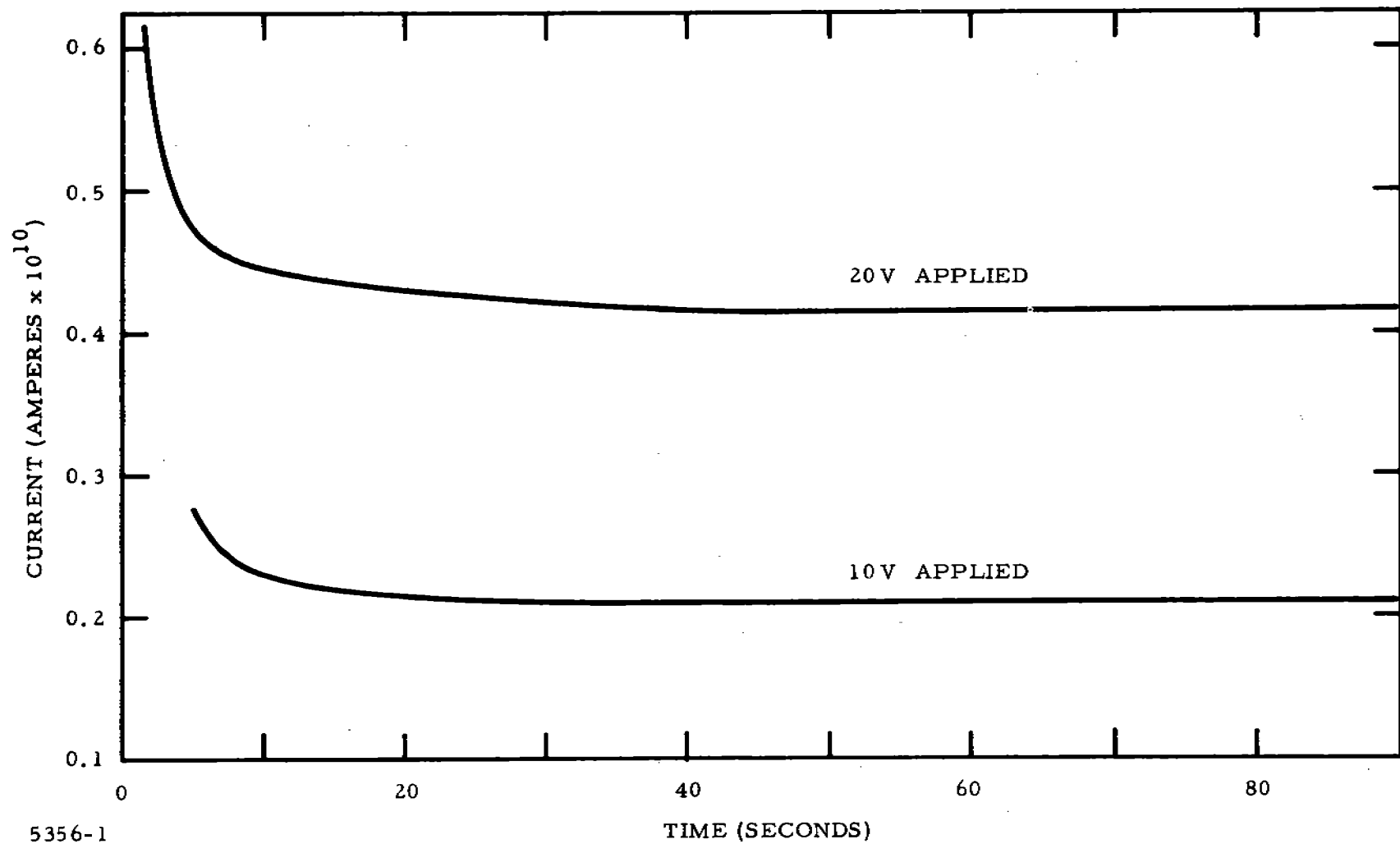
III. RESISTIVITY OF SENSOR MATERIAL

One of the more important physical properties of the sensor materials is the sample resistivity. This property measures the effectiveness of the dopant process and can be used to determine the homogeneity as well as the reproducibility of the sensor material. It was employed as a screening procedure to eliminate certain material samples from further consideration as sensor elements. Early work demonstrated that materials with resistivities greater than 10^{10} ohm-cm could not be used as sensors, while materials with resistivities in the range from 10^8 to 10^{10} ohm-cm were marginal. Samples with resistivities below 10^8 ohm-cm yield steady and reproducible sensors. Although sensor evaluations were carried out with an electrometer which had an input impedance of the order of 10^{13} to 10^{14} ohms, the sensor material had to have resistivities below 10^{10} ohm-cm to have steady response without going to extreme precautions of shielding the sensor and solution.

Sensor material samples (glass disks 1.1 to 1.2 cm in diameter, 0.04 to 0.06 cm thick) are prepared for the resistance measurement by polishing each surface to a mat finish with 40-6415 AB Silicon Carbide Powder- Grit No. 600 (Buehler Ltd.). Then the disk is rinsed thoroughly in deionized water and left to dry in air. Gold is evaporated onto each side of the disk, and the edges are ground with 30-5160 AB Handimet paper strips (Grit No. 400) to remove any gold that might have evaporated on the edges and could short the sample.

Each prepared disk is placed in a shielded can, pressure contacts are made with the gold on each side of the disk, and the shielded can is evacuated. A furnace which fits around the can is used to raise the temperature of the sample. A voltage is applied to the sample by a Harrison Laboratories 6264A DC Power Supply, and the current is monitored by a Keithley 610B Electrometer used as an ammeter. The resistance of the sample is calculated from current-voltage data. The current-time behavior is recorded on a Model 341 function/riter,[®] which is connected to the output of the Keithley 610B Electrometer. Figure 9 shows the typical current-time behavior observed for doped and undoped 1173 glass samples. In this case the glass is 2 mole % MnSe-1173 glass, and the two curves are for 20 V and 10 V of applied voltage. In each case, the current used for the calculation of sample resistivity is the steady-state value. The sharp increase in current at the beginning of each curve, followed by the gradual decrease, is characteristic for all samples. It has not been determined if this effect is the result of ionic conduction, a charging current, or a combination of the two. The resistivity of the sensor material is calculated from the geometry of the sample and the current voltage data by solving the two equations

$$V = IR \quad (1)$$



5356-1

Figure 9 Current-Time Behavior for 2.0 Mole % MnSe-1173 Glass

$$R = \rho(\ell/A) \quad (2)$$

for ρ , the resistivity.

$$\rho = \frac{VA}{I\ell},$$

where V is applied voltage, I is measured current, A is a cross-sectional area of sample, and ℓ is sample thickness.

A summary of resistivity at ambient temperature of the various sensor materials prepared is presented in Table III. Unless otherwise indicated, the samples were ohmic. The value of resistivity presented for the non-ohmic samples is the value calculated at 20 V applied dc.

The effect of concentration of dopant on resistivity for the Fe^0 and Mn^0 doped 1173 glass is shown in Figure 10. The dopant concentration for the Fe^0 -1173 glass has a greater effect on resistivity than does that for the Mn^0 -1173 glass. For the Mn^0 -doped glasses, crystallites (probably MnSe) are dispersed uniformly throughout the glass and have little effect on its resistivity until the concentration level is high enough for the crystallites to make contact with each other and essentially short the glass host. The Fe^0 -1173 glass samples are completely different. As the concentration of Fe in the glass is increased, significant decreases in the resistivity are apparent. Crystallites do not form. Fe goes into solution during glass preparation and remains in solution. Small clusters of what appears to be a different phase are noted in the 2.0 and 2.39 mole % Fe^0 -1173 glass samples. The clusters are randomly distributed in the glass and are larger in the 2.39 mole % sample, probably giving rise to a short, which would account for the sharp decrease in resistivity. Electron microprobe analysis of the Fe^0 -doped samples containing the clusters indicated no difference in the elemental composition of the regular glassy phase and the cluster phase.

The effect of temperature on the resistivity was measured for undoped 1173 and 1.0 mole % MnCl_2 -1173. As shown in Figure 11, the resistivity is exponentially related to the temperature and follows the simple Arrhenius-type equation which also describes electrolytic conduction in alkali silicate glasses,

$$\rho = \rho_0 e^{E_a/kT},$$

where ρ is the resistivity, ρ_0 is a pre-exponential factor, and E_a is the activation energy or energy barrier. In our experiments the temperature is varied from 25°C to 260°C, annealing temperature for the undoped glass. The

TABLE III

Specific Resistivities of Undoped and Doped Sensor Material Samples

<u>Sample No.</u>	<u>Sample Description</u>	<u>Resistivity (Ω-cm)</u>
1	Undoped 1173	2×10^{14}
2	Undoped 1173	1.5×10^{14}
3	0.1 mole % CaCl_2 -1173	8.5×10^{13}
4	2.0 mole % CdSe -1173	5.8×10^{13}
5	1.0 mole % MnCl_2 -1173	4.8×10^{13}
6	1.0 mole % KCl -1173	2.7×10^{13}
7	4.0 mole % KI -1173	2.3×10^{13}
8	2.0 mole % KI -1173	1.7×10^{13}
9	2.0 mole % MnSe -1173	1.1×10^{13}
10	2.0 mole % AgCl -1173	9.0×10^{11}
11	10.0 mole % CdSe -1173	$1.8 \times 10^{6*}$
12	1 mole % Mn^0 -1173	2.2×10^{13}
13	1173-Mn evaporated	$1.4 \times 10^{13*}$
14	2 mole % AgCl -1173	3.8×10^{10}
15	5 mole % MnSe -1173	$2.8 \times 10^{10*}$
16	1 mole % Fe^0 -1173	1.4×10^{10}
17	10 mole % CdSe -1173	$2.1 \times 10^{6*}$
18	5 mole % FeSe_2 -1173	$8.6 \times 10^{2*}$
19	$\text{Ge}_{28}\text{Se}_{72}$	8.8×10^{13}
20	3.0 mole % CaSe -1173	1.4×10^{13}
21	1.0 mole % Na^0 -1173	5.2×10^{12}
22	2.0 mole % Mn^0 -1173	2.8×10^{12}
23	5.0 mole % CaSe -1173	7.8×10^{11}
24	1.5 mole % Na^0 -1173	1.6×10^9
25	$\text{Ge}_{20}\text{Se}_{75}\text{Mn}_{05}$	6.3×10^8
26	1.62 mole % Fe^0 -1173	1.8×10^8
27	3.0 mole % Mn^0 -1173	6.7×10^1
28	1.5 mole % FeSe -1173	6.0×10^8
29	1.5 mole % FeSe_2 -1173	5.9×10^8
30	1.5 mole % FeTe -1173	3.5×10^9
31	2.0 mole % Ag_2Se -1173	8.4×10^9
32	1.5 mole % Na^0 -1173	2.0×10^{10}
33	5.0 mole % Na^0 -1173	2.0×10^{10}
34	5.0 mole % Pb^0 -7.0 mole % Na^0 - $\text{Ge}_{29}\text{S}_{71}$	3.2×10^9
35	2.0 mole % Fe^0 - $\text{Ge}_{29}\text{S}_{71}$	1.5×10^{14}
36	1.0 mole % Fe^0 - $\text{Ge}_{29}\text{S}_{71}$	1.2×10^{14}
37	2.3 mole % Pb - $\text{Ge}_{29}\text{S}_{71}$	5.6×10^{13}
38	1.5 mole % CaF_2 -1173	9.8×10^{13}
39	0.5 mole % Ba^0 -1173	6.7×10^{13}
40	2.0 mole % Mn^0 -1173	1.3×10^{13}
41	1.0 mole % Ca^0 -1173	9.4×10^{12}
42	1.0 mole % Ni^0 - $\text{Ge}_{29}\text{S}_{71}$	4.1×10^{11}
43	1.0 mole % Co^0 - $\text{Ge}_{29}\text{S}_{71}$	1.4×10^{11}
44	0.5 mole % Ba^0 -0.5% Ni^0 -1173	$1.4 \times 10^{10*}$
45	10.0 mole % MnSe -1173	1.5×10^9

TABLE III
(Continued)

<u>Sample No.</u>	<u>Sample Description</u>	<u>Resistivity (Ω-cm)</u>
46	1.62 mole % Fe ⁰ -1173	2.5×10^8
47	0.5 mole % Ni ⁰ -1173	$2.3 \times 10^{8*}$
48	2.0 mole % Fe ⁰ -1173	7.8×10^7
49	2.0 mole % Fe ⁰ -1173	$3.3 \times 10^{2\dagger}$
50	2.5 mole % Fe ⁰ -1173	$2.4 \times 10^{2\dagger}$
51	1.5 mole % Ni ⁰ -1173	$1.63 \times 10^{2\dagger}$
52	1.5 mole % Co ⁰ -1173	$1.47 \times 10^{2\dagger}$
53	2.0 mole % Fe ⁰ -Ag ₂₀ Ge ₃₀ Se ₅₀	$1.49 \times 10^{2\dagger}$
54	2.0 mole % Fe ⁰ -1173	$7.6 \times 10^{1\dagger}$

* Exhibited non-ohmic behavior

† Voltage applied is 1.0 V dc instead of 20 V dc

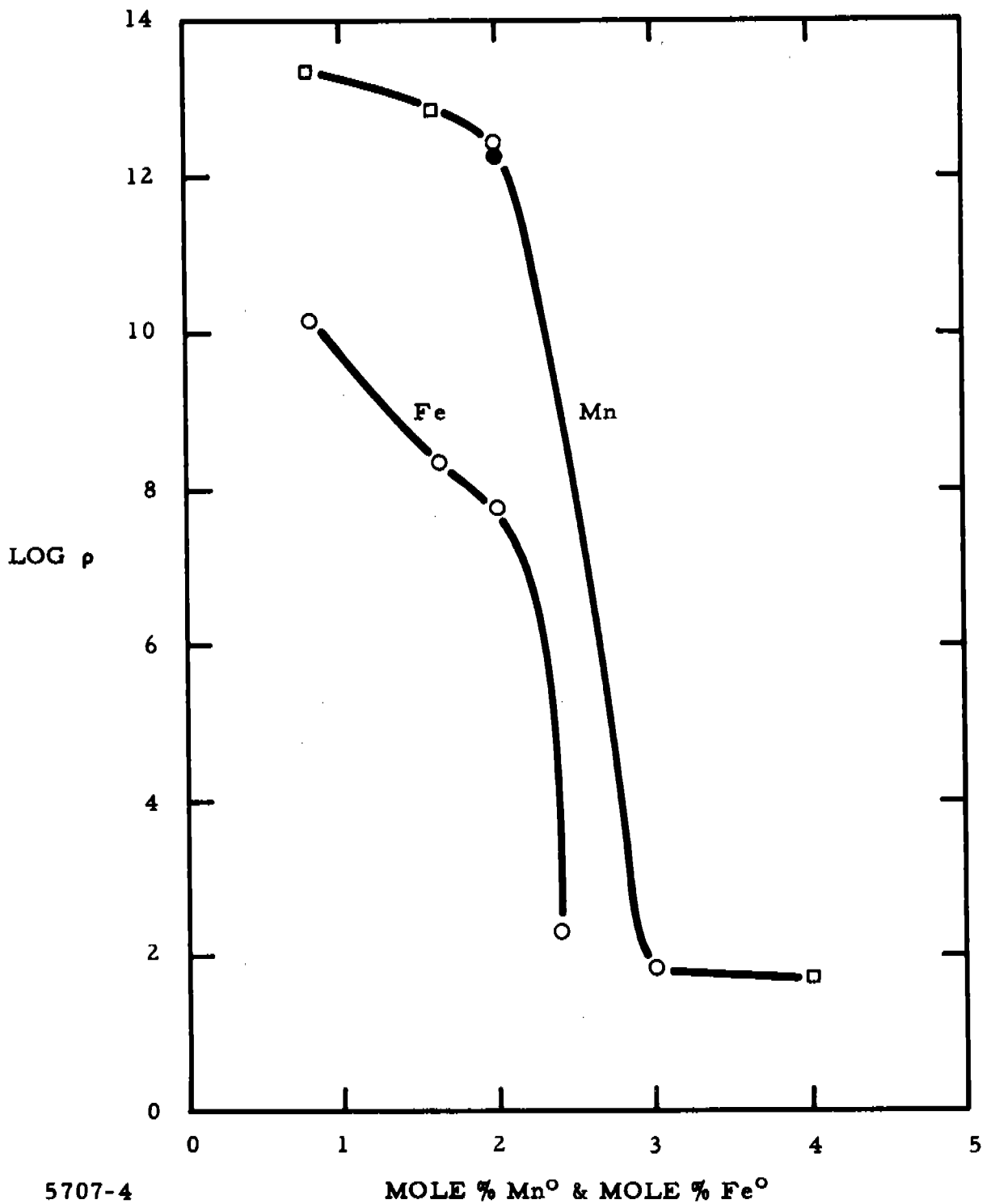
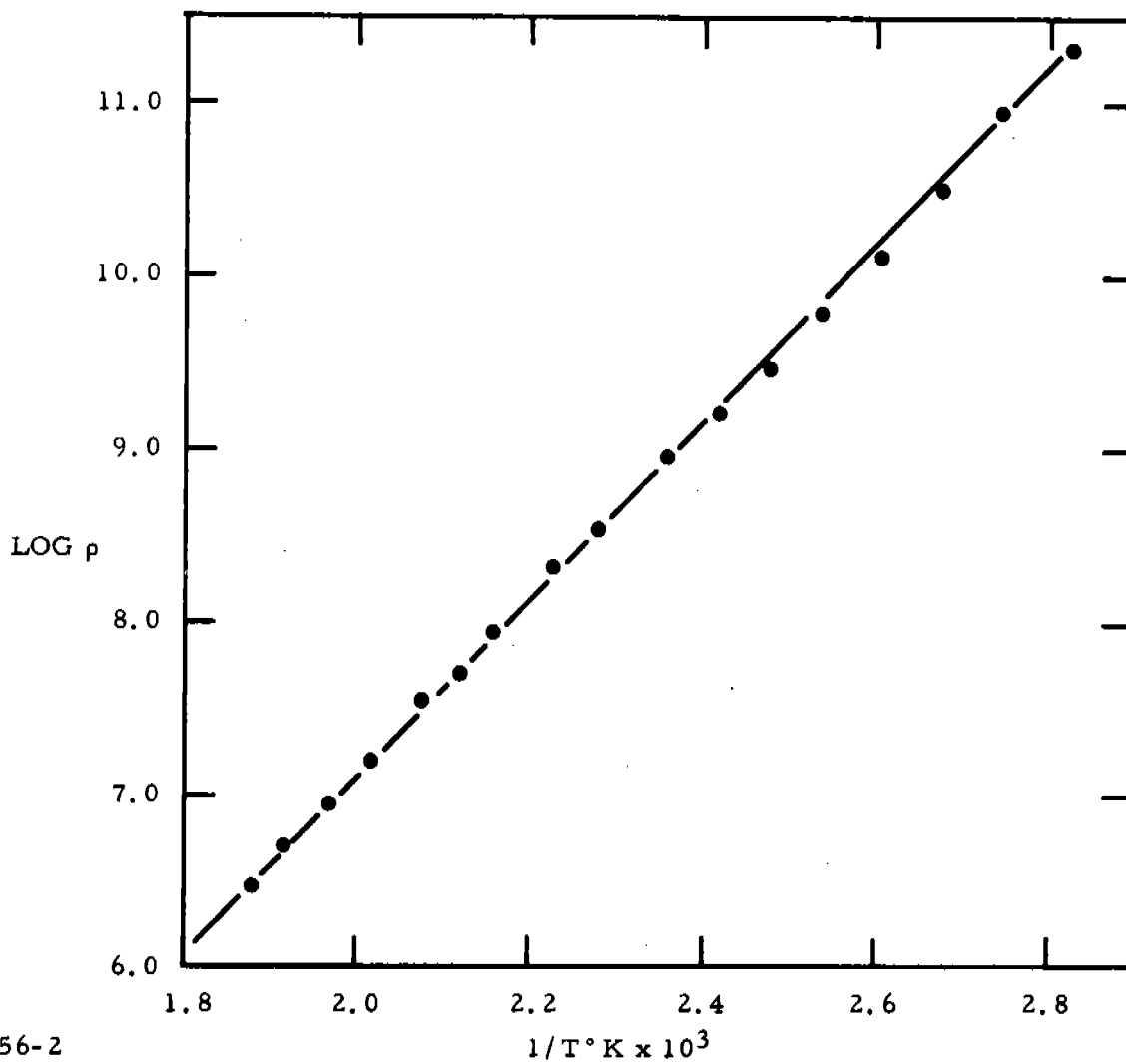


Figure 10 Effect of Mn⁰ and Fe⁰ Concentrations on the Specific Resistivities of Doped 1173 Glasses



5356-2

Figure 11 Effect of Temperature on the Resistivity of 1.0 Mole % MnCl₂-1173 Glass

slope (2.0 eV) of the $\log \rho - 1/T$ plot is not altered significantly by the direction of the temperature change, increasing or decreasing. Excursion through the temperature cycle does not affect the ambient resistivities of the glasses.

The resistivities of 5 mole % MnSe-1173 and 10 mole % CdSe-1173 were measured as a function of temperature at 20 V dc. The results are shown in Figure 12. For the 5 mole % MnSe-1173 there is no linear region in the $\log \rho - 1/T$ plot, indicating that MnSe behavior does not follow the simple Arrhenius-type expression in the temperature range 25°C to 255°C. The 10 mole % CdSe-1173 exhibited a linear region in the $\log \rho - 1/T$ plot up to 75°C, and the activation energy calculated from the slope was 0.4 eV. Between 140° and 150°C, there was a resistance breakdown which caused disfiguration of the sample. This breakdown was found to be dependent on the voltage and temperature and is believed to be associated with a hot spot in the glass which essentially shorts the glass.

Ge₂₈Se₇₂ and Ge₂₀Se₇₅Mn₅ samples were new glass compositions which were tested. The subscripts represent the mole % of each element present in the glass. Both glasses are rich in Se, the bridging atom in the glass structure. The resistivity of Ge₂₈Se₇₂ is about the same as that for undoped 1173 ($2.0 \times 10^{14} \Omega\text{-cm}$), but the resistivity of Ge₂₀Se₇₅Mn₅ is much higher than that of even the 3.0 mole % Mn⁰-1173 glass. Current-time curves for the Ge₂₈Se₇₂ at 20 V applied voltage indicate this sample exhibits a detectable amount of ionic conduction. Electronic conduction, however, is the major mechanism for charge transfer through the glass in the Ge₂₀Se₇₅Mn₅ sample.

The Ge₂₉S₇₁ samples varied in conduction mechanism depending on the dopant added. The Fe⁰ and Pb⁰ doped Ge₂₉S₇₁ exhibited ionic conduction, requiring approximately 15 minutes to reach a steady-state current. In addition, the resistivity values obtained at 10 V dc were about 20% higher than those obtained at 20 V dc. With the Ni- and Co-doped samples, ohmic behavior was observed; the apparent conducting mechanism was electronic.

The 0.5% Ni⁰-1173 and 0.5% Ba⁰-0.5 Ni⁰-1173 samples were not ohmic. The resistivity of the 0.5% Ni⁰-1173 glass increased by an order of magnitude when the voltage was decreased from 20 V to 10 V. The Ba-Ni doped 1173 sample increased about 30% in resistivity under the same conditions. The non-ohmic behavior of these two samples appears to be related to the Ni concentration in 1173.

Sensor evaluation experiments indicate that samples with a resistivity greater than $10^{10} \Omega\text{-cm}$ do not make responsive sensor elements. Glasses with resistivities between 10^8 and $10^{10} \Omega\text{-cm}$ make suitable electrodes, but their response is a bit sluggish. For the best potential stability and best response time characteristics, the resistivity values should be less than $10^8 \Omega\text{-cm}$.

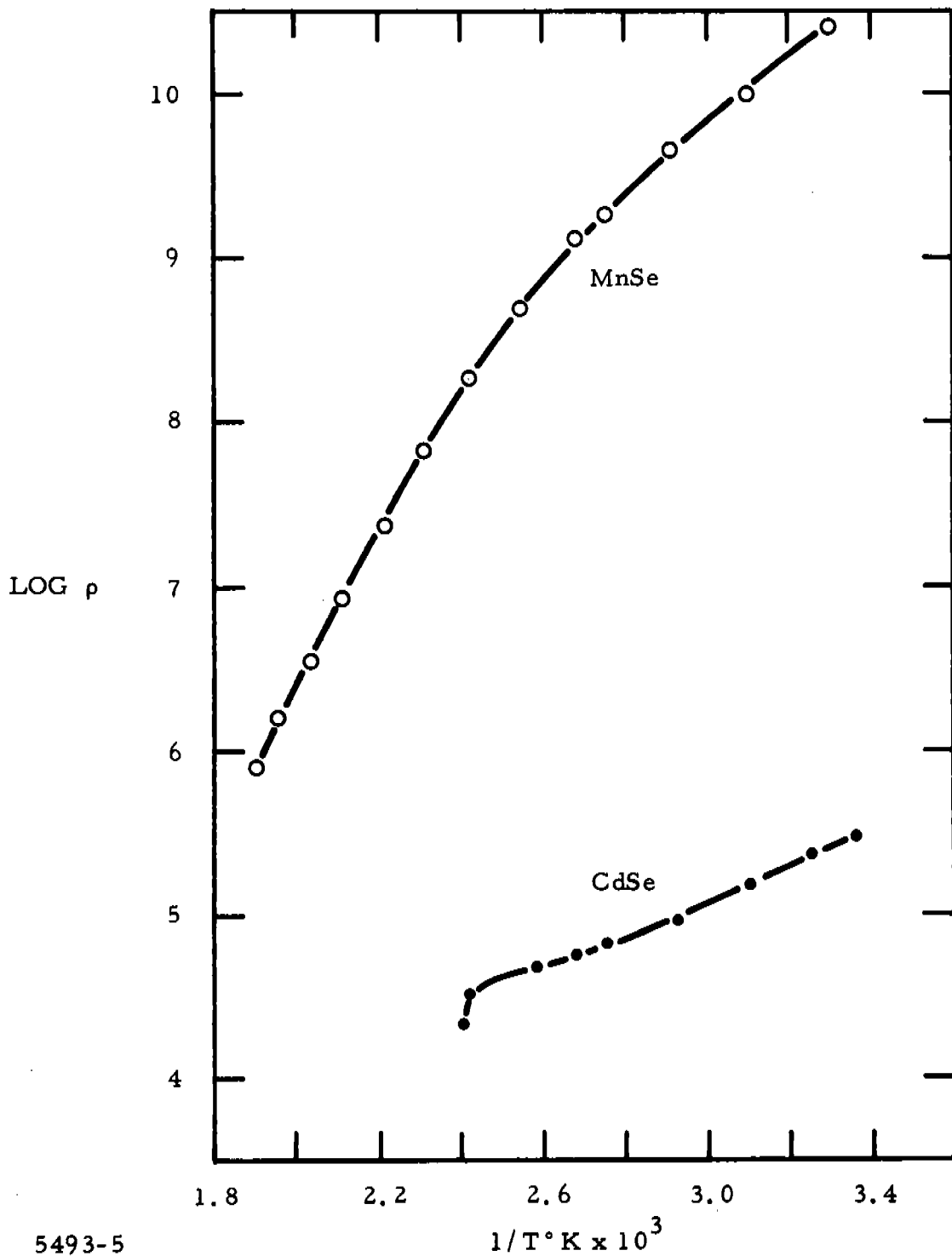


Figure 12 Effect of Temperature on the Resistivity of 5 Mole % MnSe-1173 and 10 Mole % CdSe-1173 Glasses

In all probability, the exchange current of the very high resistance sensor elements is limited by charge transfer in the glass instead of at the electrode-solution interface; therefore, the electrode does not attain equilibrium, and the electrode potential is not stable.

IV. SENSOR EVALUATION AND DISCUSSION

Two configurations (Figure 13) have been used in testing the response of the sensors to specific ions. In the first, the glass is used as a membrane or solid electrolyte like the glass in a conventional pH electrode. The sensor element is sealed in the end of a Plexiglas tube with Plexiglas adhesive such that one surface of the disk is exposed to the test solution and the other is exposed to the internal reference solution. The internal reference solution is composed of a concentration of the ion being measured (usually 10^{-3} M) in 0.1 M KNO_3 . A saturated calomel reference electrode (SCE) or a Ag/AgCl reference electrode makes contact with the internal reference solution and completes the assembly for the membrane configuration. The second configuration is an electrode in which gold is evaporated on one side of the glass disk, and a Pt-wire lead makes contact with the gold by Silver Micropaint SC 13 (Micro-Circuits Company, New Buffalo, Michigan). The lead side of the glass electrode is kept from making contact with test solutions by seating the glass disk in a Plexiglas tube sealed with Plexiglas adhesive.

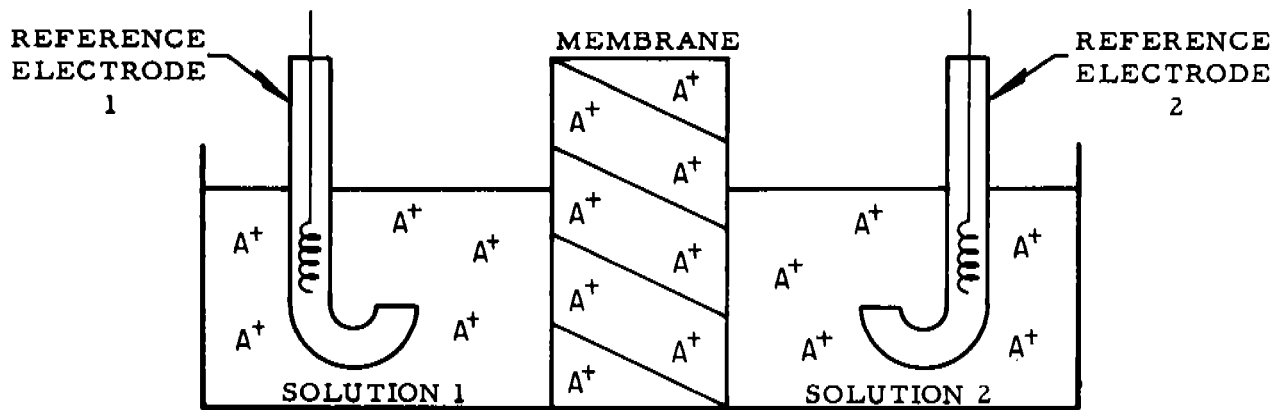
The potential response of the sensors is ideally related to the Nernst equation:

$$E \propto \frac{2.3RT}{nF} \log [X].$$

If the potential mechanism involves a redox process, then n is equal to the number of electrons transferred per ion. If the mechanism is due to a phase boundary potential based on the ion exchange theory (assuming no diffusion potential contribution), then n represents the charge of the ion measured. R , T , and F are conventional constants. $[X]$ is the concentration of the ion of interest and is directly related to the E by a logarithmic function as long as the ionic strengths of all the solutions measured are constant. (E is a function of the $\log A_X$, where A is the activity of ion X .)

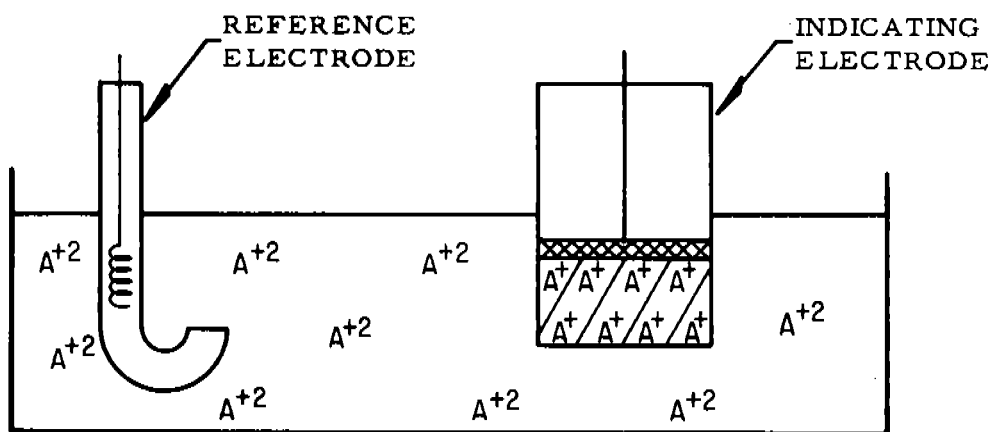
Some of the sample electrodes and membranes were not responsive as prepared, and required special pretreatments and conditioning before they became active. Descriptions of some of the activating procedures and pretreatments are presented.

The 5 mole % FeSe_2 -1173 glass as prepared does not yield a potential response to either Fe^{+2} or Fe^{+3} . Several activation and conditioning procedures were tested. The most successful procedure involves etching the solution side of the electrode with a 10 wt % KOH - 10 wt % NaH_2PO_2 solution for about 15 seconds at room temperature, anodizing the electrode in 0.1 M KNO_3 at 100 volts applied potential and approximately 1 mA of current for about 15 minutes, then soaking it in 0.1 M Fe^{+3} - 0.1 M KNO_3 solution for about 15 minutes.



$$E \propto 2.3RT/nF \text{ LOG } a_{A^+}_1/a_{A^+}_2$$

MEMBRANE CONFIGURATION



5552-3

$$E \propto 2.3RT/nF \text{ LOG } a_{A^{+2}}/a_{A^+}$$

ELECTRODE CONFIGURATION

Figure 13 Sensor Configurations

The Fe⁰-1173 glass electrodes underwent a number of activation processes designed to improve and extend the potential-concentration behavior. Anodization and cathodization of the electrodes did not improve the potential behavior, and in some instances they were detrimental. Etching the surface of the electrode with 10% KOH or 10% KOH-10% NaH₂PO₂ for 15 seconds as a pretreatment cleaning step was helpful, but not always necessary.

All other doped-1173 glass samples underwent the pretreatment used for the Fe⁰-1173 glasses. Anodization and/or cathodization of the electrodes did not enhance their performance. It appears that conditioning of the sensor is necessary when a thin layer of 1173 is smeared over the surface in the polishing step. The alkaline solution removes this thin layer and exposes the active sites, as well as lowering the resistance of the electrode.

The potential responses of each sensor were investigated by measuring the potential versus a saturated calomel reference electrode or a Ag/AgCl reference electrode with a Keithley 610 B or C electrometer. The unity-gain output of the Keithley electrometer was fed into a Hewlett-Packard 3440A digital voltmeter equipped with a Hewlett-Packard 3443A high gain/auto range unit for digital display of potentials. During continuous run experiments, the unity-gain output of the electrometer was fed into a Sargent Model SR recorder. The ionic strength of the solutions in a given series was held constant by the addition of a potentially inactive electrolyte such as KNO₃ so that direct correlations could be made between the potentials and concentrations of electroactive species with respect to the Nernst expression.

A conversion table of moles/liter to parts per million (ppm) for all the ions studied in this investigation is reproduced in Appendix A.

A. Fe⁺³ Sensors

The 5 mole % FeSe₂-1173 glass was prepared by the regular doping procedure utilizing commercially available FeSe₂. X-ray analysis of the FeSe₂ indicated that most of the material was FeSe.

The 5 mole % FeSe₂-1173 glass electrode did not give a potential response to Fe⁺² or Fe⁺³ when the electrode had not been pretreated; however, after conditioning, a potential response to Fe⁺³ was measured (Figure 14). The $\Delta E/\Delta[\text{Fe}^{+3}]$ was not reproducible from one run to the next, and the potential exhibited was dependent on the sequence of measurements. When the pH of the Fe⁺³ solutions was raised from 1.67 to 6.50, no potential response was found for changing Fe⁺³ concentrations because the uncomplexed Fe⁺³ concentration in all solutions was the same. This, along with some ionic strength experiments, led to the conclusion that the electrode gives a true potential response to [Fe⁺³].

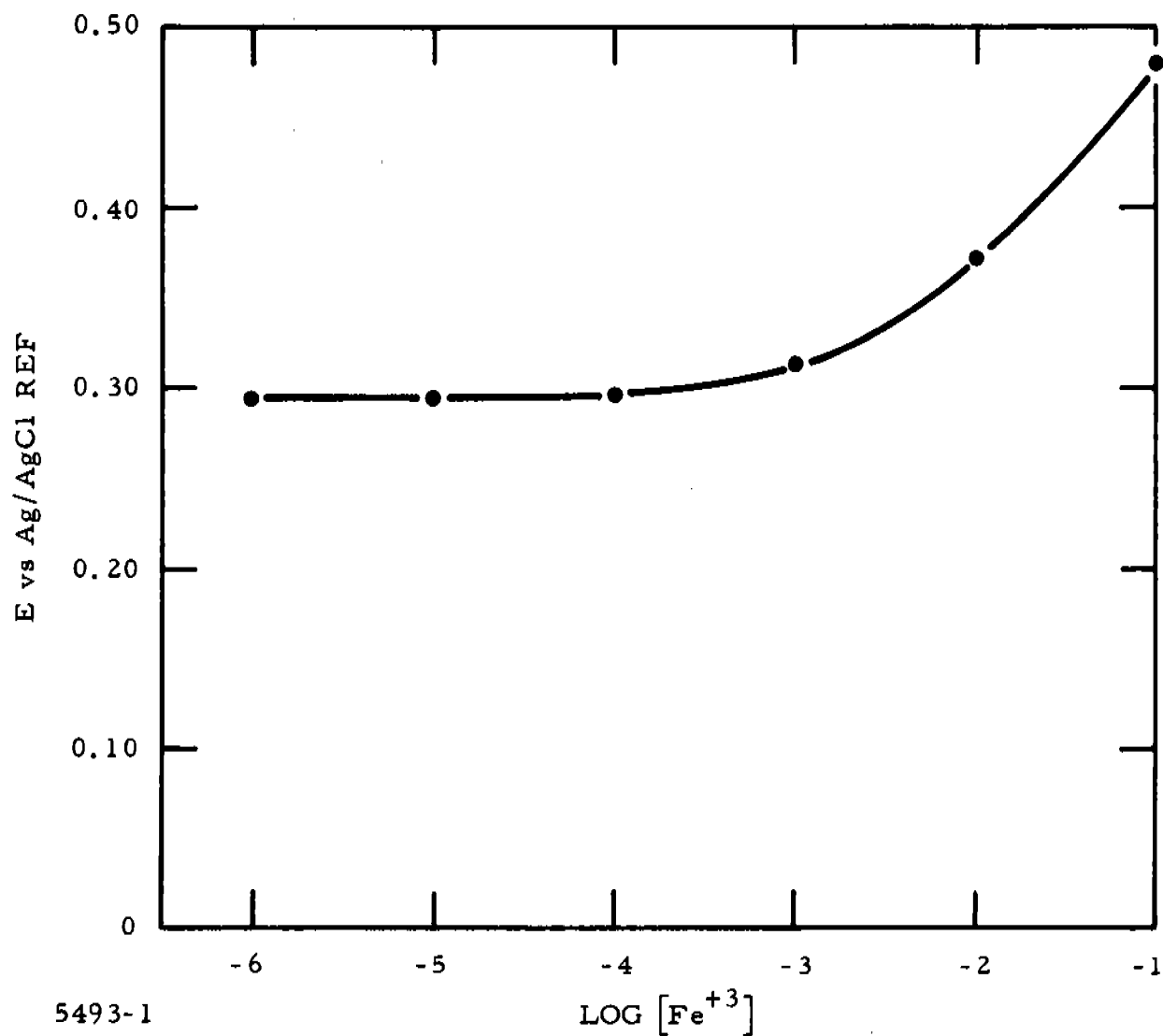


Figure 14 Effect of [Fe³⁺] on the Potential of a 5.0 Mole % FeSe₂-1173 Glass Electrode. (All solutions are 0.01 M in KNO₃ and pH = 1.67.)

Investigations of the potential response behavior of electrodes of 1.5 mole % FeTe-1173, 1.5 mole % FeSe-1173, and 1.5 mole % FeSe₂-1173 glasses to Fe⁺³, Fe⁺², and H₃O⁺ were made. Figures 15, 16, and 17 show potential responses to Fe⁺³ and Fe⁺². The responses of the FeSe and doped glasses are identical. The slopes of the E - log [Fe⁺³] curves (43 mV) are a little less than the 60 mV observed for 1.62 and 2.0 mole % Fe⁰-1173 glasses, possibly because of the presence of two glassy phases which probably contain Fe. Potential responses observed in the more concentrated Fe⁺² solutions were actually responses to Fe⁺³ present as a contaminant. Sensitivity of the FeTe-doped glass was slightly less than that of the other Fe-doped samples. Again, this is probably a function of the second immiscible glassy phase. The shape of the E-pH curves was similar for all three electrodes. Between pH 2 and pH 8, a slope of 20-30 mV/pH unit was observed; above pH 8, the response increased with increasing pH.

Electrodes prepared by encasing commercially available FeSe, FeSe₂, and FeTe were investigated for potential response to Fe⁺³, Fe⁺², and pH. The data from these experiments are given in Figures 18 through 21. None of the electrodes was responsive to Fe⁺². The FeTe electrode responded to Fe⁺³ only in the 10⁻² to 10⁻¹ M range. Both the FeSe and FeSe₂ electrodes exhibited potentials which were dependent on Fe⁺³ concentration. The slopes of the E vs log [Fe⁺³] plots were 50 mV and 212 mV for the FeSe and FeSe₂ electrodes, respectively. Of the three compound electrodes, only the FeTe exhibited an E-pH dependence.

Metallic iron was introduced into 1173 glass in an attempt to tie up the substituent of the glass which is involved in the potential determining interaction and make it become the potential active component on the glass side of the interface. The electrodes were conditioned by etching as previously described.

Samples of 1173 glass doped with 0.8, 1.62, 2.0, and 2.39 mole % Fe⁰ have been tested in the electrode configuration for potential responses to changing Fe⁺³, Fe⁺², and H₃O⁺ concentration. The results of these experiments are presented in Figures 22 through 25.

All Fe⁰-1173 glass electrodes were responsive to Fe⁺³, and the potential behavior was linear and reproducible in the concentration range from 10⁻⁵ - 10⁻⁴ to 10⁻¹ M (total salt concentration held at ~ 0.1 M by addition of KNO₃). The 0.8 and 1.62 mole % Fe⁰-1173 glass electrodes gave close to the theoretical Nernstian response of 60 mV per decade change in Fe⁺³ concentrations ($\Delta E/\Delta \log[\text{Fe}^{+3}] = 52 - 65 \text{ mV}$), but the noise pickup on these electrodes is a little higher than is desirable. The slopes of the E vs log [Fe⁺³] plots for the 2.0 and 2.39 mole % Fe⁰-1173 glass electrodes ranged from 78 to 90 mV. A

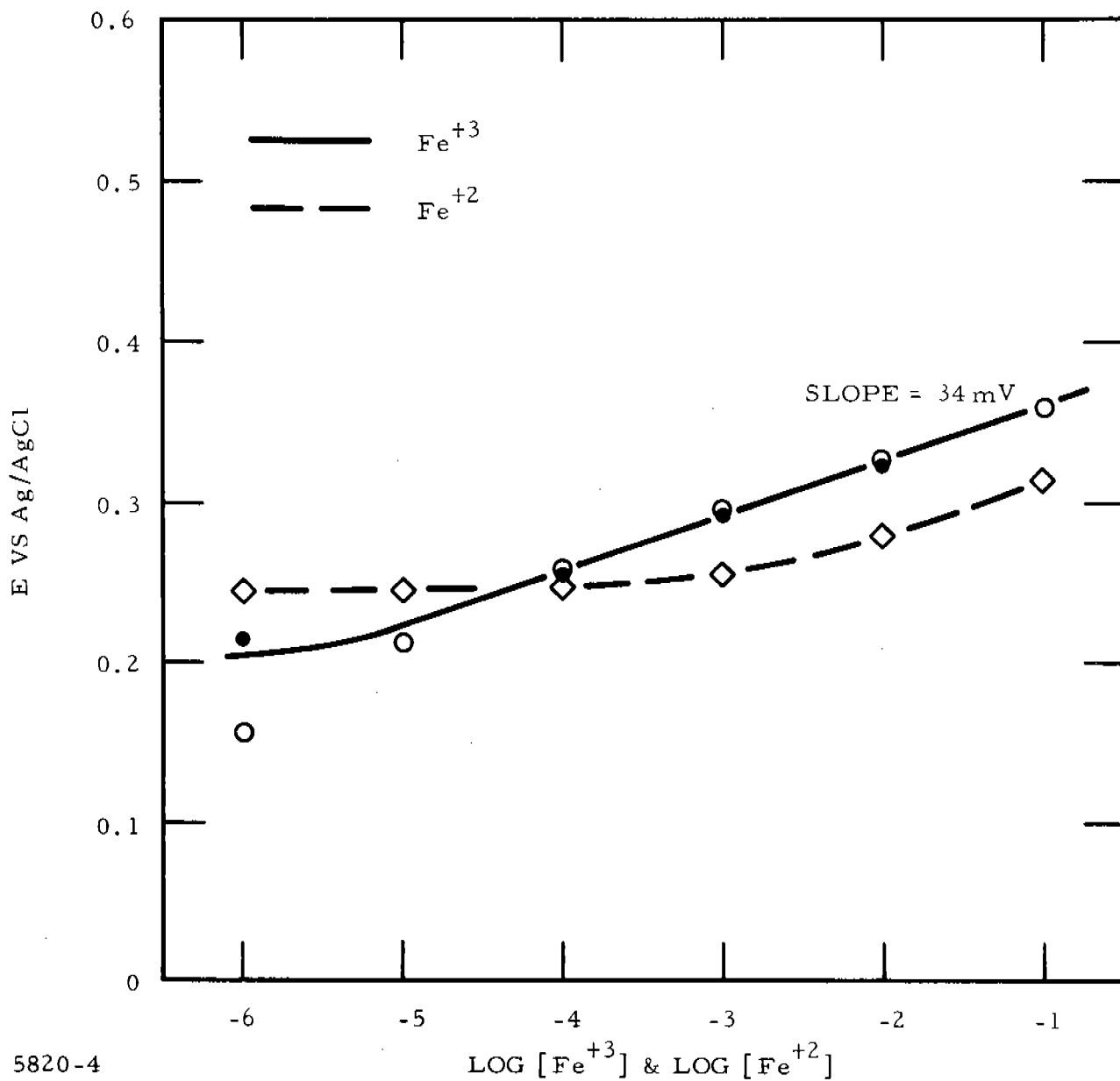
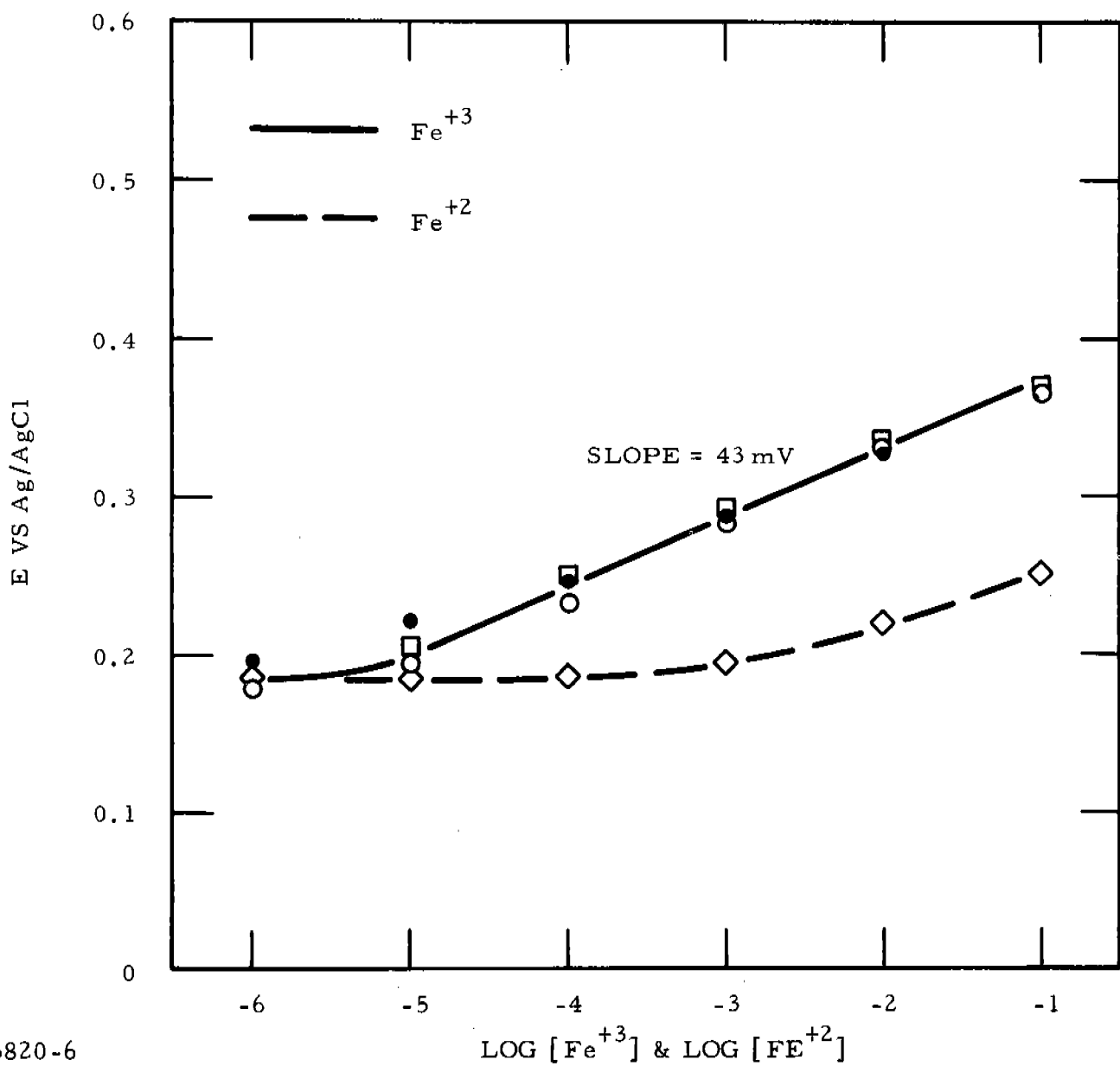


Figure 15 Potential Response of a 1.5 Mole % FeTe-1173 Glass Electrode to Fe⁺³ and Fe⁺² in 0.1 M KNO₃ at pH = 2.0



5820-6

Figure 16 Potential Response of a 1.5 Mole % FeSe-1173 Glass Electrode to Fe⁺³ and Fe⁺² in 0.1 M KNO₃ at pH = 2.0

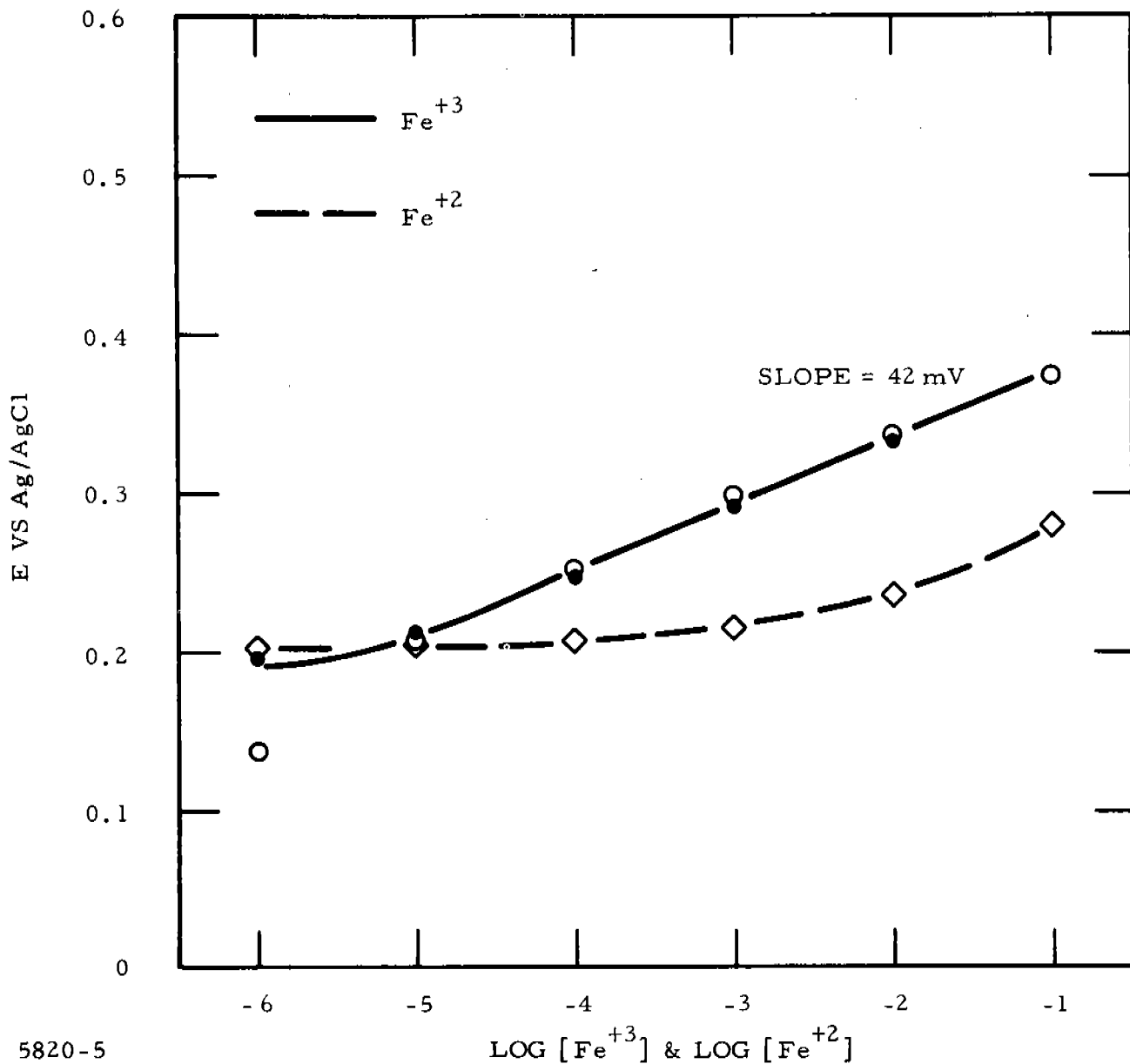
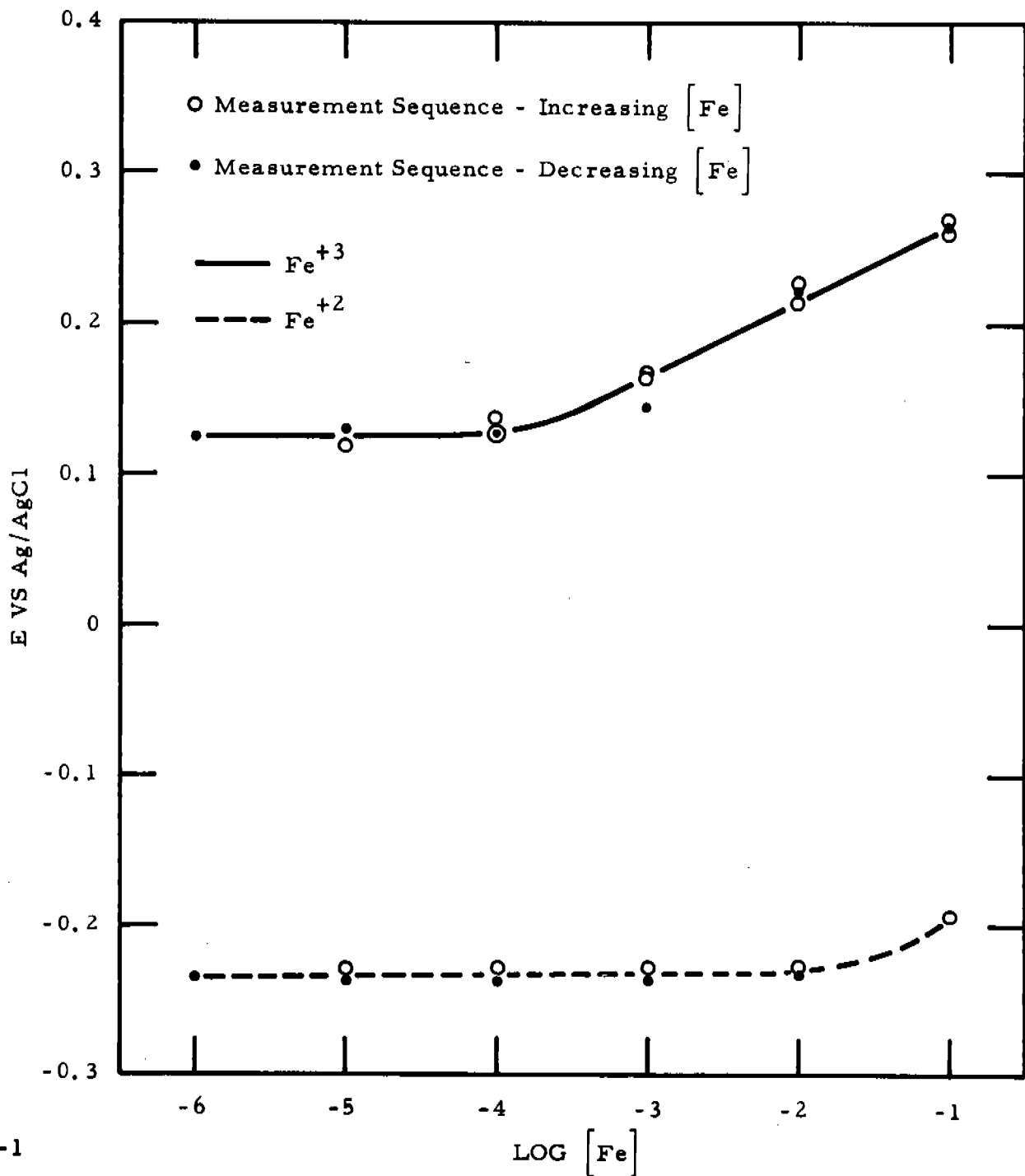
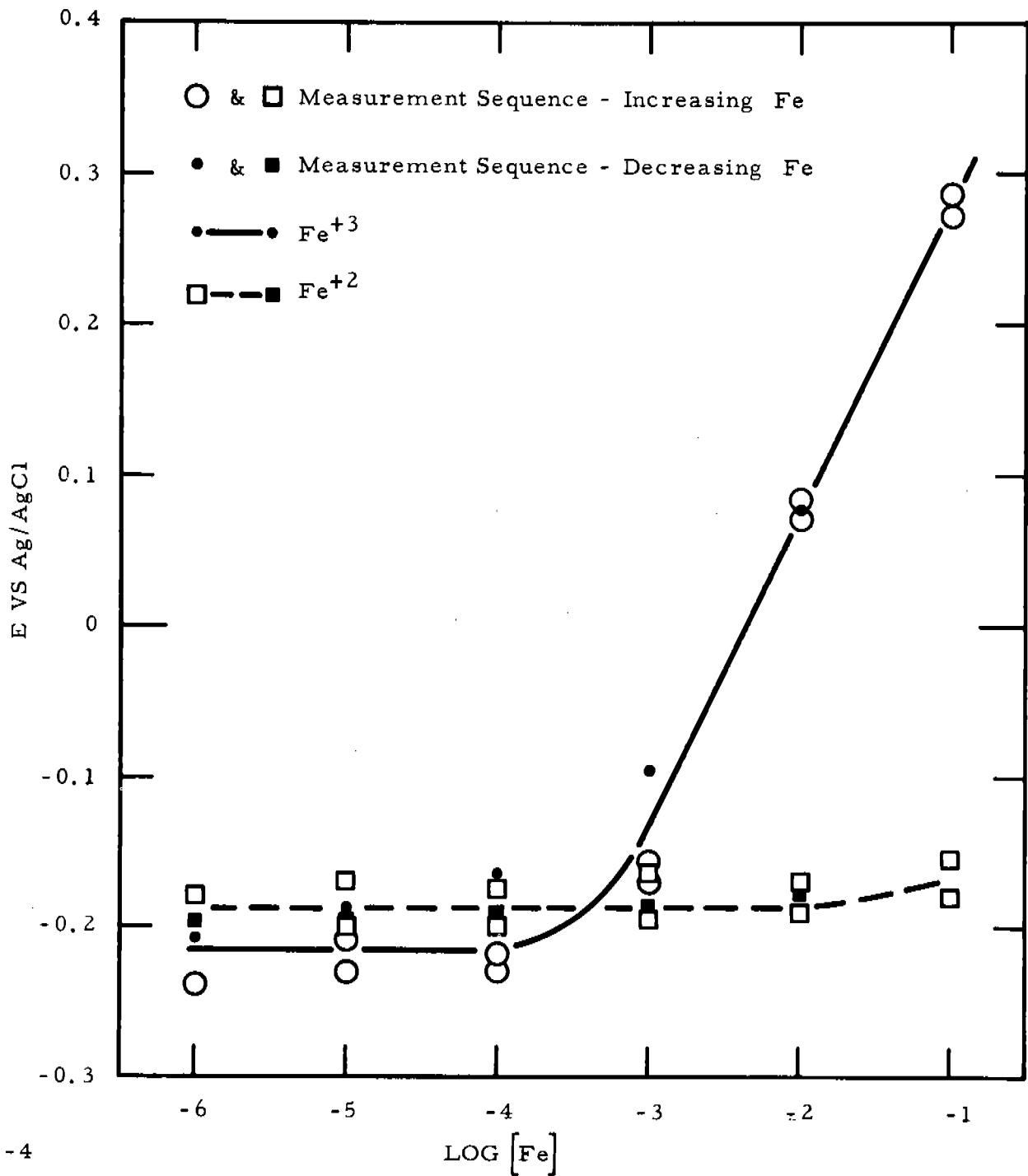


Figure 17 Potential Response of a 1.5 Mole % FeSe₂-1173 Glass Electrode to Fe⁺³ and Fe⁺² in 0.1 M KNO₃ at pH = 2.0



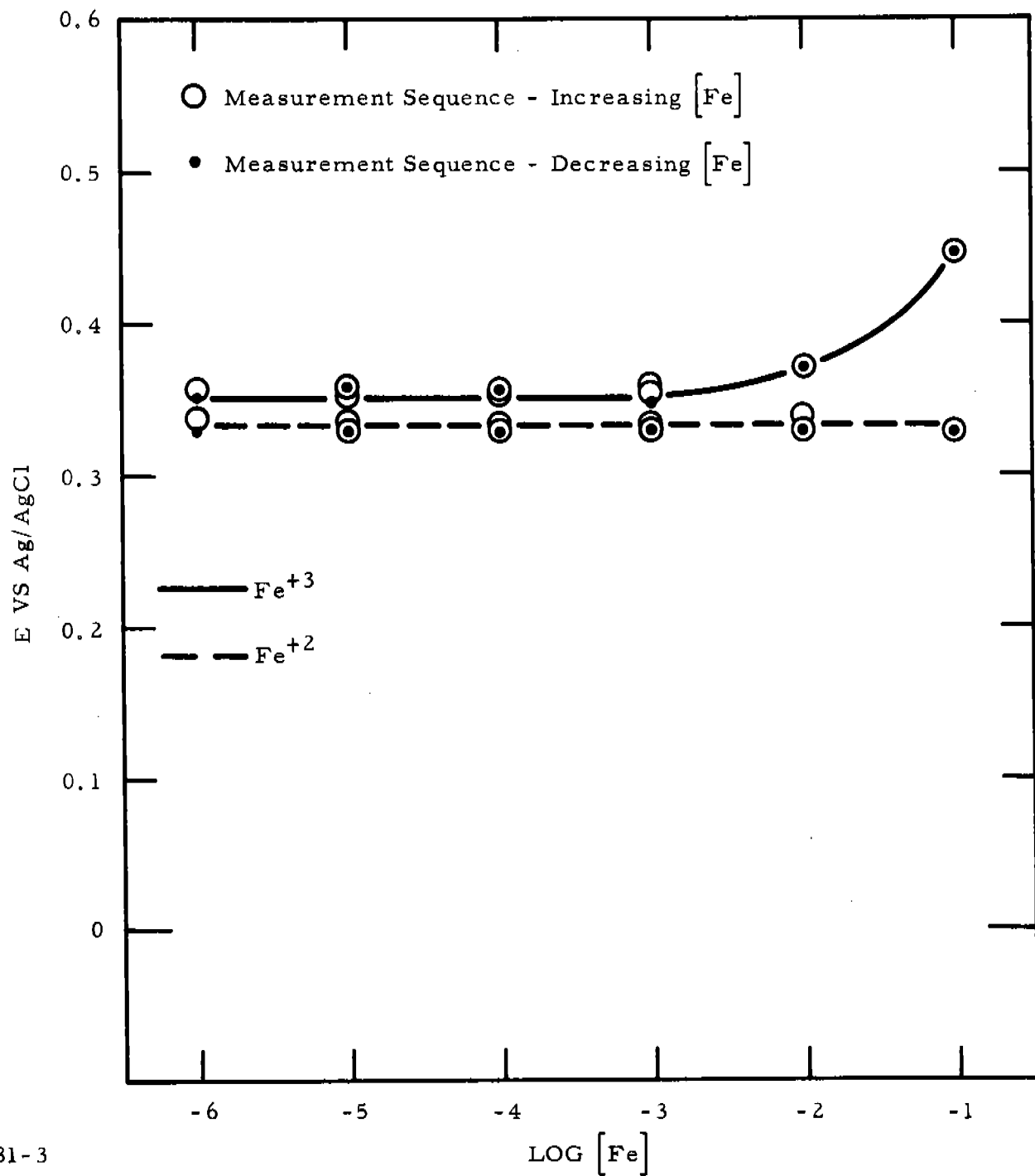
5552-1

Figure 18 Effect of $[\text{Fe}^{+3}]$ and $[\text{Fe}^{+2}]$ Concentrations and Measurement Sequence on the Potential of an FeSe-Epoxy Electrode. (All solutions are 0.1 M in KNO_3 and $\text{pH} = 1.6$.)



5581-4

Figure 19 Effect of [Fe⁺³] and [Fe⁺²] Concentrations and Measurement Sequence on the Potential of an FeSe₂-Epoxy Electrode. (All solutions are 0.1 M in KNO₃ and pH = 1.7.)



5581-3

Figure 20 Effect of $[Fe^{+3}]$ and $[Fe^{+2}]$ Concentrations and Measurement Sequence on the Potential of an FeTe-Epoxy Electrode. (All solutions are 0.1 M in KNO_3 and $pH = 1.7$.)

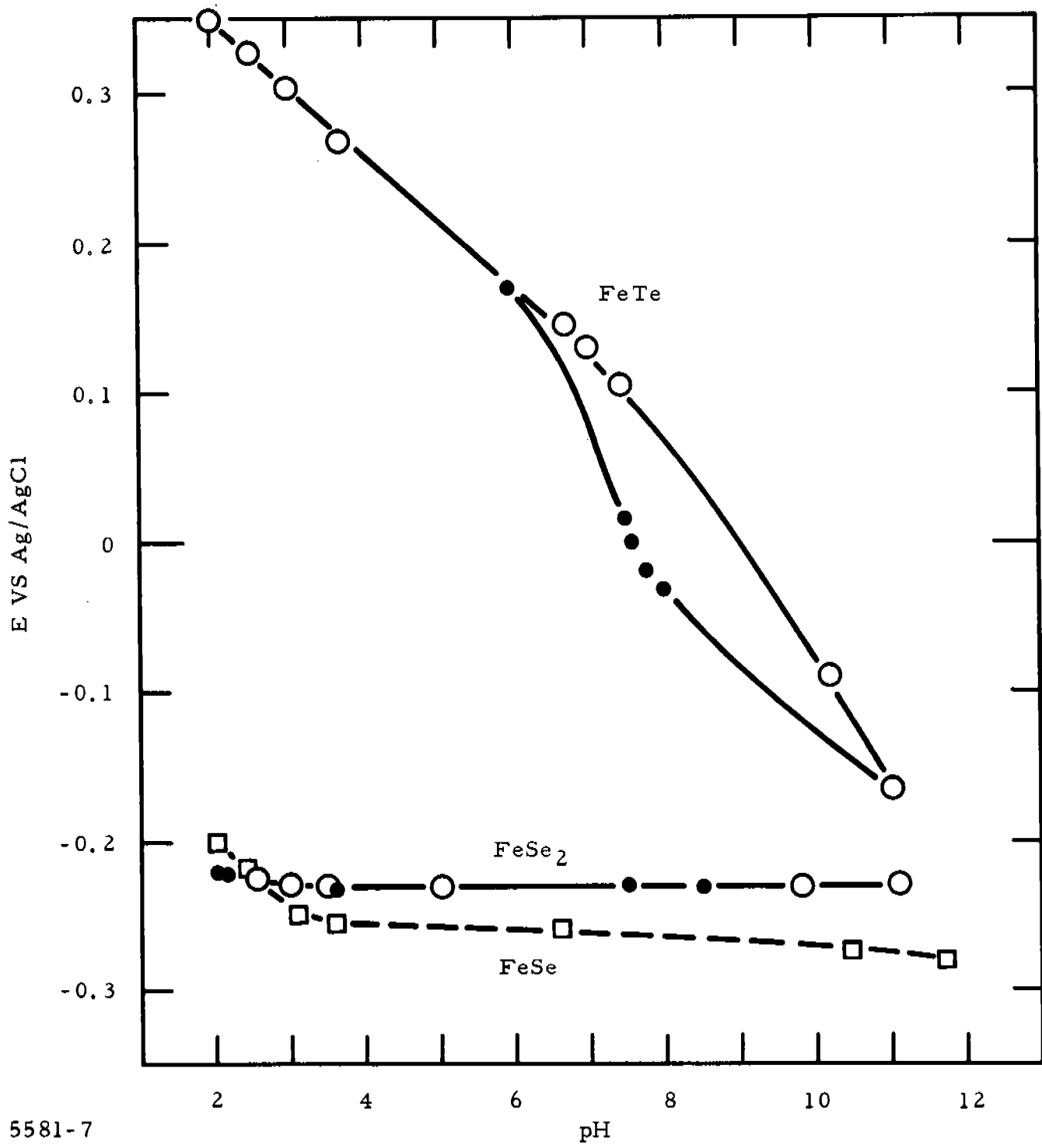


Figure 21 Effect of pH on the Potential of FeTe-, FeSe₂-, and FeSe-Epoxy Electrodes. (Solutions of 0.1 M KNO₃ made acidic and basic with HNO₃ and KOH.)

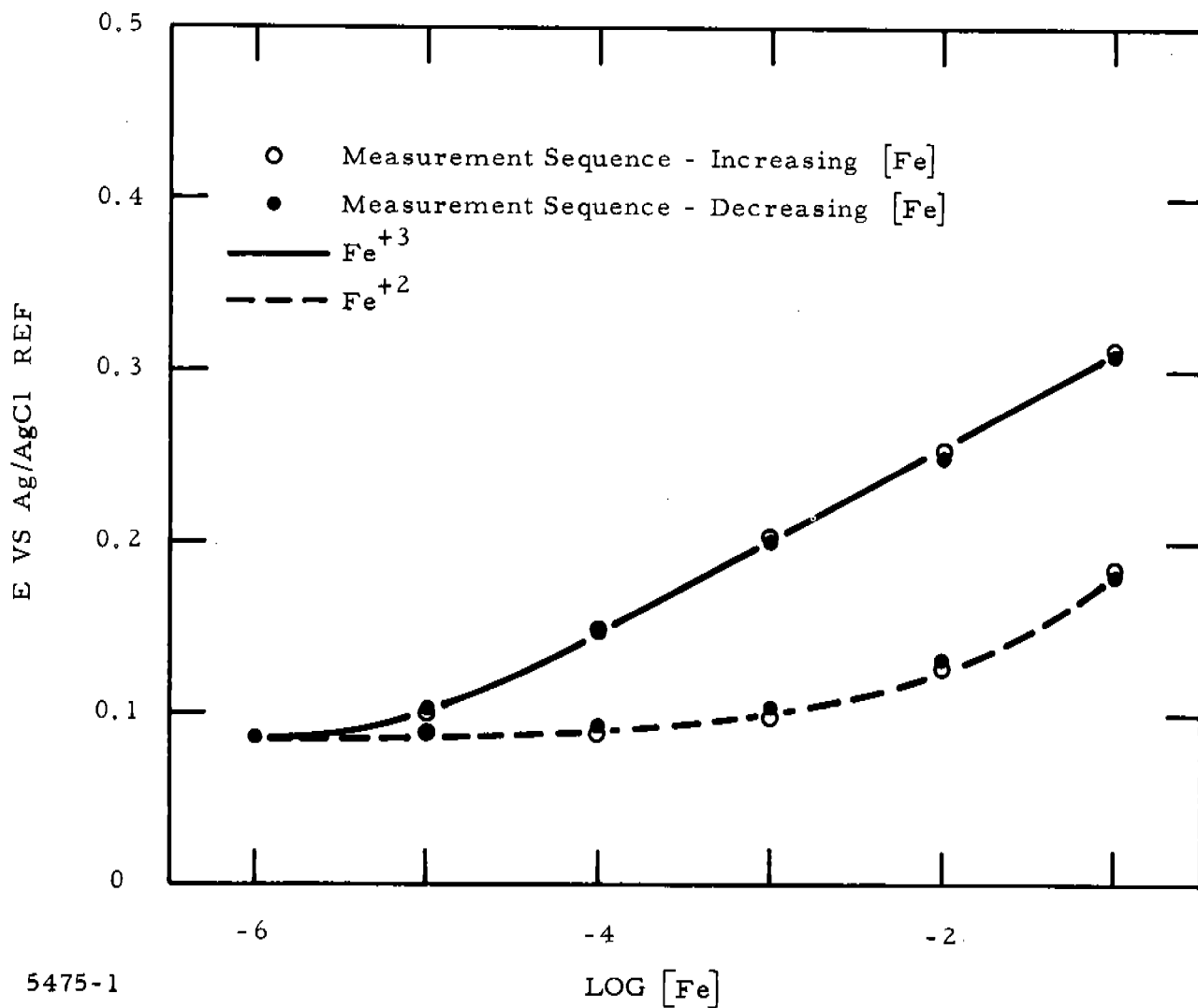
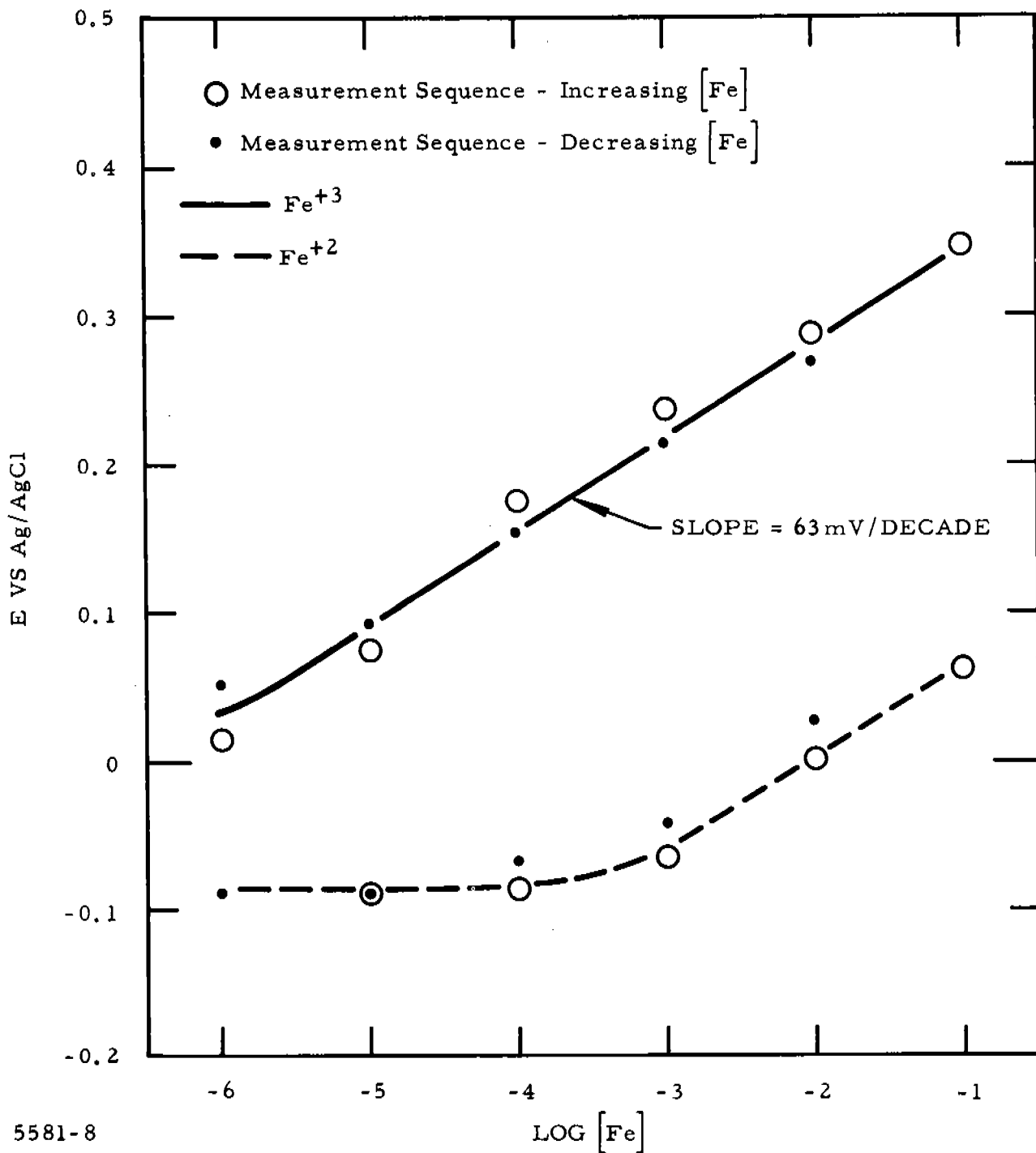
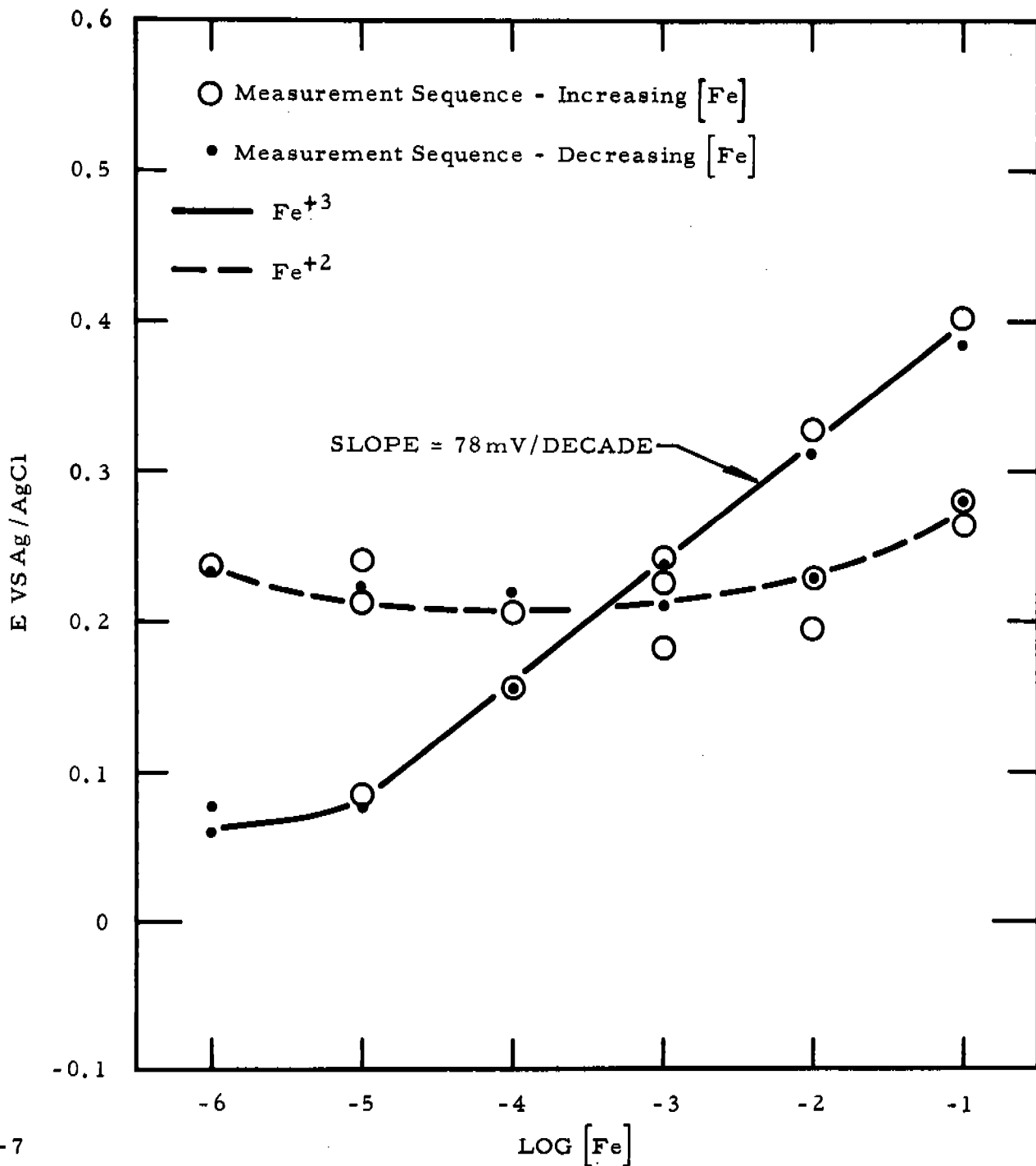


Figure 22 Effect of $[Fe^{+3}]$ and $[Fe^{+2}]$ Concentrations and Measurement Sequence on the Potential of a 0.8 Mole % FeO-1173 Glass Electrode. (All solutions are 0.01 M in KNO_3 and pH = 1.67.)



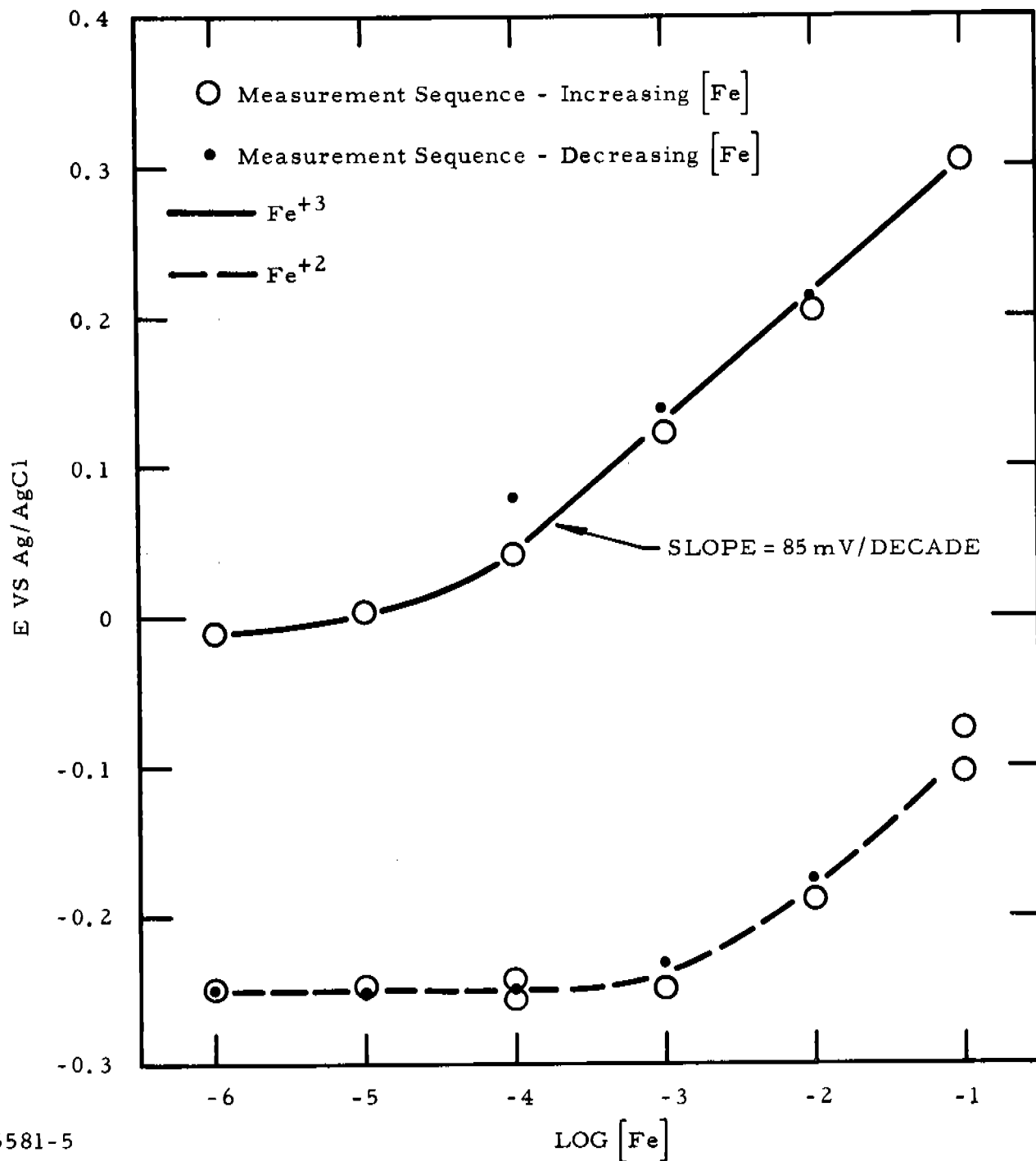
5581-8

Figure 23 Effect of $[\text{Fe}^{+3}]$ and $[\text{Fe}^{+2}]$ Concentrations and Measurement Sequence on the Potential of a 1.62 Mole % Fe^0 -1173 Glass Electrode. (All solutions are 0.1 M in KNO_3 and $\text{pH} = 1.7$.)



5581-7

Figure 24 Effect of $[Fe^{+3}]$ and $[Fe^{+2}]$ Concentrations and Measurement Sequence on the Potential of a 2.0 Mole % Fe^0 -1173 Glass Electrode. (All solutions are 0.1 M in KNO_3 and $pH = 1.7$.)



5581-5

Figure 25 Effect of [Fe⁺³] and [Fe⁺²] Concentrations and Measurement Sequence on the Potential of a 2.39 Mole % Fe⁰-1173 Glass Electrode. (All solutions are 0.1 M in KNO₃ and pH = 1.7.)

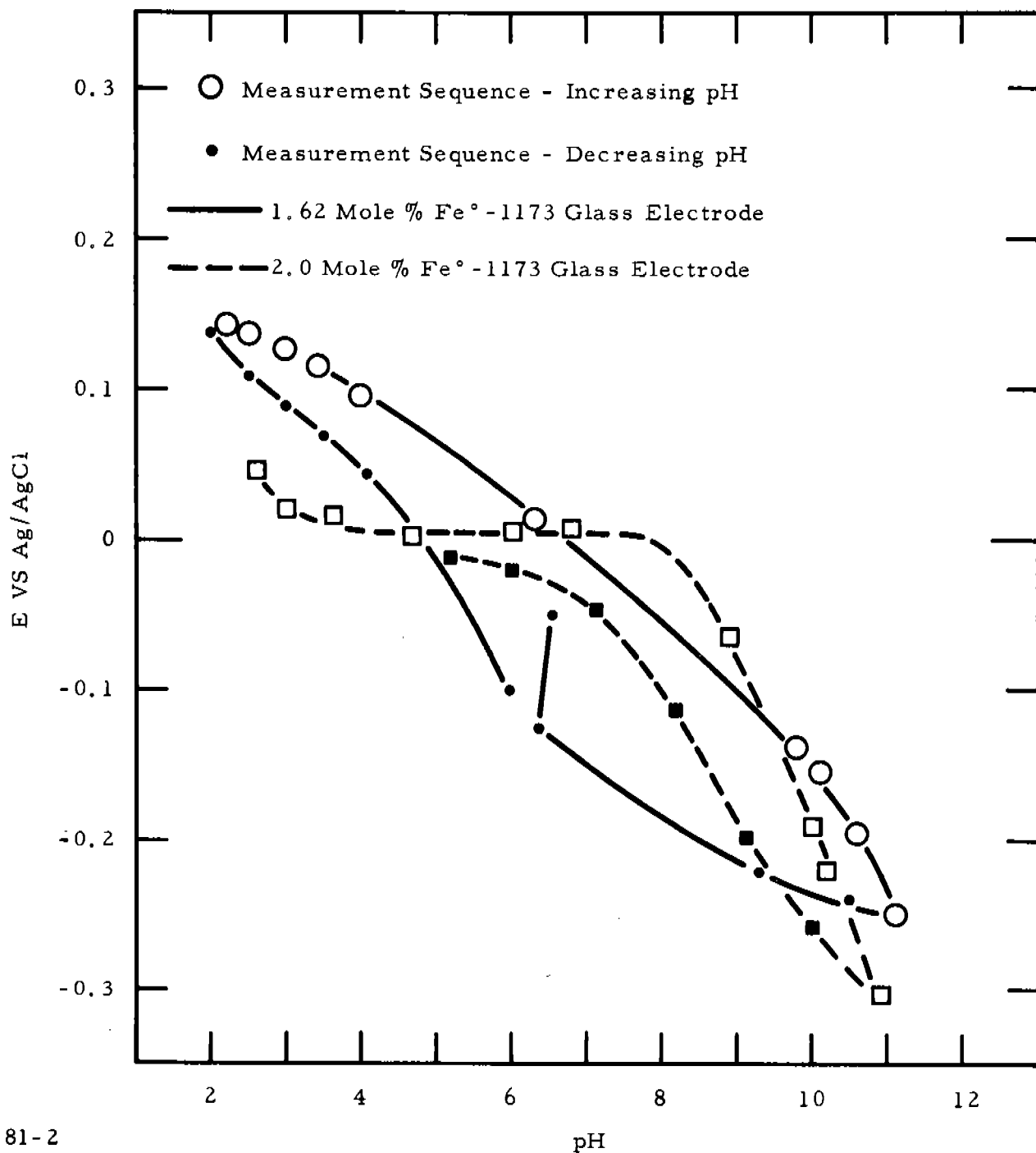
general trend is noted: as the Fe^0 content in the glass increases, the $\Delta E/\Delta \log [\text{Fe}^{+3}]$ increases. The larger than Nernstian response observed for the more concentrated Fe^0 -1173 glass electrodes is not fully understood at this time.

Experiments performed with the 0.8 mole % Fe^0 -1173 glass electrode in 1.0 M $\text{K}_2\text{C}_2\text{O}_4$ solutions with varying concentrations of Fe^{+3} indicated that the addition of strong complexing agents completely suppresses electrode response. These results support the contention that the potential is developed by free, uncomplexed Fe^{+3} .

The Fe^0 -1173 glass electrodes are essentially non-responsive to Fe^{+2} . Potential responses recorded at the higher Fe^{+2} concentration levels are attributed to Fe^{+3} present as a contaminant at concentrations < 1% of the Fe^{+2} .

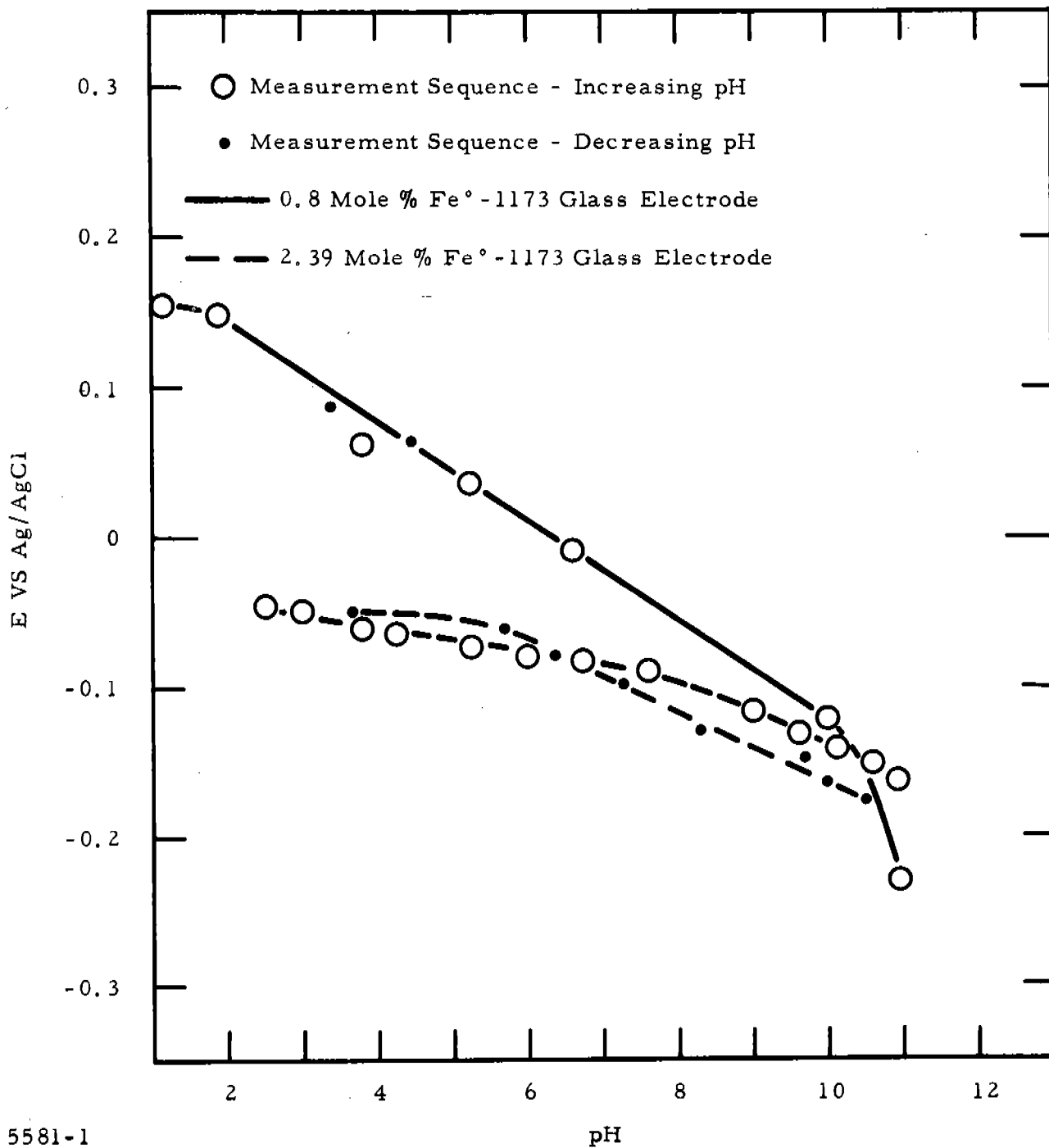
Figures 26 and 27 show the effect of pH on the electrode potential for the four Fe^0 -doped glasses. As noted, a significant pH response is exhibited by the 0.8 and 1.62 mole % Fe^0 -1173 glass electrodes, but as the Fe^0 concentration in the glass is increased, the pH response decreases. The decrease in potential at high pH's is common regardless of the dopant used in the glass. The surface of the glass is attacked by highly alkaline solutions. If the alkalinity is high enough, dissolution of the glass is visible. The response of an Fe^0 -1173 glass electrode to changing Fe^{+3} concentration is usually tested by removing the electrode from the previous test solution, rinsing it with deionized water, wiping it gently with a Kimwipe, and placing it in the next test solution. It is possible that in this procedure the surface of the electrode is altered slightly, giving rise to a slight scatter in our experimental data. Therefore, experiments were performed in which the 1.62 and 2.39 mole % Fe^0 -1173 glass electrodes were not removed from solutions during a run, but were allowed to remain in the solutions overnight. Aliquots of test solution were continually removed and replaced with aliquots of more concentrated Fe^{+3} solution or of 0.1 M KNO_3 containing no Fe^{+3} to increase or decrease the concentration of Fe^{+3} . The resulting Fe^{+3} concentration-potential plot is shown in Figure 28 for the 2.39 mole % Fe^0 -1173 glass electrode. Figure 29 shows time-response behavior observed in going to more concentrated Fe^{+3} solutions and to more dilute solutions. Overall, the potential response to changing Fe^{+3} concentration is sharp, and equilibrium is established in two to four minutes.

The effect of pH, $[\text{Fe}^{+3}]$, and $[\text{Fe}^{+2}]$ on the potential of a 2.5% Fe^0 -1173 glass electrode was measured. A potential response of 35 to 50 mV per pH unit was observed between pH 3 and pH 9. At more acidic and more basic pH's the response increased. The electrode did not respond to Fe^{+2} concentration. With Fe^{+3} , the $E - \log [\text{Fe}^{+3}]$ behavior was poorer than that observed for most



5581-2

Figure 26 Effect of pH on the Potential of Fe⁰-1173 Glass Electrodes. (Solutions of 0.1 M KNO₃ made acidic and basic with HNO₃ and KOH.)



5581-1

Figure 27 Effect of pH on the Potential of Fe⁰-1173 Glass Electrodes. (Solutions of 0.1 M KNO₃ made acidic and basic with HNO₃ and KOH.)

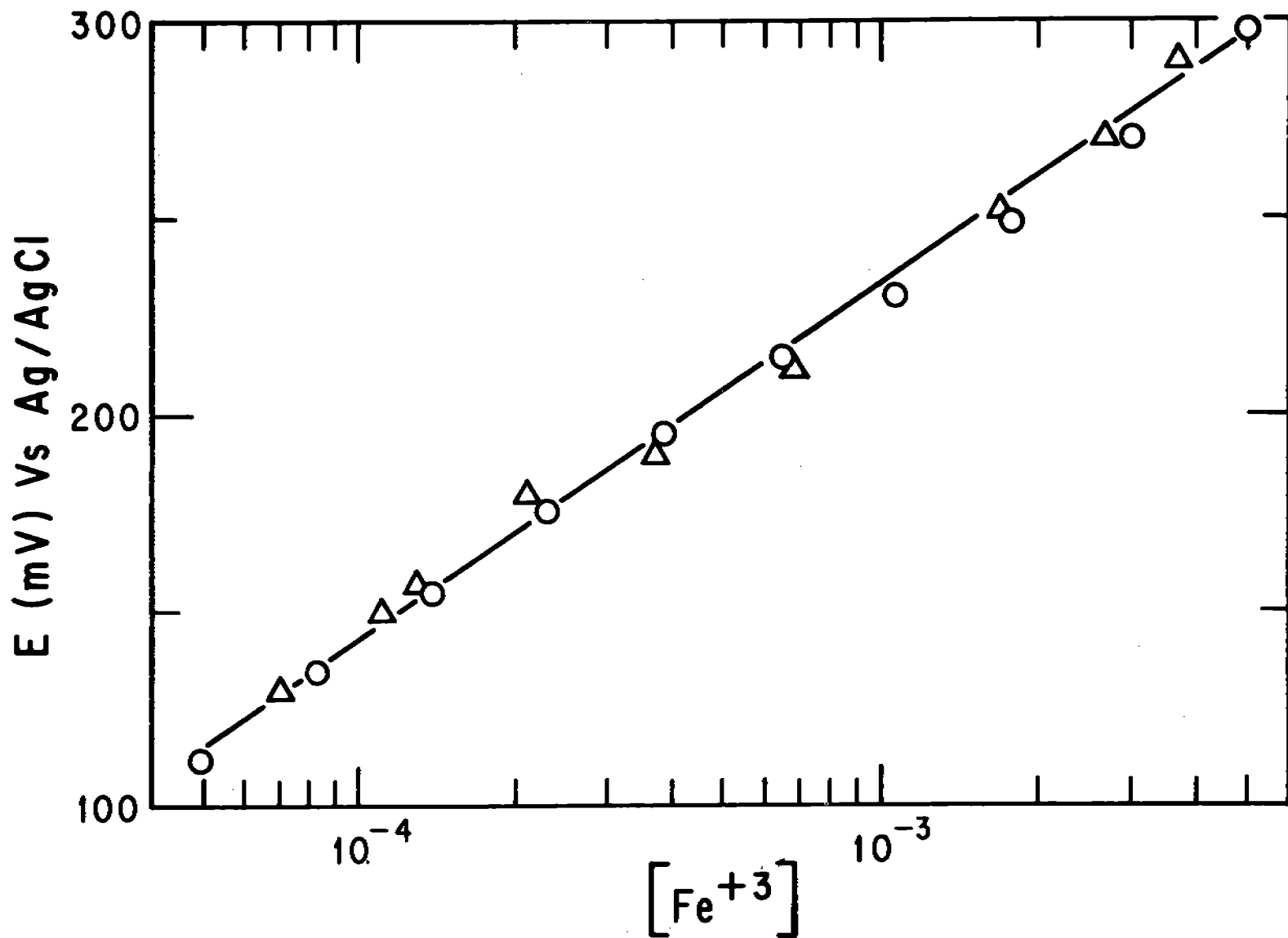
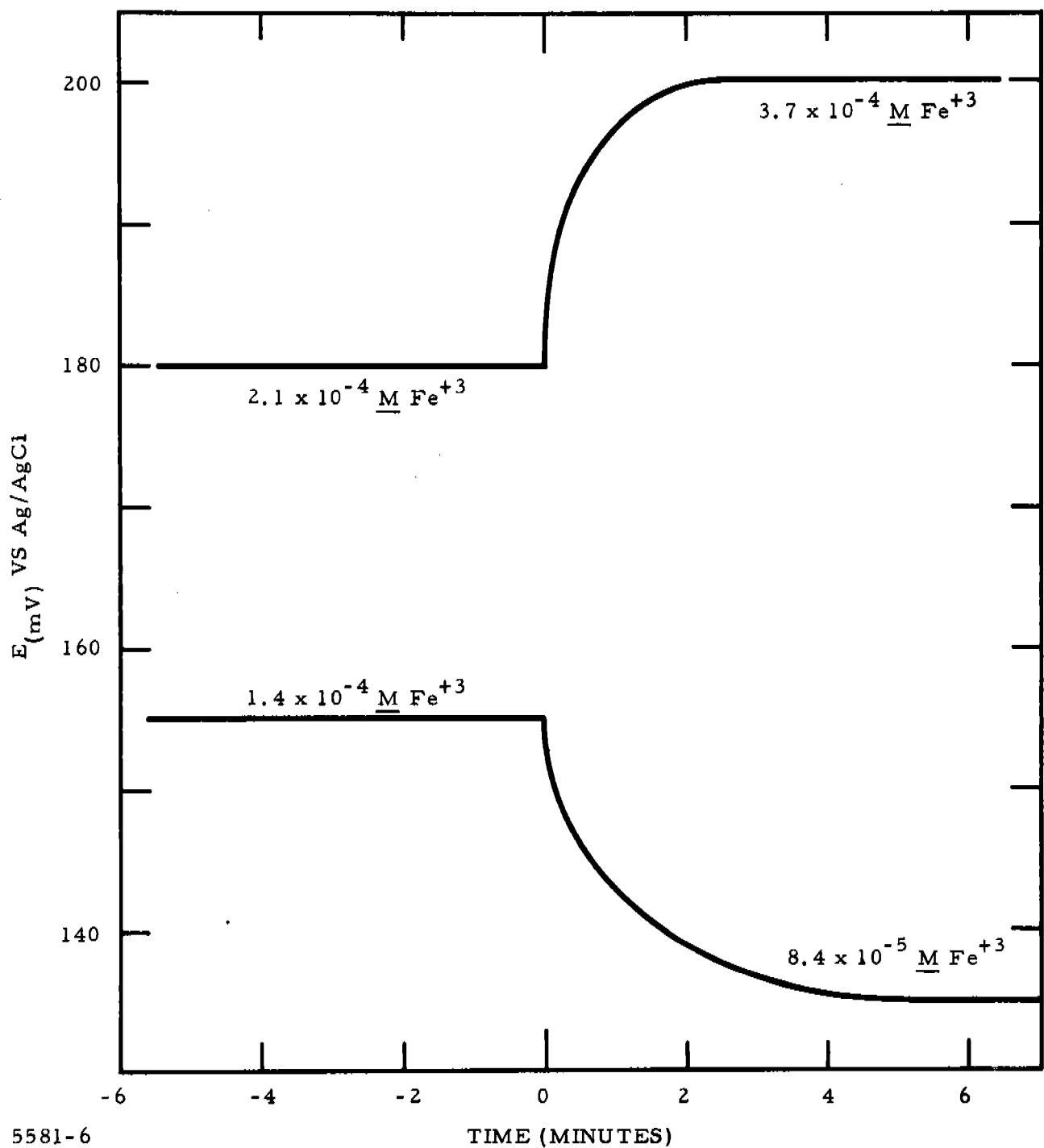


Figure 28 Effect of Varying the Fe^{+3} Concentration without Removing the 2.39 Mole % Fe^0 -1173 Glass Electrode from the Test Solution. (Solution was 0.1 M KNO_3 and pH = 1.7.)



5581-6

Figure 29 2.39 Mole % Fe^0 -1173 Glass Electrode Response Times for Changing $[\text{Fe}^{+3}]$

of the Fe-doped 1173 glass electrodes. There was no linear region in the curve, and the electrode was sensitive only to Fe^{+3} concentrations down to 10^{-4} M. For the Fe^0 -doped 1173 glasses, the optimum doping level for potential stability, response time characteristics, and Nernstian behavior is in the neighborhood of 2.0 mole % Fe^0 -1173.

2.0 mole % Fe^0 -1173 glass in the membrane configuration and the electrode configuration (Figure 13) was tested for potential response to Fe^{+3} concentration. The results of these experiments are shown in Figure 30. The responses of the two configurations were identical except for the absolute values of the potentials measured. Both gave a potential response of 62 to 63 mV per decade change in Fe^{+3} concentration in the 10^{-5} M to 10^{-1} M range. Neither responded to changing Fe^{+2} concentration.

A 2.0 mole % Fe^0 -1173 glass membrane which had been soaked in deionized H_2O for five months was retested for its responsiveness to Fe^{+3} (Figure 31). The $E - \log [\text{Fe}^{+3}]$ curve is linear from $< 10^{-4}$ to 10^{-1} M Fe^{+3} and has a slope of 62 mV. The same membrane had been tested during the fourth quarter of 1968 and was reported in Figure 3 of the Fourth Quarterly Progress Report for this contract. At that time its response was linear from $< 10^{-5}$ M to 10^{-1} M Fe^{+3} and had a slope of 63 mV. Therefore, the range of the response to concentration has decreased by an order of magnitude.

A 1.62 % Fe^0 -1173 glass electrode prepared and tested on 17 September 1968 was retested on 18 July 1969 after soaking in deionized water for two months. The results of this experiment are shown in Figure 32. A slope of 57 mV was observed in the 10^{-4} M to 10^{-1} M Fe^{+3} range. During the original investigation, a slope of 61 mV in the 10^{-5} M to 10^{-1} M Fe^{+3} range was measured. Therefore, this electrode, like the 2% Fe^0 -1173 membrane, has decreased in sensitivity by an order of magnitude. Attempts to increase the sensitivity by etching the electrode surface with 10% NaH_2PO_4 -10% KOH and by placing the electrode in 0.1 M Fe^{+3} for 50 hours reduced the performance of the sensor. The 2.0% Fe^0 -1173 membrane mentioned above developed a crack and had to be discarded. However, it is concluded from these experiments that the Fe in the glass is not readily lost by diffusion into solution.

Several interference tests were made on the 1.62 and 2.0 mole % Fe^0 -1173 glass electrodes by measuring the electrode potential as the contaminant concentration varied and the test solution remained 0.1 M in KNO_3 , 0.001 M in Fe^{+3} , and at a pH of 1.6. Figure 33 shows the effect of the ions tested on the electrode potential of a 2.0 mole % Fe^0 -1173 glass electrode. The electrode potential was independent of concentration of Ca^{+2} , Ba^{+2} , Mg^{+2} , Cu^{+2} , and Zn^{+2} . Fe^{+2} and Mn^{+2} can also be added to this list on the basis of results of earlier tests.

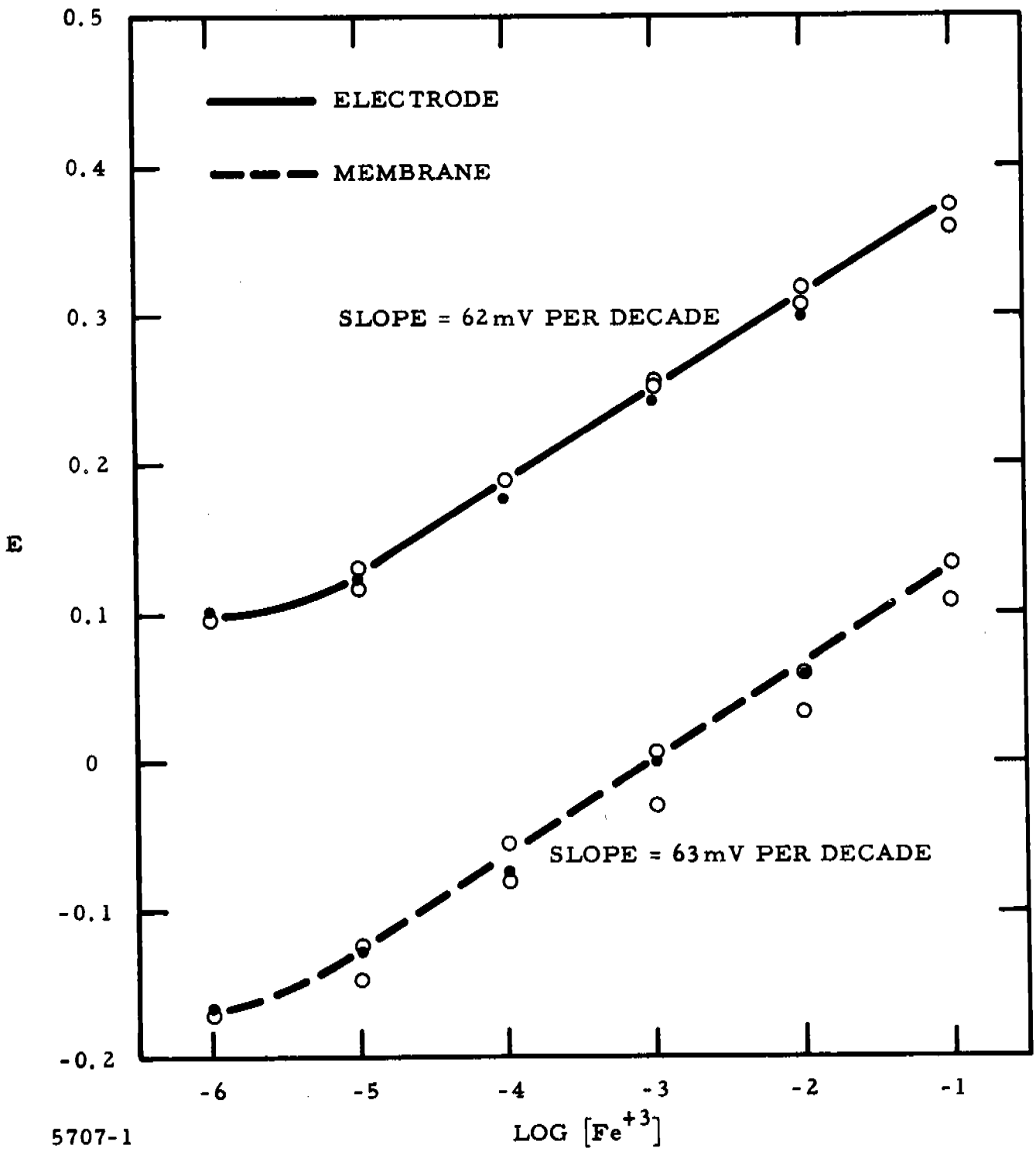
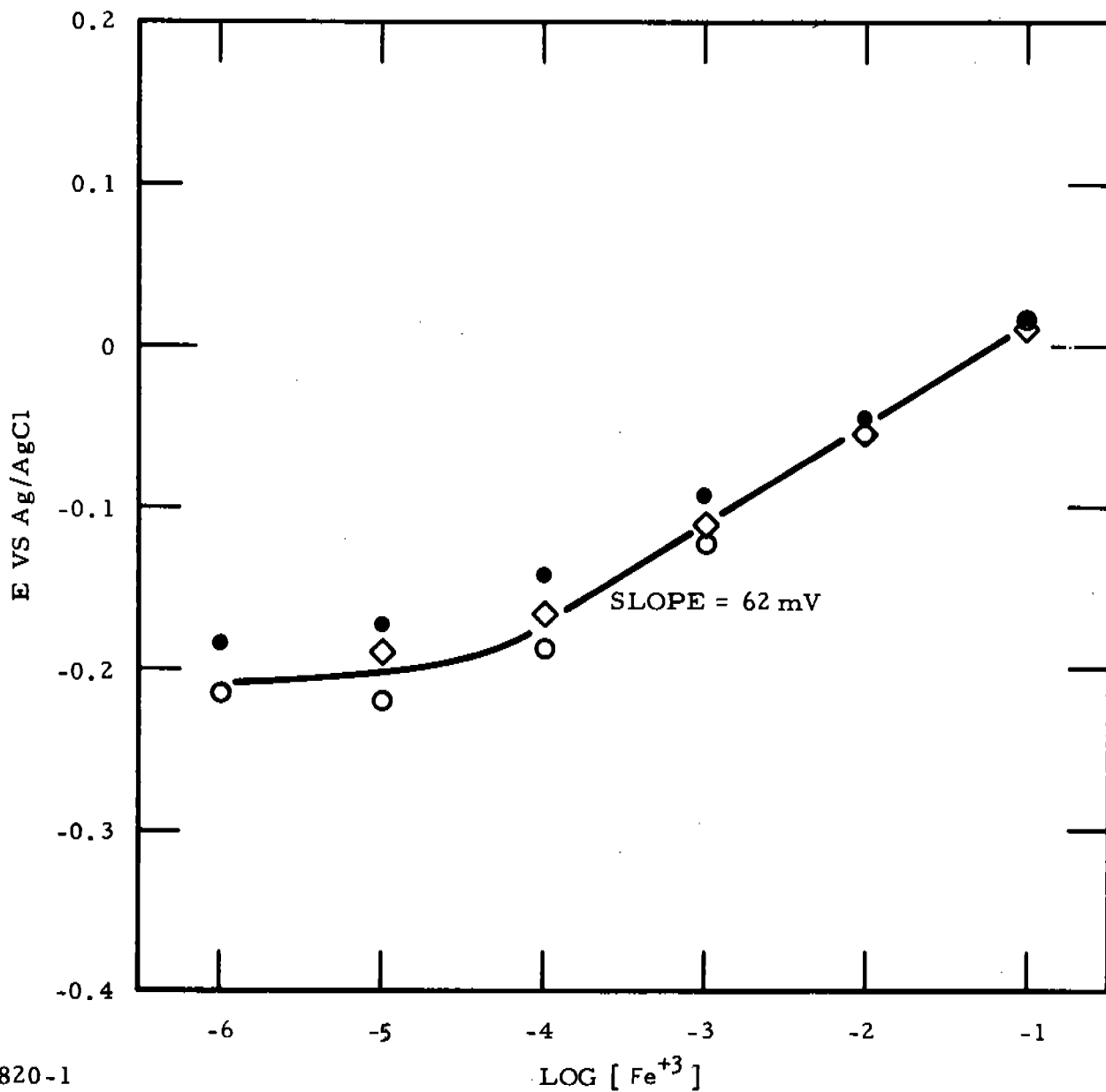


Figure 30 Potential Response of Electrode and Membrane of 2.0 Mole % Fe⁰-1173 Glass to Fe⁺³ Concentration. (All solutions are 0.1 M in KNO₃ and pH = 1.8.)



5820-1

Figure 31 Potential Response of 2.0 Mole % Fe⁰-1173 Glass Membrane to Fe⁺³ in 0.1 M KNO₃ at pH = 2.0 (Membrane soaked in deionized H₂O for 5 months.)

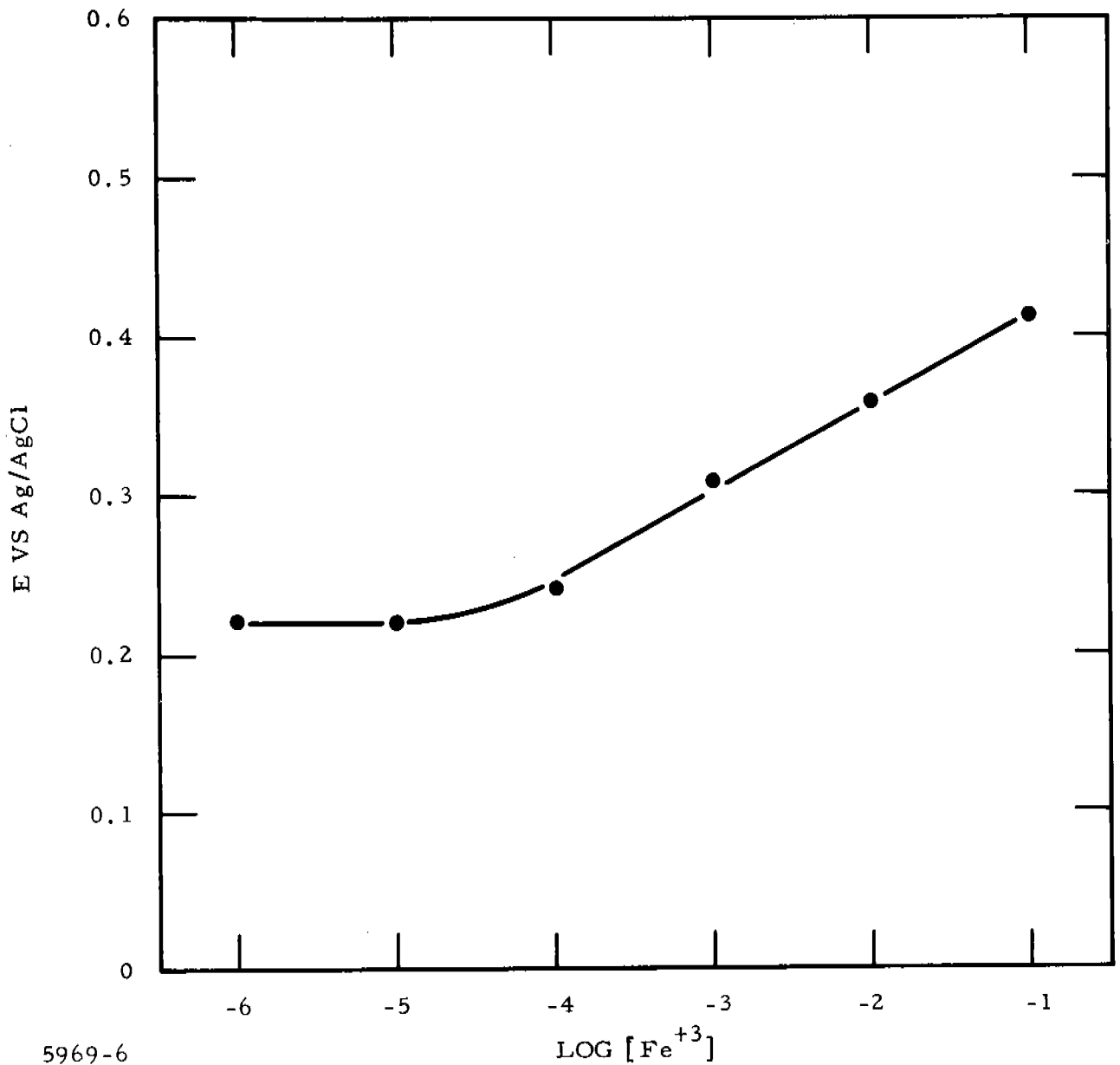


Figure 32 Potential Response of a 1.62 Mole % Fe⁰-1173 Glass Electrode to Fe³⁺. Electrode was prepared and tested on 17 September 1968 and was retested on 18 July 1969 after soaking in deionized water for two months.

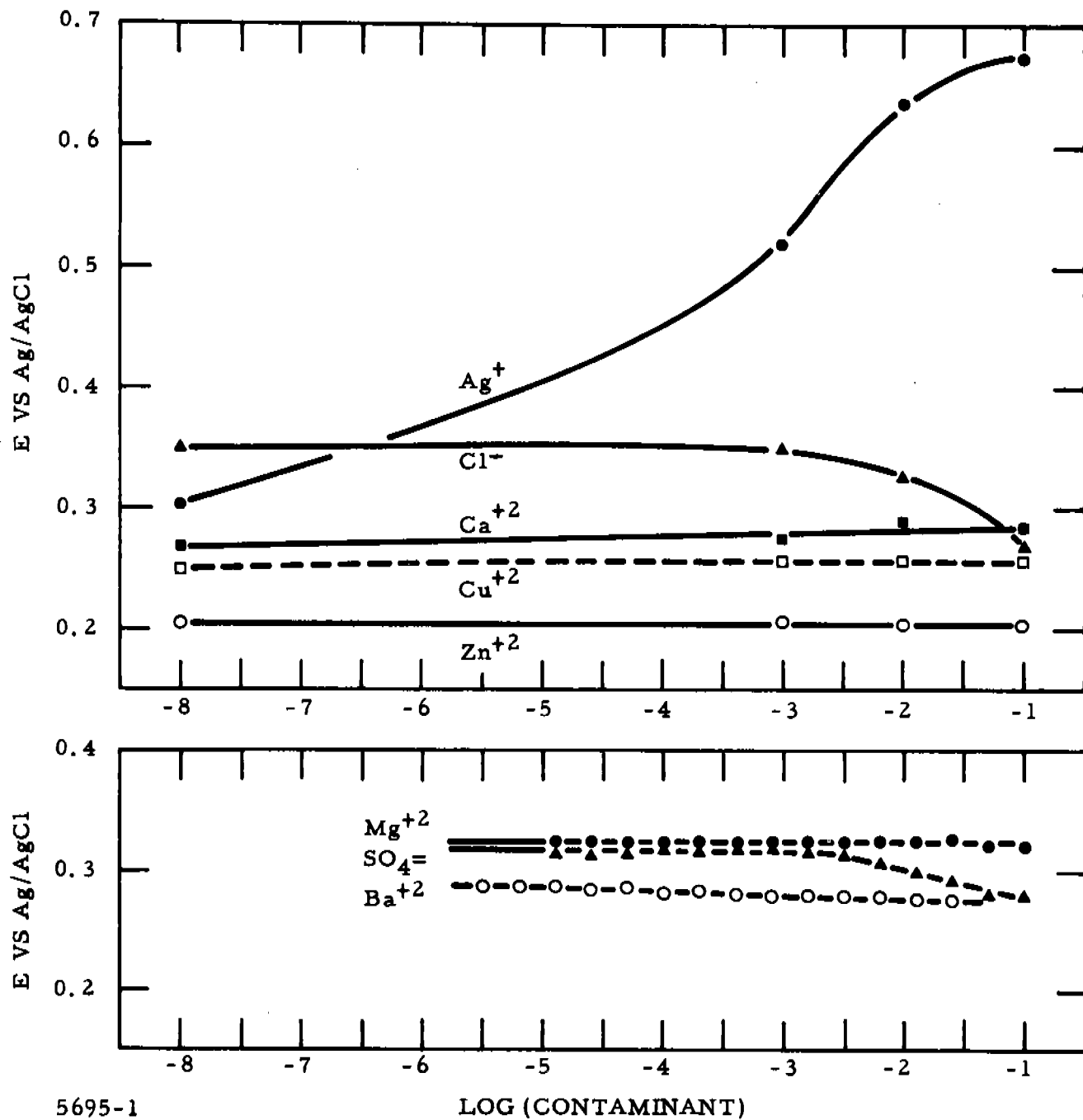


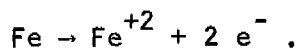
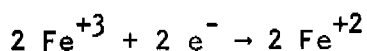
Figure 33 Effect of Contaminant Concentration on the Potential of a 2.0 Mole % Fe^0 -1173 Glass Electrode. (All solutions are 0.1 M in KNO_3 , 0.001 M in Fe^{+3} , and $pH = 1.6$.)

A large interference was observed when Ag^+ was present in solution and is believed to be due to the interaction of Ag^+ with selenium or selenide sites on the surface of the glass, similar to the potential response of the KI- and KCl-doped 1173 glasses to Ag^+ observed in the preliminary investigations of 1173 glasses.

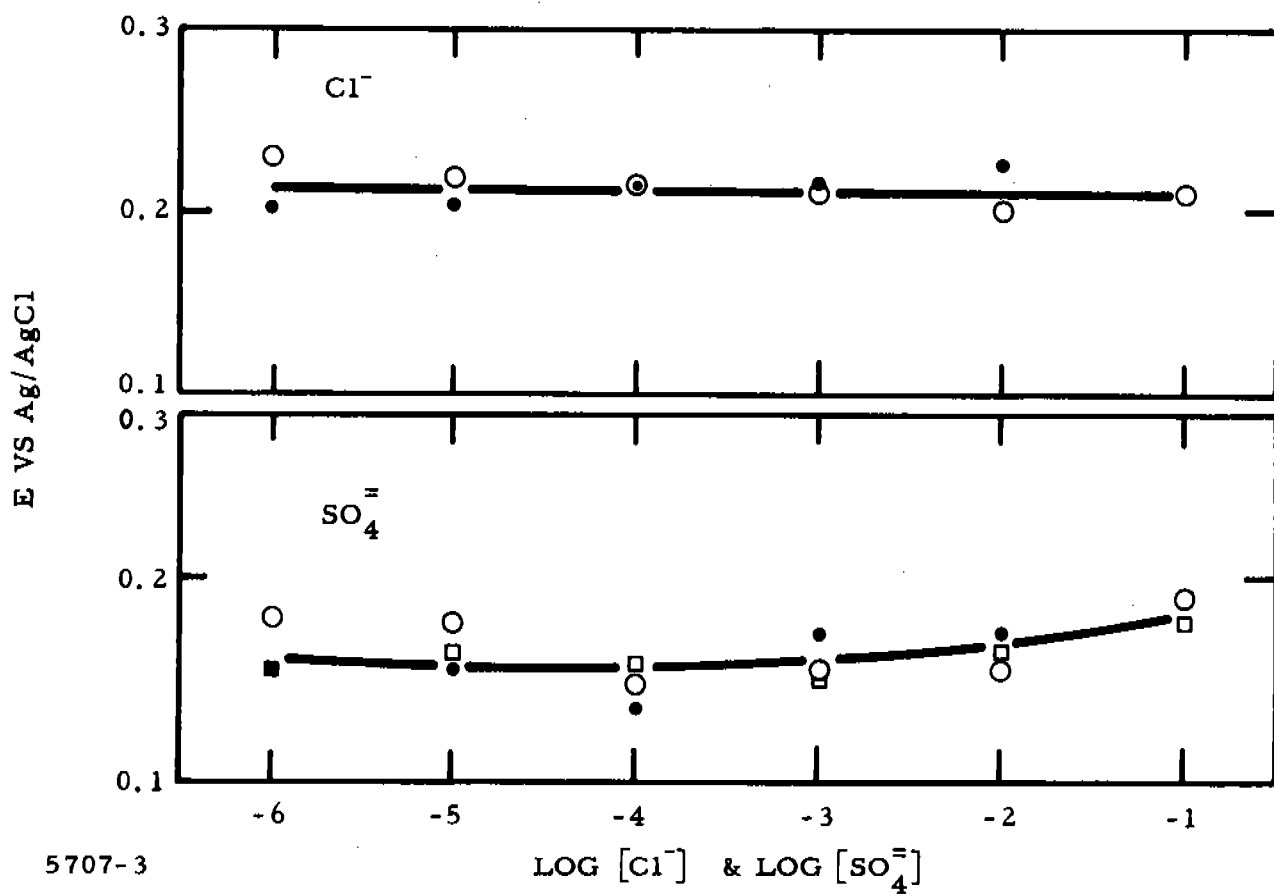
Cl^- and SO_4^{2-} also interfered when they were present at concentrations greater than 10^{-3} M. When Fe^{+3} was not present in the test solutions, the electrode potential was not dependent on the Cl^- or SO_4^{2-} concentration (Figure 34). Therefore, it is the complexing of the Fe^{+3} by the anions which interferes with the electrode potential of a 2.0 mole % Fe^0 -1173 glass electrode in a 0.001 M Fe^{+3} solution. This coordination shifts the electrode potential negatively, as would be predicted by the Nernst expression.

In the presence of excess Cl^- (1 M KCl), the potential response of Fe^{+3} is linear and yields a slope of 68 mV in the 10^{-4} to 10^{-1} M Fe^{+3} range (Figure 35). The electrode sensitivity has decreased by an order of magnitude.

Potential response experiments to this point indicate that the Fe in the Fe^0 -1173 glasses may be present as Fe^{+2} . The slope of 60 mV per decade change in Fe^{+3} concentration can be explained by a redox potential with Fe^{+2} representing the other half of the redox couple. If the Fe is present in 1173 as metallic Fe^0 , then the slope is not a simple Nernst equation calculation, and the potential exhibited is really a mixed potential based on the following two electrode reactions occurring simultaneously:



This type of behavior may explain the abnormally high slopes found for the 2.39 mole % Fe^0 -1173 glass electrodes and some of the 2.0 mole % Fe^0 -1173 glass electrodes. The clusters found in these glasses may be rich in elemental Fe. X-ray diffraction of the FeSe_2 used in the compound FeSe_2 -epoxy electrode indicates the presence of metallic Fe, and this electrode exhibited a slope of 212 mV.



5707-3

Figure 34 Effect of Cl⁻ and SO₄⁼ Concentration on the Electrode Potential of a 2.0 Mole % Fe⁰-1173 Glass Electrode when Fe⁺³ is not Present in Solution. (All solutions are 0.1 M in KNO₃ and pH = 1.8.)

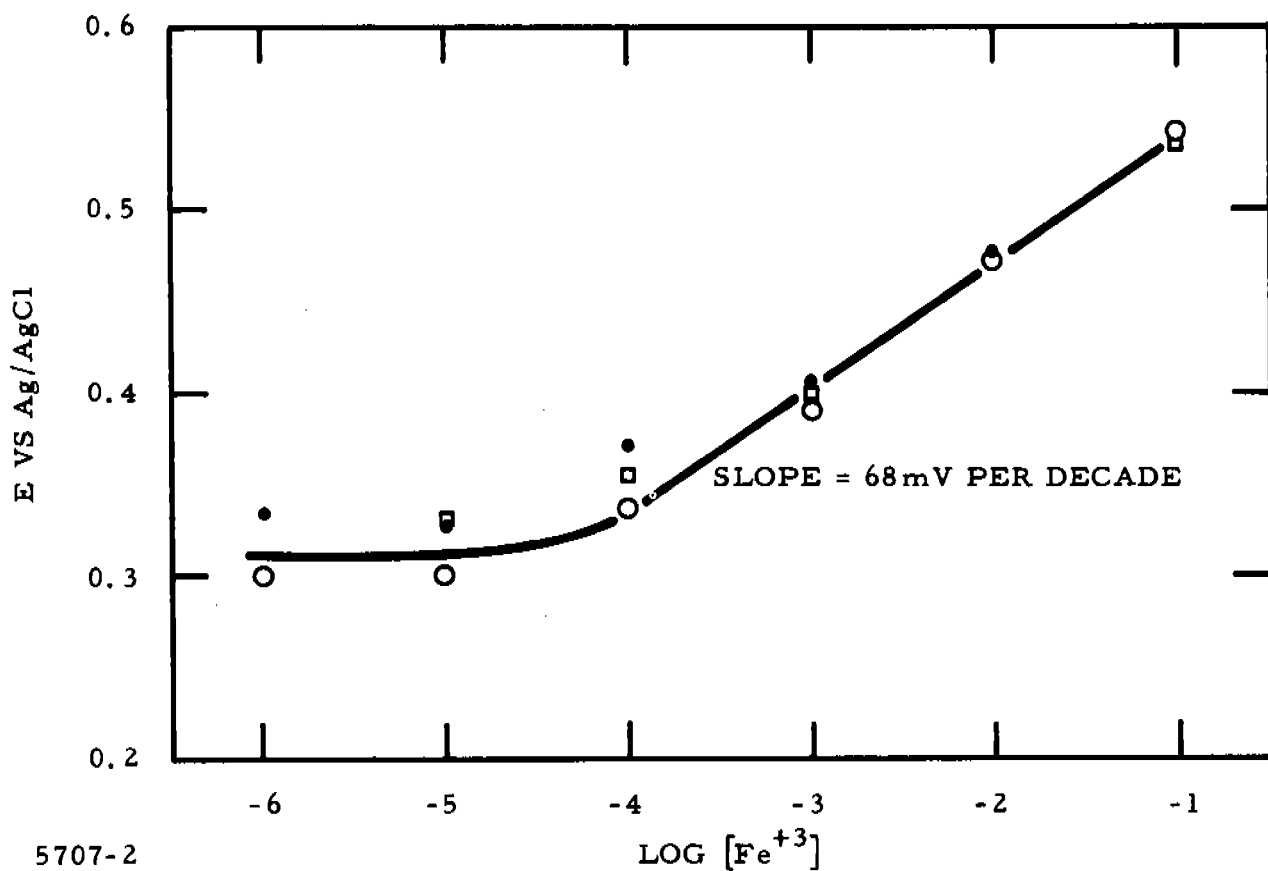


Figure 35 Response of 2.0 Mole % Fe⁰-1173 Glass Electrode to Fe³⁺ Concentration in an Excess Cl⁻ Medium. (All solutions are 1.0 M in KCl and pH = 1.7.)

If the electrode potential is due to a membrane potential and Fe^{+3} is present in the 1173 glass, then a 20 mV response per decade change in Fe^{+3} concentration is predicted from

$$E = \text{Constant} + \frac{2.3 RT}{nF} \log [\text{Fe}^{+3}],$$

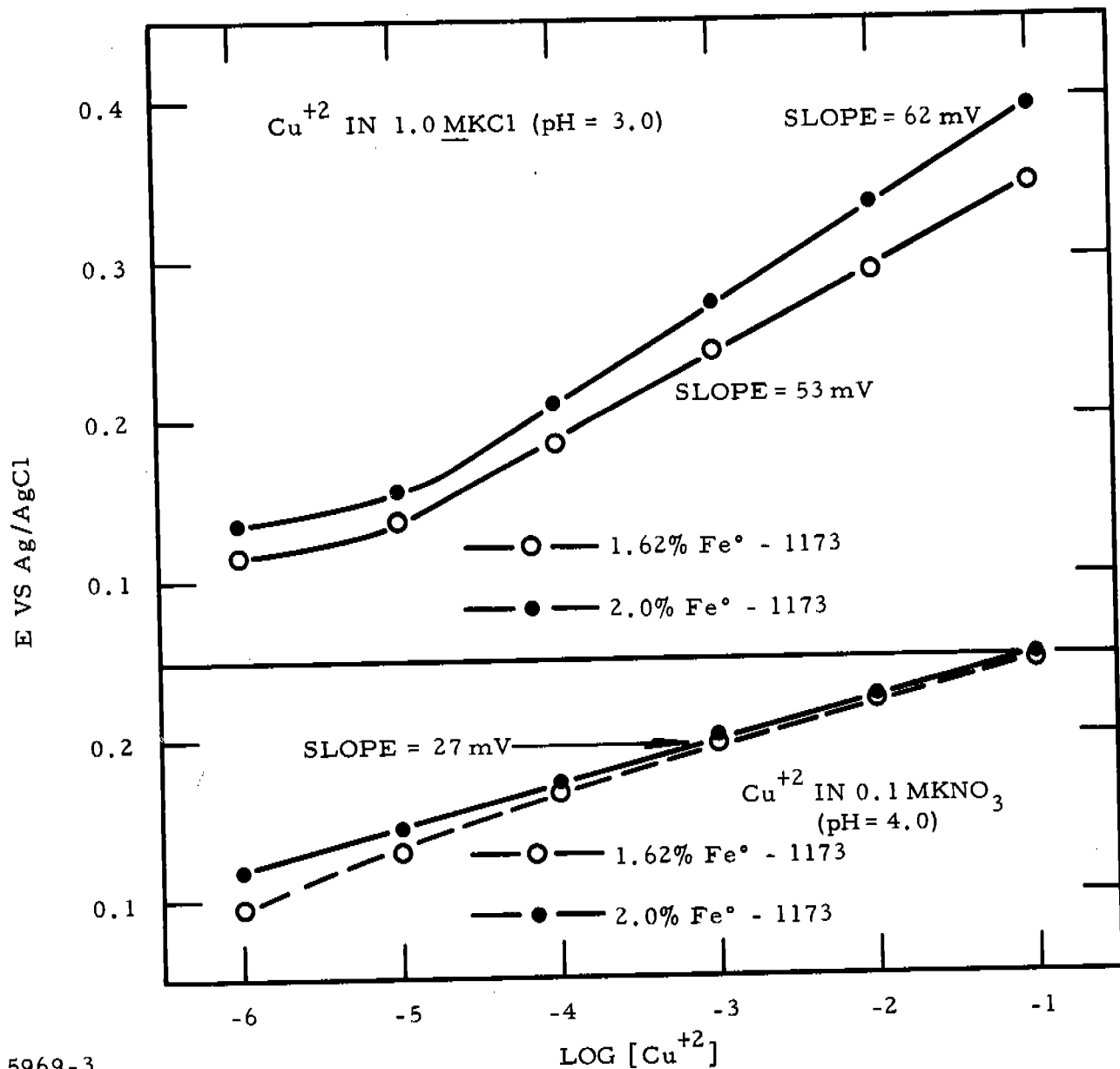
where $n = 3$, the oxidation state of the ion. A membrane potential with Fe^{+2} present in the 1173 glass is ruled out because none of the electrodes tested to date responds to Fe^{+2} .

Therefore, the potential response displayed by Fe-doped 1173 glasses with no clusters of elemental Fe^0 present is attributed to a redox potential with the Fe^{+2} half of the couple present in the 1173 glass.

The poor reproducibility of the 5 mole % FeSe_2 -1173 glass electrode to $\Delta[\text{Fe}^{+3}]$ raised the question of whether the potential response might be partly attributed to a surface phenomenon -- perhaps a reaction between Fe^{+3} and the Se of the glass. Therefore, some non-iron-containing 1173 glasses were tested for potential response to changing Fe^{+3} concentration. It was concluded that the 1173 glass itself exhibits a potential response to $\Delta[\text{Fe}^{+3}]$.

In view of the potential responses of Fe-doped 1173 glasses and some non-iron-containing glasses to Fe^{+3} , some doped-1173 glass electrodes were evaluated as sensors for other reversible redox systems.

Electrodes of 1.62% Fe^0 -1173 and 2.0% Fe^0 -1173 were tested for potential responses to Fe^{+3} , Cu^{+2} (in a NO_3^- medium), Cu^{+2} (in a Cl^- medium), Sn^{+4} , Ce^{+4} , and PO_4^{\equiv} . Both electrodes responded to Fe^{+3} . The potential behavior of the electrodes to Cu^{+2} in NO_3^- and Cl^- media is shown graphically in Figure 36. The slopes of the $E - \log [\text{Cu}^{+2}]$ curves for Cu^{+2} in 0.1 M KNO_3 (27 mV) are those that would be expected for a $2e^-$ redox process or an ion exchange reaction involving a cation with a +2 charge. In the Cl^- medium, slopes of 53 mV and 62 mV for the 1.62% Fe^0 -1173 and 2.0% Fe^0 -1173 respectively, are indicative of a $1e^-$ redox process, especially in light of the fact that Cu^{+1} is known to be stable in an excess Cl^- medium. This redox type behavior for Cu^{+2} supports further the $1e^-$ redox potential mechanism for Fe^{+3} . For the Ce^{+4} solutions, a sigmoidally shaped curve was obtained. The Fe-doped 1173 glass electrodes were not responsive to Sn^{+4} or PO_4^{\equiv} .



5969-3

Figure 36 Potential Response of 1.62 Mole % Fe^0 -1173 and 2.0 Mole % Fe^0 -1173 Glass Electrodes to Cu^{+2} in Cl^- and NO_3^- Media

Because the periodic properties of Co and Ni were similar to those of Fe, electrodes of 1.5% Co⁰-1173 and 1.5% Ni⁰-1173 were prepared. These electrodes were found to be insensitive to Ni⁺² and Co⁺², but were responsive to pH (40 mV/pH unit from pH 1.5 to pH 10) and Fe⁺³ concentration. The potential response to Fe⁺³ was over the entire concentration range tested (10⁻⁶ M to 10⁻¹ M Fe⁺³) and approached a linear Nernstian response in the 10⁻⁵ M to 10⁻¹ M Fe⁺³ range (Figure 37).

Figures 38 and 39 show the response of the 1.5% Ni⁰-1173 and 1.5% Co⁰-1173 electrodes to Cu⁺² in NO₃⁻ and Cl⁻ media. In a NO₃⁻ medium, the response to Cu⁺² is linear in the 10⁻⁵ M to 10⁻¹ M range with a slope of ~ 30 mV. In a Cl⁻ medium, the slope increased to 44 or 54 mV, depending on the sequence of measurements. Like those for the Fe-doped 1173 electrodes, these results indicate that the potential determining process shifts from a 2e⁻ mechanism to a 1e⁻ mechanism in going from a NO₃⁻ medium to a Cl⁻ medium.

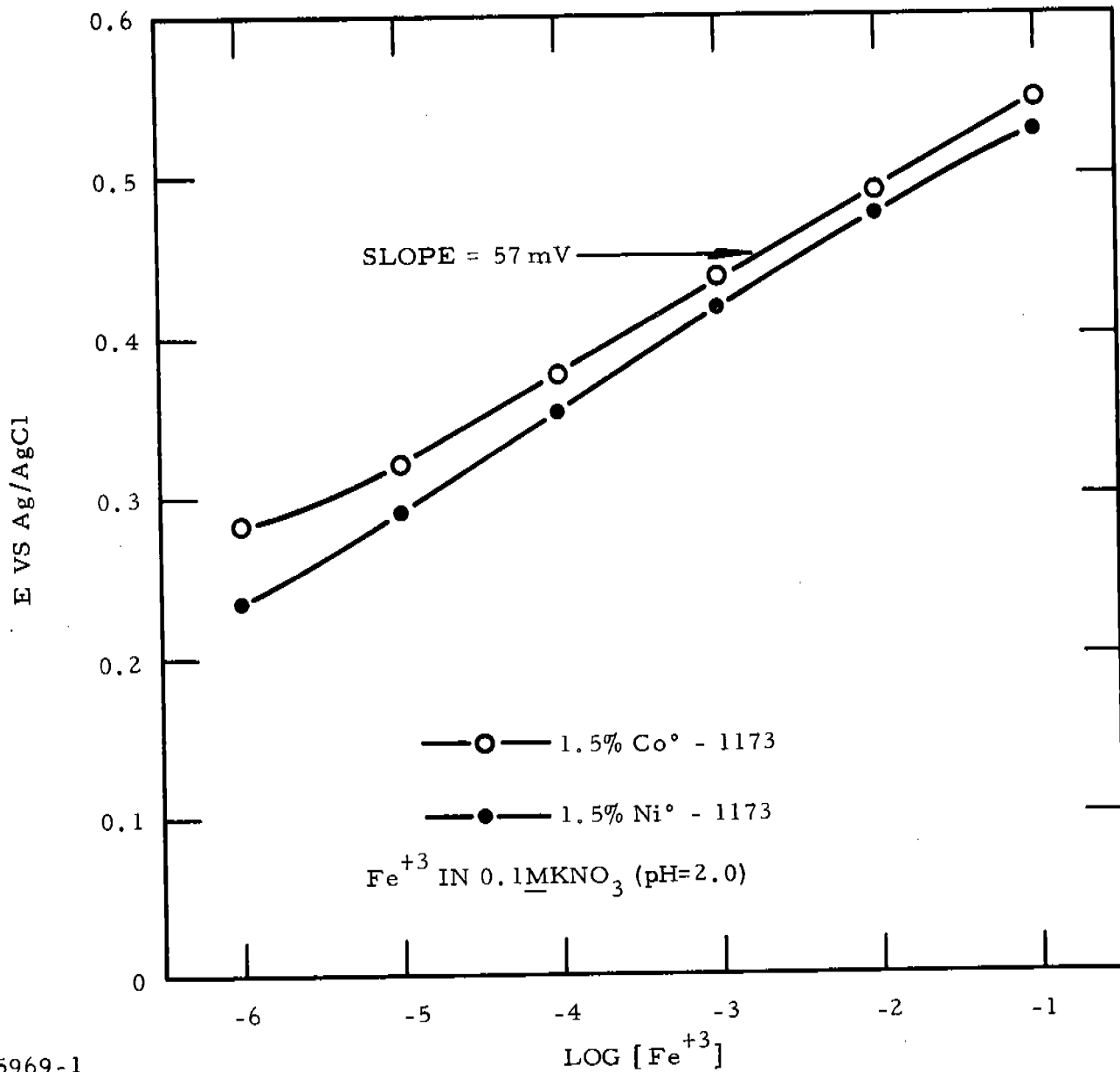
The 1.5% Ni⁰-1173 and 1.5% Co⁰-1173 electrodes were also tested for potential responses to Hg⁺² and PO₄⁼. A sigmoidal E - log [Hg⁺²] curve with the inflection point between 10⁻⁴ and 10⁻³ M Hg⁺² was obtained for Hg⁺². The electrode was insensitive to [PO₄⁼].

A 0.5% Ni⁰-1173 sensor exhibited the same potential response pattern as the 1.5% Ni⁰-1173 sample, but the sensitivity decreased.

B. Mn⁺² Sensors

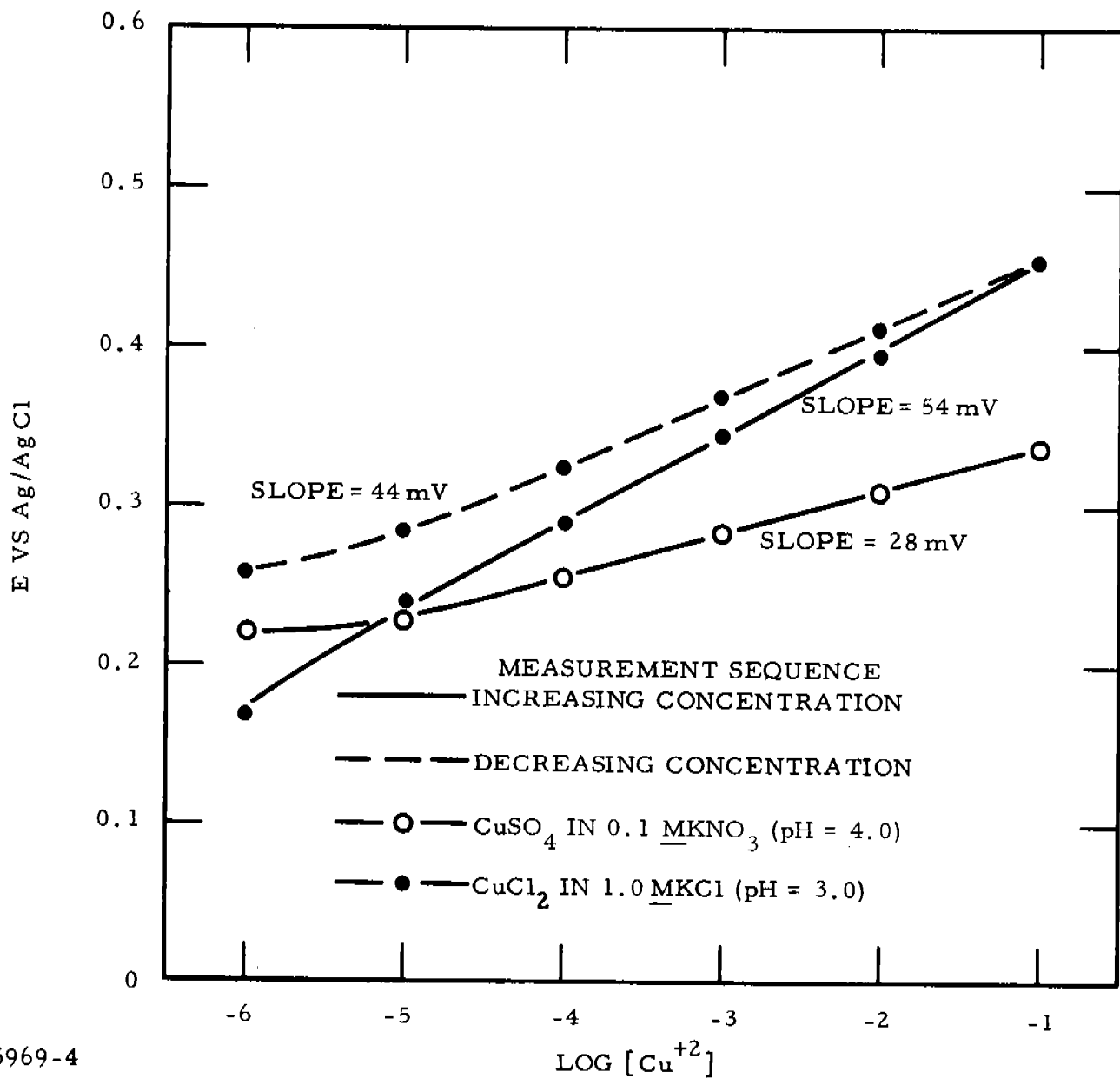
Electrodes and/or membranes of 1.0% MnCl₂-1173, 2.0% MnO₂-1173, 2.0% MnSe-1173, 5.0% MnSe-1173, 0.8% Mn⁰-1173, 1.62% Mn⁰-1173, 2.0% Mn⁰-1173, and 4.0% Mn⁰-1173 were evaluated for potential responses to changing Mn⁺² concentrations. None exhibited a potential dependence on Mn⁺². Of these samples, only the 5.0% MnSe-1173 and the 4.0% Mn⁰-1173 had resistivities in the desirable range (< 10⁸ Ω-cm).

Attempts were made to activate the 2.0 mole % Mn⁰-1173 glass so that it would give a potential response to Mn⁺² in solution. The activation process involved formation of low-resistance paths through the glass disk by probing the heated disk with an ac signal. However, this did not improve the potential-concentration behavior of the electrode. Although Mn in various oxidation states has been added to 1173, no encouraging results indicating sensing of Mn⁺²



5969-1

Figure 37 Potential Response of 1.5 Mole % Co^O -1173 and 1.5 Mole % Ni^O -1173 Glass Electrodes to Fe^{+3} .



5969-4

Figure 38 Potential Response of a 1.5% Ni⁰-1173 Glass Electrode to Cu²⁺ in NO₃⁻ and Cl⁻ Media

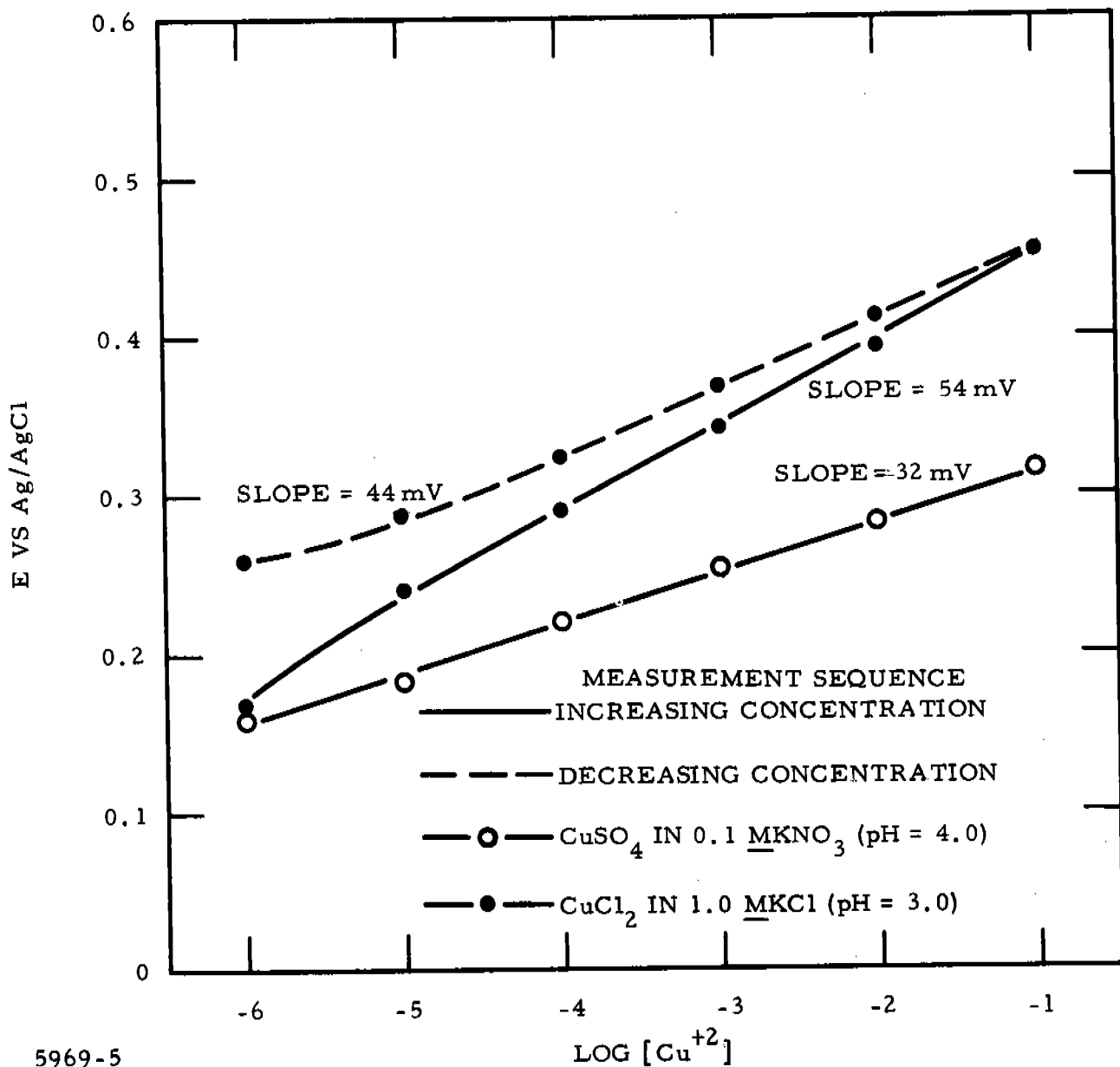


Figure 39 Potential Response of a 1.5 Mole % Co^0 -1173 Glass Electrode to Cu^{+2} in NO_3^- and Cl^- Media

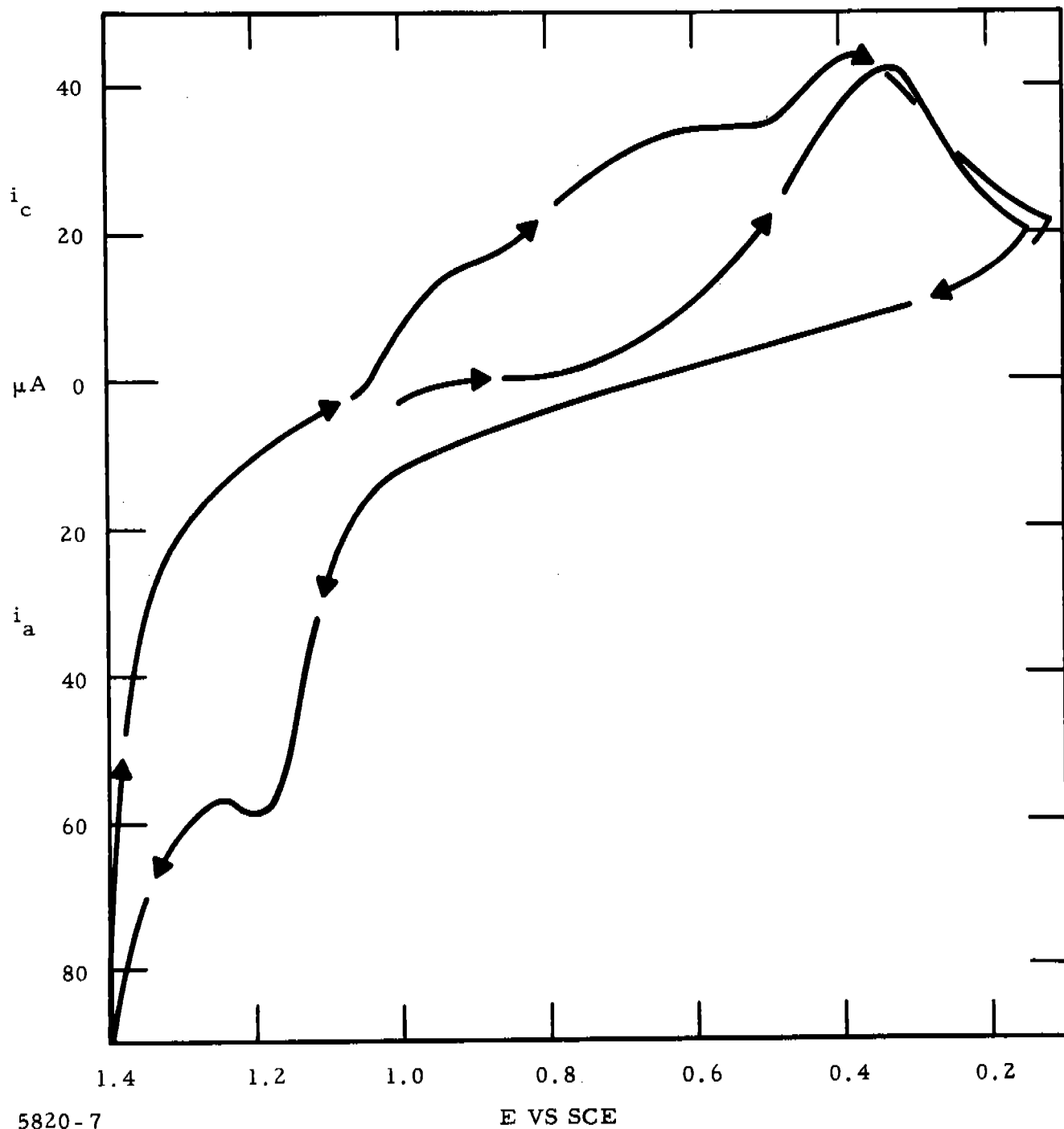
have been obtained. Larger concentrations (10% MnSe-1173) and mixtures of various oxidation states of Mn (2.0% MnSe-2.0% MnO₂-1173) have been added to 1173, but these samples have not been evaluated.

An electrode of 4.0 mole % Mn⁰-1173 glass was tested for a potential response to Mn⁺³, which was generated electrochemically from Mn⁺² in a H₂SO₄ - pyrophosphate medium. The Mn (P₂O₇)₃⁻³ complex is stable (violet color; like MnO₄⁻) and does not disproportionate readily. Figure 40 shows the cyclic voltammogram of a Pt electrode in 10⁻² M Mn⁺³, 10⁻¹ M Mn⁺², 0.4 M Na₄P₂O₇, and 2 M H₂SO₄. The anodic peak at +1.2 V is the oxidation of Mn⁺² to Mn⁺³. The cathodic shoulder at 0.95 - 1.0 V is believed to be the cathodic reduction of Mn⁺³ to Mn⁺². The identity of the cathodic peak at 0.6 - 0.7 V is unknown; the cathodic peak at 0.4 V is the reduction of a Pt-oxide film. Electrochemical generation of Mn⁺³ was carried out at a Pt-flag electrode by constant current electrolysis where concentration of Mn⁺³ was directly proportional to time of electrolysis. In arriving at the concentration of the test solutions, a 100% current efficiency was assumed for the electrolysis. Although the absolute values of Mn⁺³ concentrations might be in error, the $\Delta \log [\text{Mn}^{+3}]$ should be correct as long as current efficiency for the electrochemical generation remained constant. Figure 41 shows the potential response of the electrode to Mn⁺³. In the 10⁻⁵ M to 10⁻² M Mn⁺³ range, a linear response was observed and a slope of 99 mV was calculated. A Pt electrode showed a linear response over the same Mn⁺³ concentration range (Mn⁺² held at 0.1 M) and exhibited a slope of 85 mV.

The 4.0 mole % Mn⁰-1173 glass electrode was also evaluated for its responsiveness to MnO₄⁻ and was found to be insensitive in the 10⁻⁶ N to 10⁻⁴ N range. At higher concentrations (10⁻³ N to 10⁻¹ N), the MnO₄⁻ oxidized the electrode surface.

As a follow-up to the behavior observed with Ni-doped, Co-doped, and Fe-doped 1173 sensors to Fe⁺³ and Cu⁺² in NO₃⁻ and Cl⁻ media, the 4.0% Mn⁰-1173 electrode was evaluated for its potential response to Fe⁺³ and Cu⁺² under the same conditions. The response to Fe⁺³ was not Nernstian, but the response to Cu⁺² was (30 mV slope in NO₃⁻ medium; 60 mV slope in Cl⁻ medium).

A different glass composition doped with Mn⁰, Ge₂₀Se₇₅Mn₀₅, was tested in the membrane and electrode configurations for a response to Mn⁺². No response was observed, and the glass was not chemically stable in an aqueous medium.



5820-7

Figure 40 Voltammogram of Pt in $10^{-2} \text{ M Mn}^{+3}$, $10^{-1} \text{ M Mn}^{+2}$, $0.4 \text{ M Na}_4\text{P}_2\text{O}_7$, and $2 \text{ M H}_2\text{SO}_4$

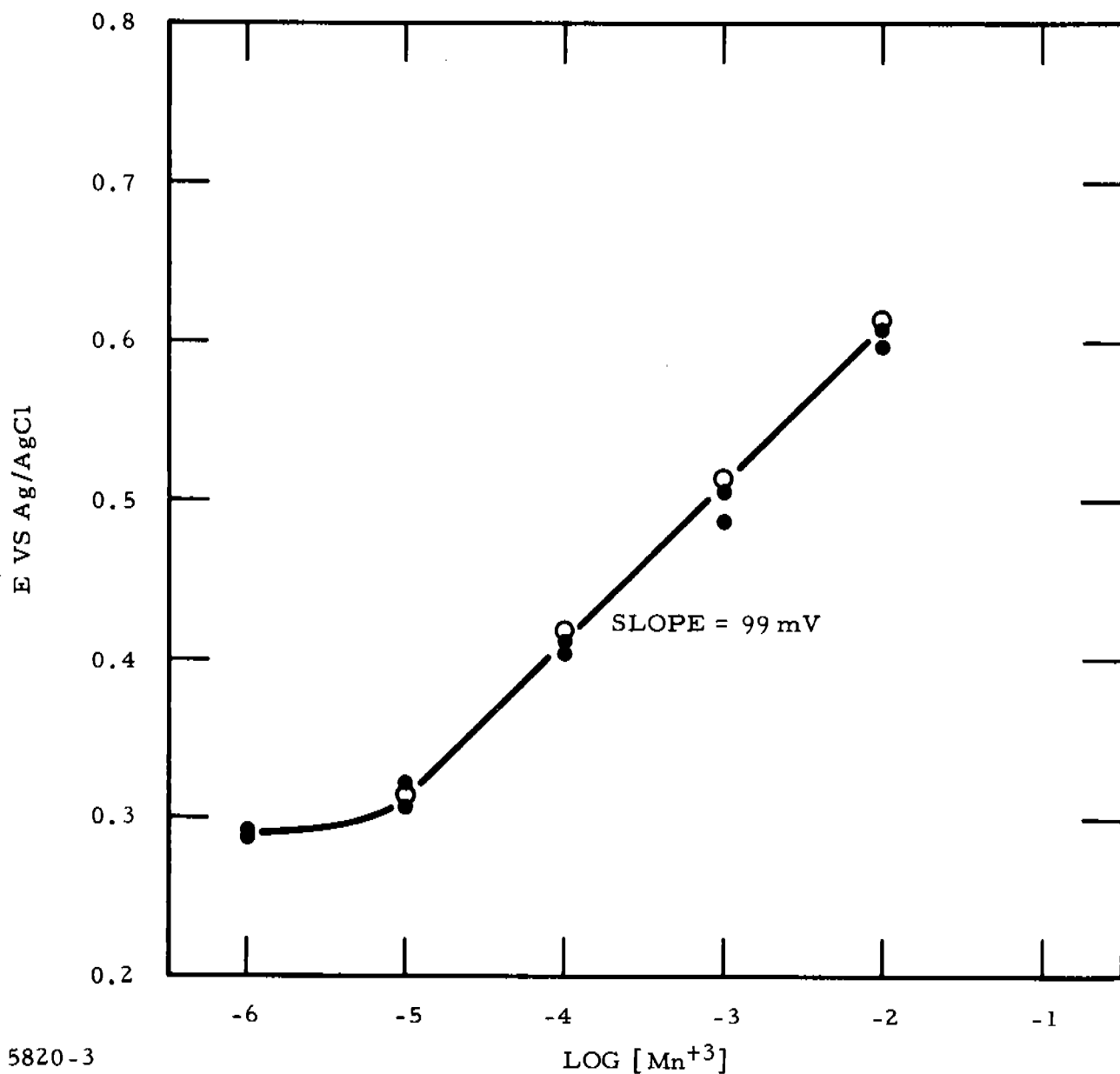


Figure 41 Potential Response of a 4.0 Mole % Mn⁰-1173 Glass Electrode to Electrochemically Generated Mn³⁺ in 0.1 M MnSO₄, 0.4 M Na₄P₂O₇, and 2 M H₂SO₄

Another approach to development of a sensor for Mn^{+2} was also initiated. Elemental Mn^0 was evaporated on slices of heavily doped n-type Si ($\rho = 0.007 \Omega\text{-cm}$ - phosphorus) and heavily doped p-type Si ($\rho = 0.0015 \Omega\text{-cm}$ - boron). The slices were heated at 700°C for 72 hours in a H_2 atmosphere in an attempt to thermally diffuse the Mn into the Si. Electron microprobe profile analyses (Figures 42 and 43) showed that Mn diffused into the Si to a depth of from 6 to $30 \mu\text{m}$. Evaluation of the respective samples as sensors for Mn^{+2} indicated they were insensitive to Mn^{+2} . They were responsive, however, to Fe^{+3} , Cu^{+2} , and pH, but the responses were not Nernstian. Deeper diffusions of Mn into Si at higher temperatures will be required.

C. Ca^{+2} Sensors

A sample of 0.1% $CaCl_2$ -1173 glass was tested in the membrane configuration and was found to be as inert to Ca^{+2} concentration as the undoped 1173. The resistivity of the sample indicates the doping level is too low, but autoradiograms showed this concentration of $CaCl_2$ is not dissolved or dispersed uniformly throughout the glass. The $CaCl_2$ is rejected by the glass. Attempts to prepare 1.0 mole % $CaCl_2$ -1173 glass were unsuccessful, yielding a crumbly ingot which had lost its glassy characteristics. It does not seem likely that a Ca-1173 glass with good potential response characteristics can be obtained using the present $CaCl_2$ doping procedure.

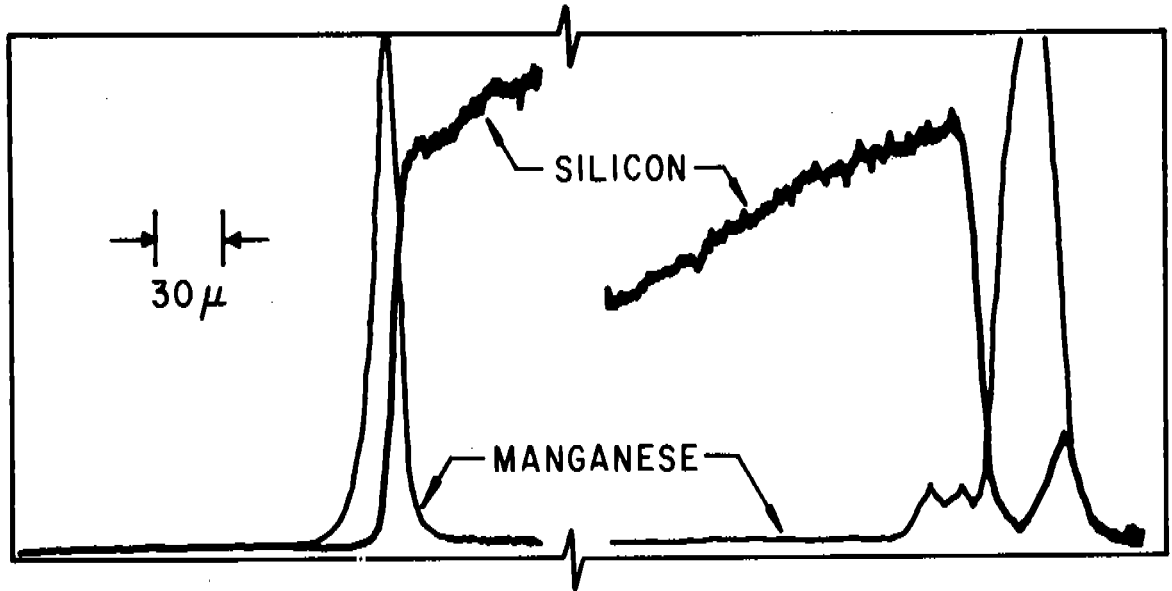
Electrodes and membranes of 3.0% $CaSe$ -1173, 5.0% $CaSe$ -1173, 1.0% Ca^0 -1173, and 1.5% CaF_2 -1173 were also insensitive to Ca^{+2} concentration. Although there appeared to be no dopant rejection, the resistivities of all the samples were too high.

D. Mg^{+2} Sensors

Samples of 1173 glass doped with 1.5 and 3.0 mole % Mg^0 and with 1.5 mole % $MgSe$ were prepared, but none of the Mg-doped glasses was mechanically or chemically stable.

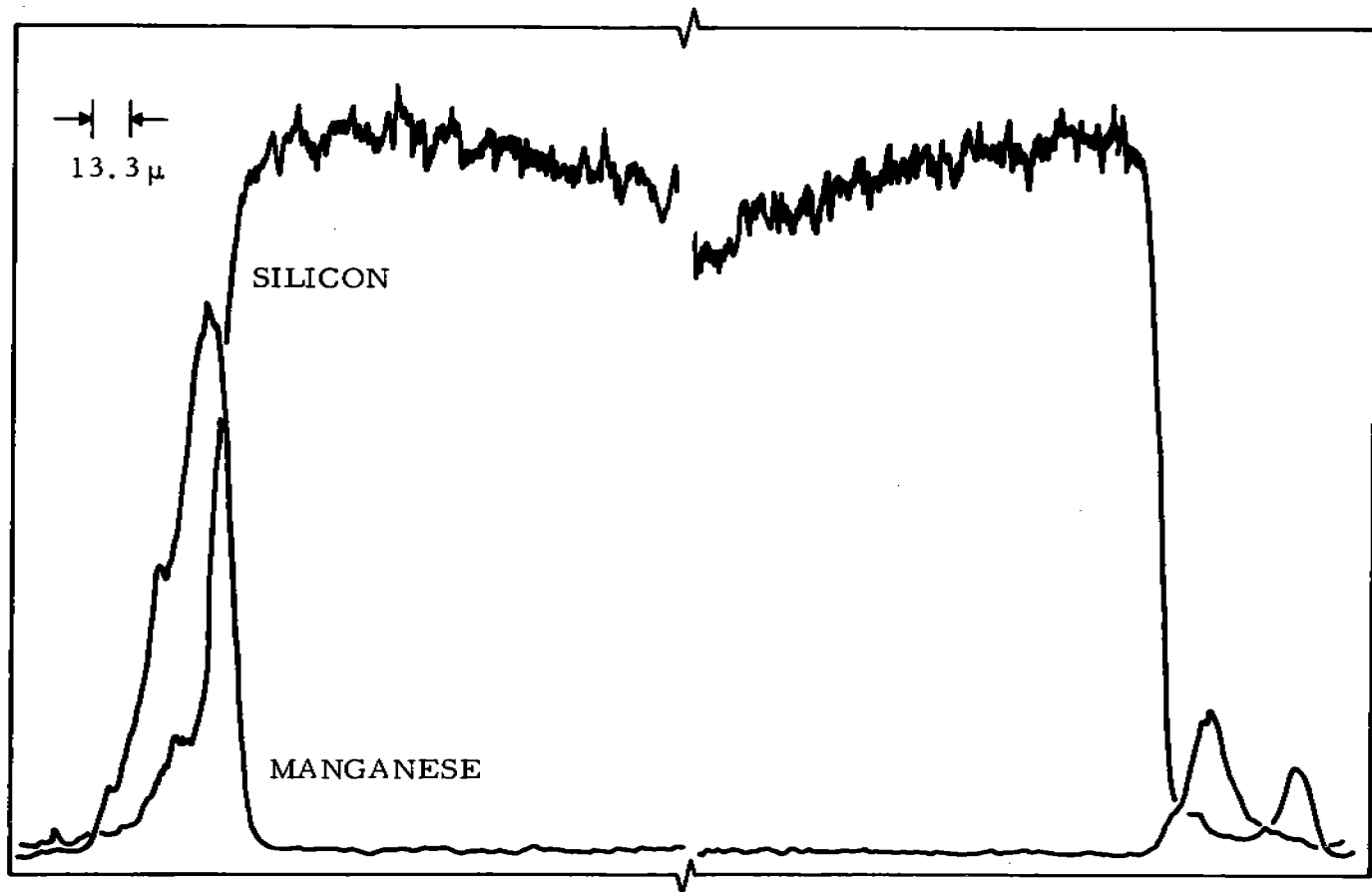
E. Na^+ , K^+ , Ag^+ , Cl^- , and I^- Sensors

Electrodes of 1.0, 1.5, and 5.0 mole % Na^0 -1173 glasses were prepared and evaluated as sensors for Na^+ . None of the electrodes was responsive to Na^+ concentration or pH. The resistance of the Na-doped glasses is borderline for sensor application.



5820-11

Figure 42 Electron Microprobe Profile Analysis of the Diffusion of Mn^0 into n-type Si ($\rho = 0.007 \Omega\text{-cm}$ - phosphorus doped)



5820-8

Figure 43 Profile Analysis of the Diffusion of Mn^0 into p-type Si
($\rho = 0.0015 \Omega\text{-cm}$ - boron doped)

A 1.0 mole % KCl-1173 glass electrode was found to be insensitive to K^+ concentration and Cl^- concentration. For the effect of changing K^+ concentration, the total salt concentration was held at 0.1 M by adding NaCl while the KCl concentration was varied from 10^{-4} M to 0.1 M. For the response to Cl^- experiment, KNO_3 was used instead of NaCl. The potential response of the electrode to Ag^+ concentration has been observed and is shown in Figure 44. The electrode is sensitive to Ag^+ concentration in the 10^{-4} M through the 10^{-1} M range. The $\Delta E/\Delta[Ag^+]$ varies from ~ 150 mV/decade at the low concentration end to ~ 100 mV/decade at the high concentration end. By making the appropriate ionic strength correction and plotting E versus the activity of the Ag^+ , the non-linearity of the plot can be decreased, but it does not become linear.

Results obtained from 2 mole % KI-1173 glass electrodes and membranes indicate the glass is sensitive to Ag^+ concentration. Figure 45 shows the potential response of the 2.0 mole % KI¹³¹-1173 glass electrode to Ag^+ concentration. The slope of the plot over the linear region is 53 mV/decade. The curve for the electrode is entirely different from that for the membrane of the same glass. The membrane exhibited a sigmoidal E vs log $[Ag^+]$ curve with increasingly negative potentials for increasing $[Ag^+]$.

Testing a 2 mole % KI-1173 electrode in solutions of varying pH revealed a pH response. Figure 46 shows the effect of pH on the electrode potential. Sargent buffers were used in one case and 0.1 M NaCl adjusted to various pH's with HCl and NaOH in the other. The pH values for the NaCl solutions were obtained with a Sargent Model LS pH meter. The difference between the E values for the two experiments and between the $\Delta E/\Delta pH$ implies that the components of the buffer system may influence the potential of the electrode. The effect of the NaCl solutions at the various pH's shows, however, that the pH affects the potential of the 2 mole % KI-1173 glass electrode.

In early experiments 2 mole % KI¹³¹-1173 glass used in the membrane and electrode configurations was found to be insensitive to changing I^- concentration. Figure 47 shows the data from a later experiment using a 2 mole % KI¹³¹-1173 glass electrode. As seen from the data, there is a definite potential response to changing I^- concentration. The discrepancy in response among the experiments has not yet been explained. This experiment also provided information about the effect of additional light on the potential of the electrode. As seen from the data, additional light raised the potential by approximately 9 mV. The origin of this photopotential may be similar to that found in some semiconductors.

The 2.0 mole % AgCl-1173 glass electrode potential was dependent on Ag^+ concentration and Cl^- concentration (Figure 48). The potential response to Ag^+ concentration was quite good over the concentration range from 10^{-6} M

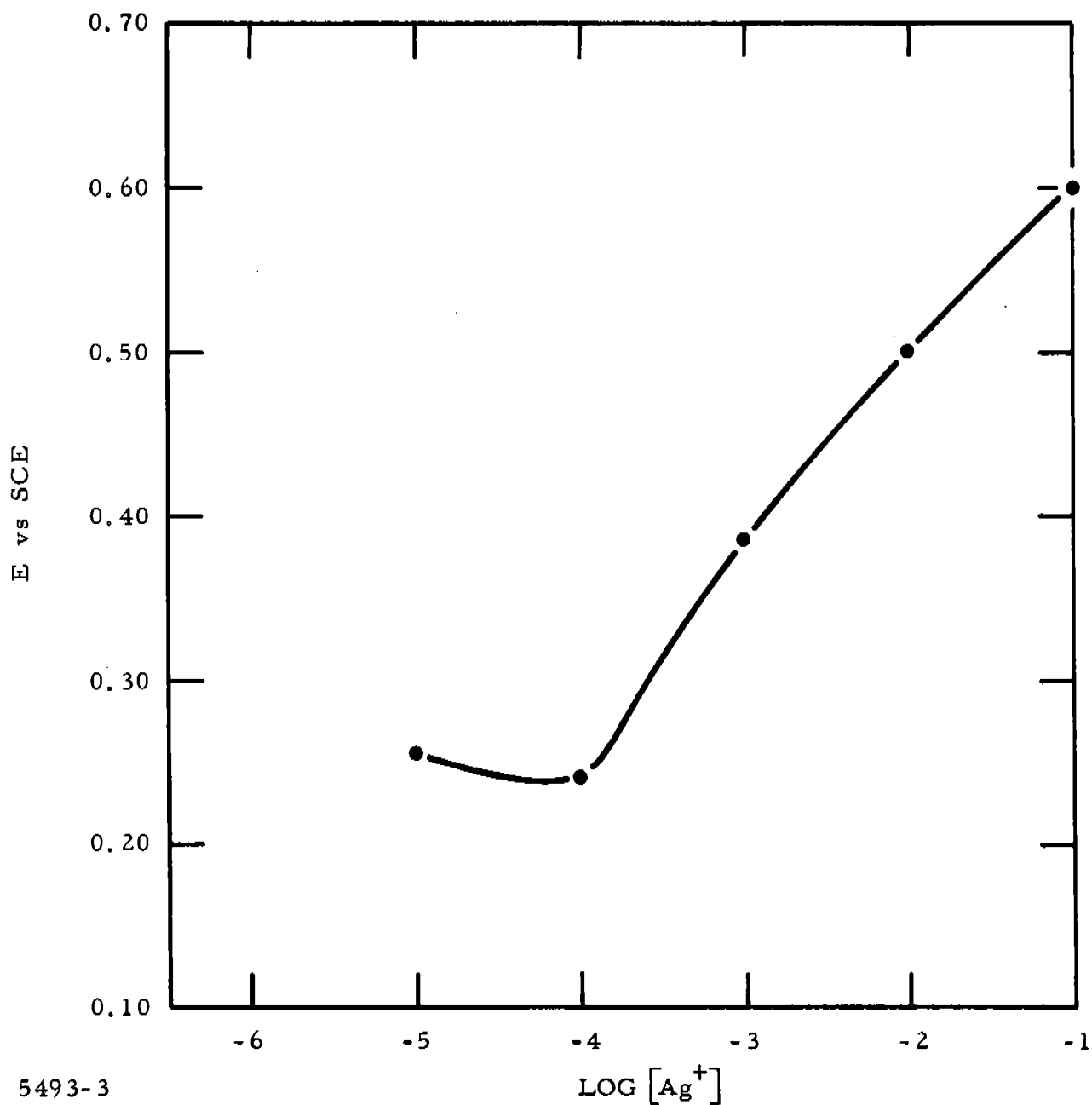
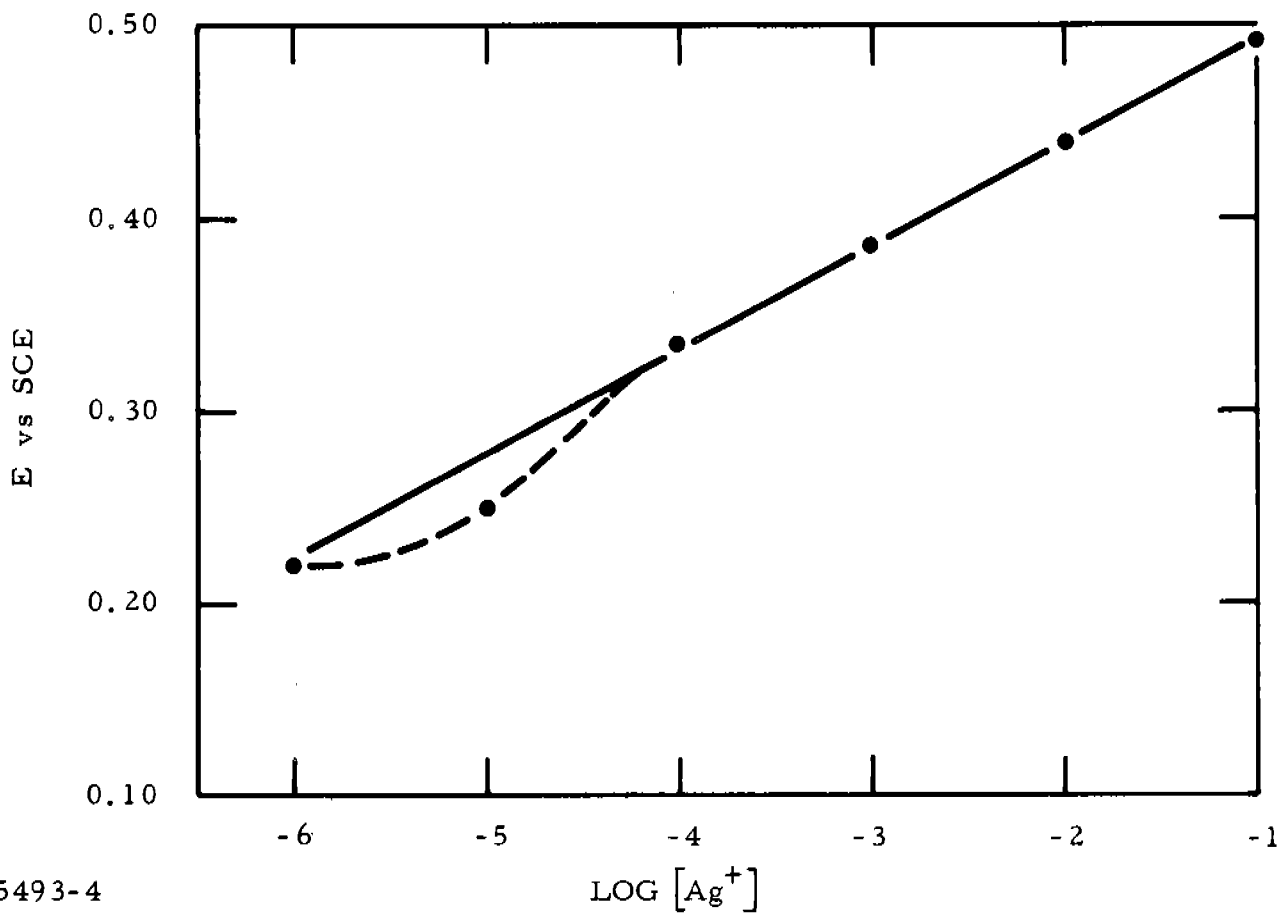
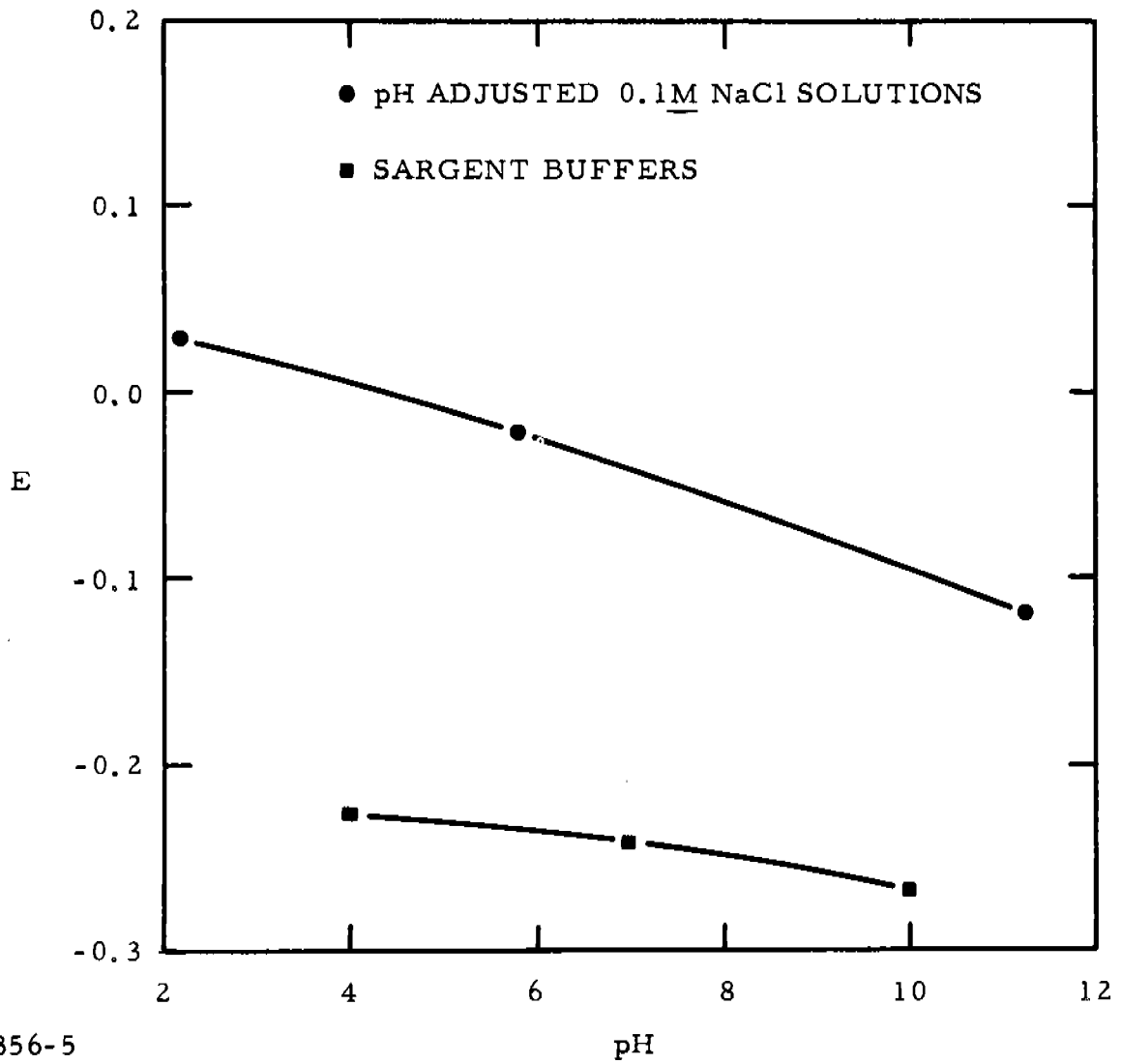


Figure 44 Effect of [Ag⁺] on the Potential of the 1.0 Mole % KCl-1173 Glass Electrode. (All solutions were 0.01 M in KNO₃.)



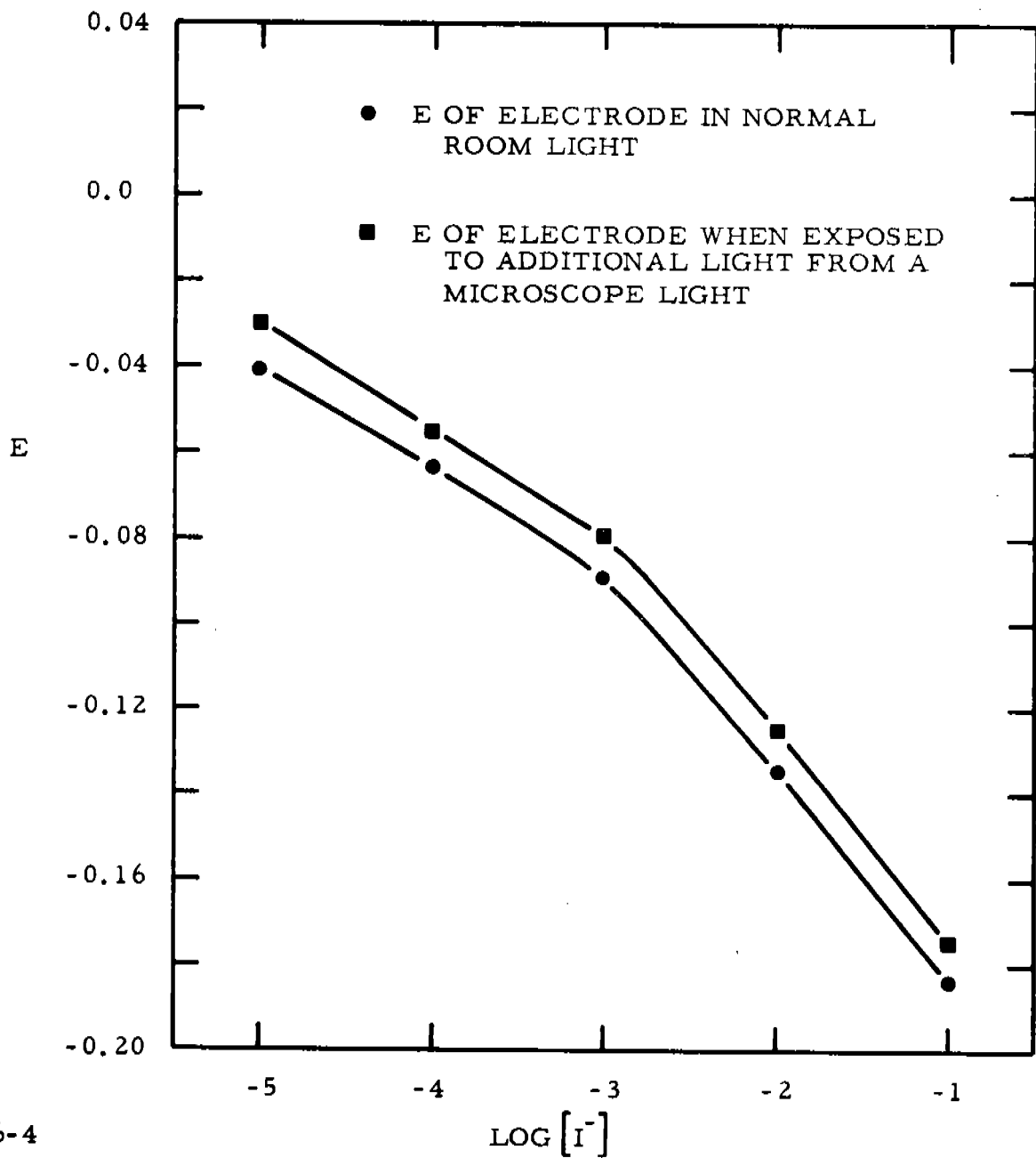
5493-4

Figure 45 Effect of $[\text{Ag}^+]$ on the Potential of the 2 Mole % KI^{131} -1173 Glass Electrode. (All solutions were 0.01 \underline{M} in KNO_3 .)



5356-5

Figure 46 Effect of pH on the Potential of a 2.0 Mole % KI-1173 Glass Electrode



5356-4

Figure 47 Effect of [I⁻] on the Potential of a 2.0 Mole % KI¹³¹-1173 Glass Electrode. (Total salt concentration held at 0.1 M by addition of KNO₃.)

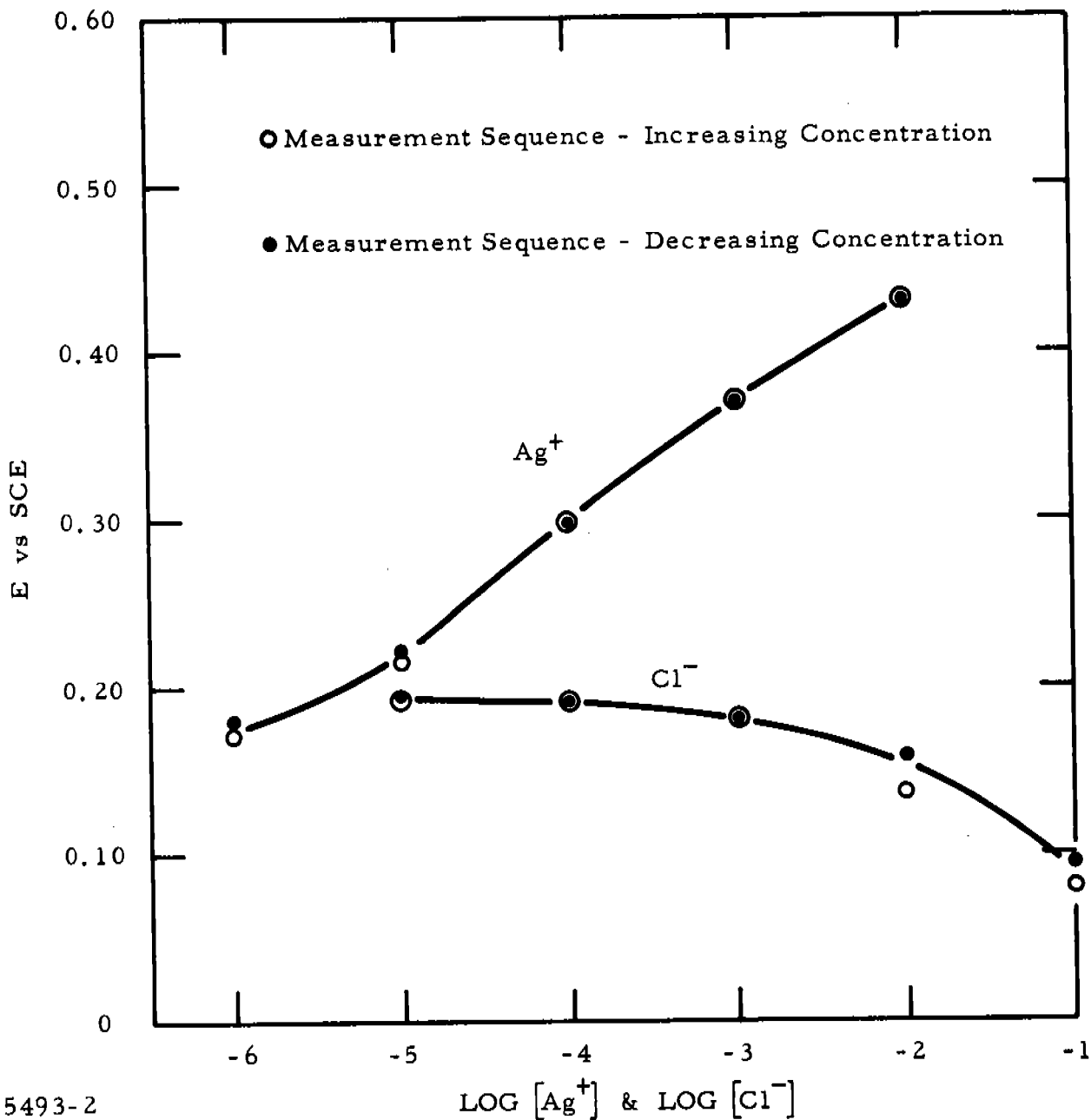


Figure 48 Effect of $[Ag^+]$ and $[Cl^-]$ on the Potential of a 2.0 Mole % AgCl-1173 Glass Electrode. (All solutions are 0.1 M in KNO_3 .)

through 10^{-2} M Ag^+ (highest concentration tested); the $\Delta E/\Delta[\text{Ag}^+]$ varied from 50 mV to 80 mV/decade over this concentration range. Perhaps the most outstanding feature of this electrode was reproducibility of the potential regardless of the sequence of measurements. The Cl^- response was poor and was dependent on the sequence of measurements.

The potential response of a 2.0 mole % Ag_2Se -1173 glass electrode to Ag^+ and Cl^- was measured (Figure 49). The response to Ag^+ concentration was not Nernstian, but the $E - \log [\text{Ag}^+]$ curve was sigmoidal in shape. Potential-time behavior in the 10^{-4} - 10^{-3} M Ag^+ range indicated that a titration or adsorption process was occurring at the electrode surface. In Cl^- solutions, the potential of the electrode decreased with increasing Cl^- concentration, as would be expected for a potential which is dependent on Ag^+ . The response to Cl^- was linear in the 10^{-4} - 10^{-1} M Cl^- range and had a slope of 33 mV. This potential response indicates that the Ag is in the Ag^{+2} state and a 1:1 relationship exists between Ag^{+2} and Cl^- . Another possible explanation for the slope of 33 mV is that the potential is a complex function of the Ag in the glass structure and the Ag in the crystallites dispersed in the glass. The E-pH curve for the electrode was linear from pH 2 to pH 8, but above pH 8 the potential change increased with increasing pH.

F. Cd^{+2} Sensors

A 2 mole % CdSe -1173 glass membrane does not give a potential response to Cd^{+2} , and the resistivity of the glass (5.8×10^{13} $\Omega\text{-cm}$) makes it incompatible with most electrometers.

Membranes and electrodes of 10 mole % CdSe -1173 give reasonably good potential responses to changing Cd^{+2} concentration. Here again, the potential response is better when the sequence of measurements is from the dilute solutions to the concentrated ones. Adsorption and/or dissolution rates at the glass interface cause problems when the measurement sequence is reversed. This is shown in Figure 50 for a membrane and an electrode. The theoretical response is 30 mV per decade change in Cd^{+2} concentration, and the response approaches theoretical as the concentration increases. ΔE for a series of solutions is reproducible from one day to the next for a given electrode, but the absolute potential values indicate that the initial conditions existing at the glass interface are not reproducible.

The 10 mole % CdSe -1173 glass is sensitive to illumination and displays a photopotential nine times greater than that for the 2 mole % KI^{131} -1173 glass and

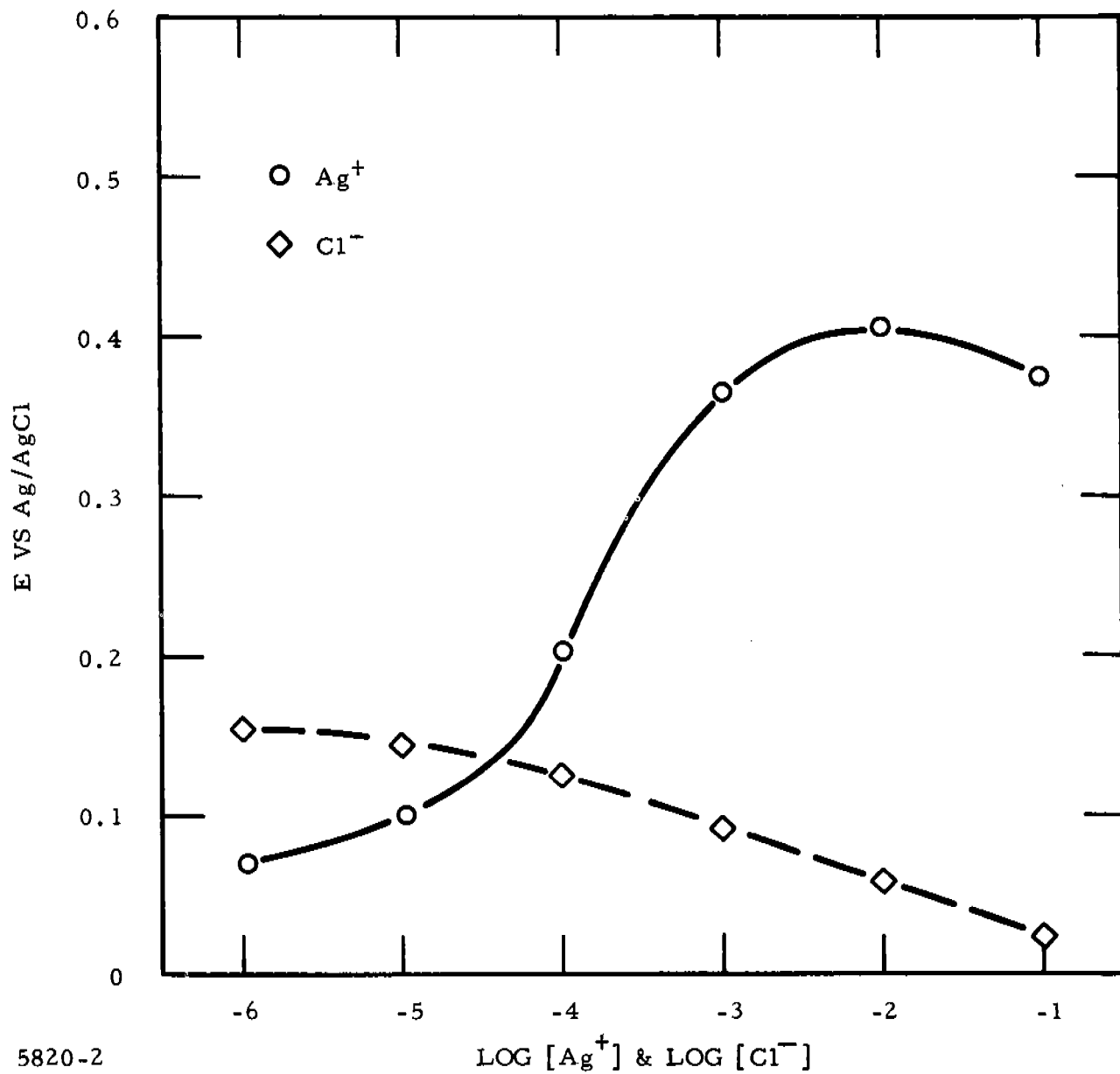
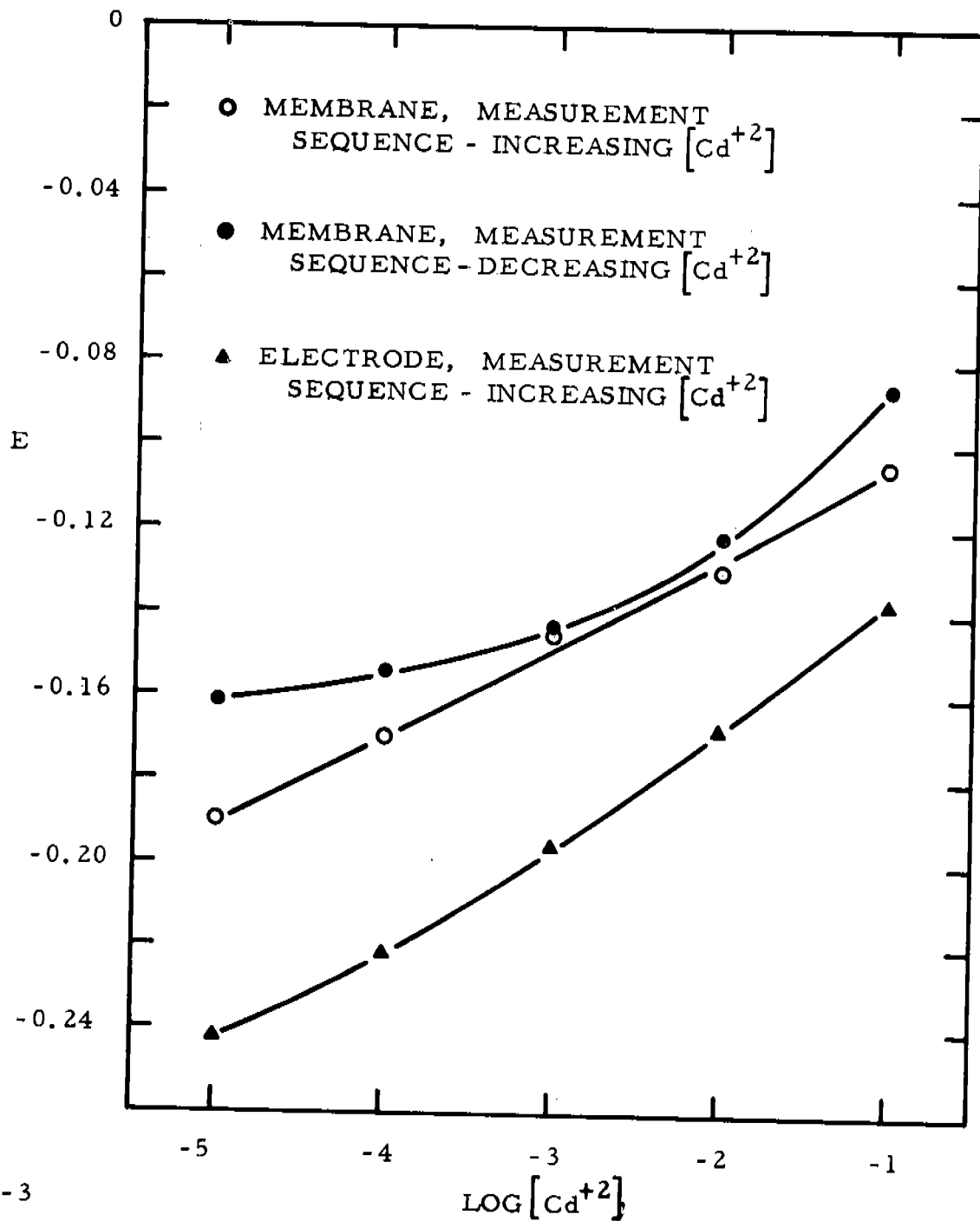


Figure 49 Potential Response of a 2.0 Mole % Ag_2Se -1173 Glass Electrode to Ag^+ and Cl^- in 0.1 M KNO_3 at $\text{pH} = 5.4$



5356-3

Figure 50 Effect of $[Cd^{+2}]$ and Measurement Sequence on Membrane and Electrode Potentials for 10 Mole % CdSe-1173 Glass. (Total salt concentration held at 0.1 M by addition of KNO_3 .)

opposite in sign (~ -80 mV). Although x-ray analysis indicates that the crystals dispersed in the glass are not simple CdSe crystals, the photopotential observed is assumed to be similar to that reported for CdSe.

G. $\text{SO}_4^{=}$ Sensors

The adverse effects observed with the CaCl_2 -1173 were even more pronounced in the BaCl_2 -1173 prepared. Therefore, it was impossible to test the BaCl_2 -doped samples.

A 0.5% Ba^0 -1173 electrode was fabricated as a possible sensor for $\text{SO}_4^{=}$, but was found to be insensitive to Ba^{+2} , Fe^{+3} , and $\text{SO}_4^{=}$. The resistivity of the glass was too high ($6.7 \times 10^{13} \Omega\text{-cm}$).

The effect of small amounts of Ni on the resistivity of 1173 glass opened the possibility of using multiple dopants to attain samples with the desired resistance. As a result, a 0.5% Ba^0 - 0.5% Ni^0 -1173 sample was prepared and evaluated as a sensor. The electrode was not responsive to Ba^{+2} or $\text{SO}_4^{=}$, but it did exhibit a potential dependence on $\text{S}_2\text{O}_8^{=}$. Figure 51 shows the effect of $\text{S}_2\text{O}_8^{=}$ concentration on a 1.5% Ni^0 -1173 electrode and a 0.5% Ba^0 - 0.5% Ni^0 -1173 electrode. The response of the Ni^0 -1173 sensor indicates that the potential mechanism is probably the same as that observed for Fe^{+3} and Cu^{+2} , with the $\text{S}_2\text{O}_8^{=}$ being the higher oxidation state of the $\text{S}_2\text{O}_8^{=}/\text{SO}_4^{=}$ redox couple. The response observed with the Ba-Ni -1173 electrode represents a significant difference and implies that the addition of the Ba altered the potential determining step.

H. $\text{Ge}_{29}\text{S}_{71}$ Sensors

Electrodes of 2.0% Pb^0 - $\text{Ge}_{29}\text{S}_{71}$, 2.0% Fe^0 - $\text{Ge}_{29}\text{S}_{71}$, and 1.0% Mn^0 - $\text{Ge}_{29}\text{S}_{71}$ were evaluated as sensors. All were found to be unresponsive. Although these materials have good chemical and mechanical characteristics, the resistivities are so high that equilibration at the electrode-solution interface is masked by charge transfer in the glass. The addition of Co and Ni (1.0% Co^0 - $\text{Ge}_{29}\text{S}_{71}$ and 1.0% Ni^0 - $\text{Ge}_{29}\text{S}_{71}$) improved the resistivities, but still did not bring them into the desired range. Further improvements in the resistivities must be made if these materials are to be useful as sensors.

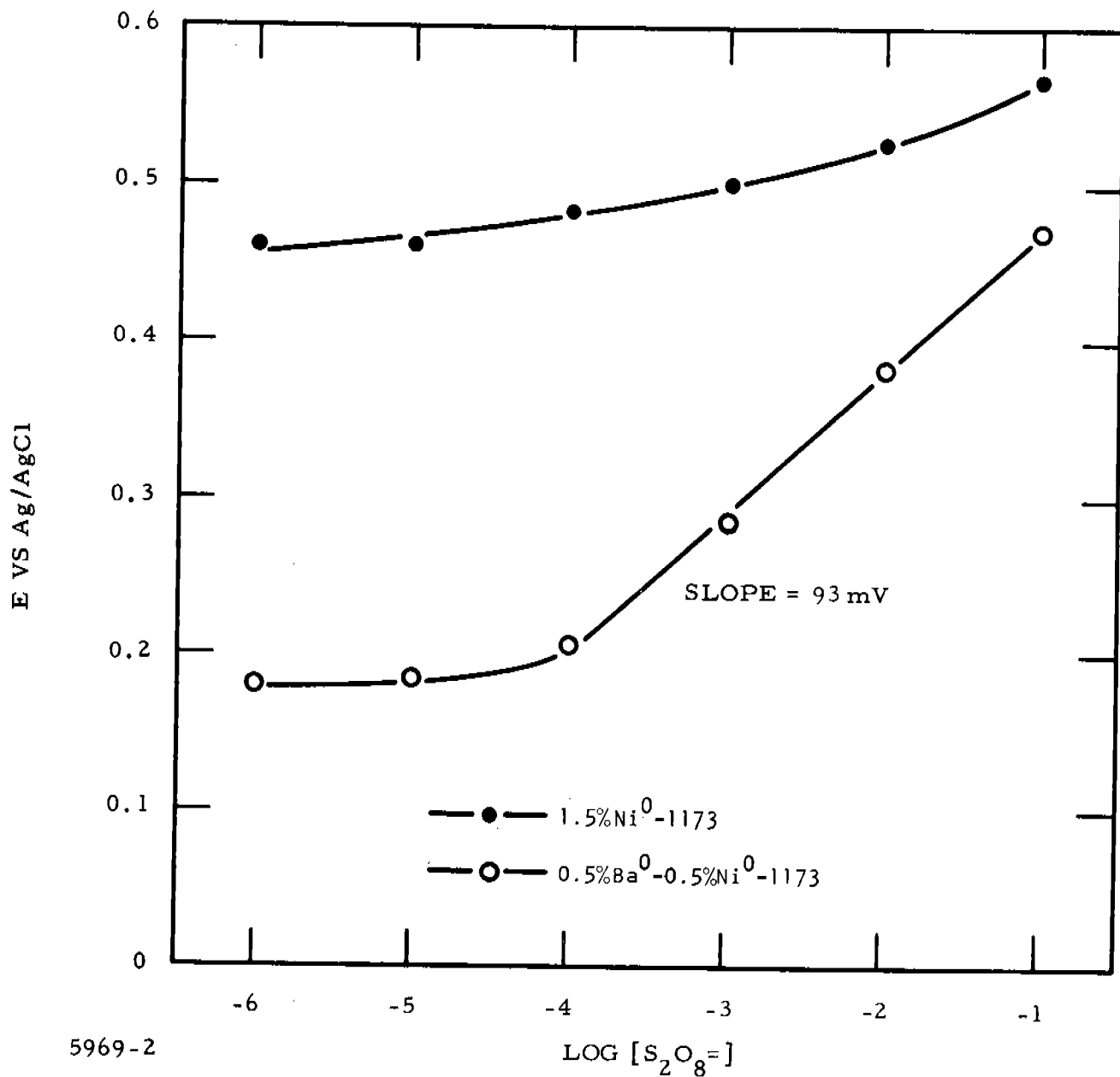


Figure 51 Potential Response of 0.5 Mole % Ba⁰-0.5 Mole % Ni⁰-1173 and 1.5 Mole % Ni⁰-1173 Glass Electrodes to S₂O₈ in 0.1 M KNO₃ (pH = 3.65)

2. Conclusion of Sensor Evaluation

Sensors made of doped 1173 glasses can be prepared in either membrane or electrode configurations. The potential response of these sensors supports a redox potential mechanism as opposed to either the membrane potential or the ion exchange mechanism. The sensors appear to respond only to the high oxidation state of reversible redox couples in which each ion of the couple is stable in solution. While this greatly limits the applicability of doped 1173 sensors to certain ions, it also eliminates many of the interferences. Interferences may be expected only from the high oxidation of redox couples other than the specific ion of interest or from ions (usually anions) which complex with the specific ion of interest. However, selectivity can be improved by adjusting the dopant and its concentration.

The sensor itself does not appear to be inert. It acts as a reducing agent which generates the lower oxidation state of the redox couple and maintains a constant activity. Tests for extended time periods (up to 5 months) indicate that some sensitivity at the lower concentration levels is lost with time. This evidence further supports the redox potential mechanisms.

Sensors have been prepared which respond to Fe^{+3} , Mn^{+3} , Cu^{+2} , Cd^{+2} , Ag^{+} , and $\text{S}_2\text{O}_8^{=}$. Most sensors respond to ions in the range between 10^{-5} and 10^{-1} moles/liter, with several sensors showing good response even below 10^{-6} moles/liter.

V. SUMMARY AND RECOMMENDATIONS

Several ion-selective electrochemical sensors prepared during the course of this research program have shown selective response to specific ions. The Fe^{+3} sensors are the most promising sensors in this study. A chalcogenide glass (TI No. 1173 - 28% Ge, 60% Se, 12% Sb) was doped with various amounts of Fe and Fe compounds. Sensors produced from this material yielded very selective response to Fe^{+3} , even in the presence of Fe^{+2} . Response has been observed at concentrations as low as 10^{-6} moles/liter (0.056 ppm). The preferred working range is 10^{-5} to 10^{-1} moles/liter. The sensor has maintained its selectivity after five months in solution. The ability to reproduce the sensor has also been established.

The major results of these investigations are summarized below.

A successful process for doping nonoxide chalcogenide glasses, particularly 1173 glass, has been demonstrated. Although these materials contain varying amounts of doping elements and compounds, they still retain good mechanical and chemical properties which permit their fabrication and use as ion-selective electrochemical sensors. The doped 1173 varies from totally glassy samples at low dopant concentration (< 1.5 mole %) to samples with a crystalline phase dispersed in the glass matrix. Variations in compounding the materials from the elements or from doping prereacted 1173 were negligible. Good sensors have been prepared by both compounding procedures and from sensor material which exhibited single and multiple phases.

A basic criterion for the use of a doped material as a sensor element is that the resistivity of the material must be $< 10^{10}$ Ω -cm. The sensor elements with the best potential stability and best response time characteristics have resistivities $< 10^8$ Ω -cm. The major mode of conduction in doped 1173 samples is electronic. If the material resistivity is borderline, the sensor may be potentially responsive, but the noise pickup is so great that elaborate shielding of the test cell is required. For the higher resistance sensor material, the exchange current is apparently limited by charge transfer in the glass instead of at the electrode-solution interface. In this case, the electrode does not attain equilibrium, and the electrode potential is not stable.

Attempts have been made to develop sensors for all the major ions commonly found in saline and brackish water. To date, only a sensor selectivity responsive to Fe^{+3} has been developed. Indirect sensors for Mn^{+2} and $\text{SO}_4^{=}$ have been prepared, in that responses have been observed to Mn^{+3} and $\text{S}_2\text{O}_8^{=}$ respectively. The sensors for the other ions were limited by high resistance

of sensor material, lack of potential response from a reversible redox couple, or ion exchange.

For the Fe-doped 1173 glasses, the best potential stability, response time characteristics, and Nernstian behavior were obtained when the doping level of elemental Fe was in the neighborhood of 2.0 mole % (2.0 mole % Fe⁰-1173). At lower Fe⁰ doping levels, noise pickup increased; at higher levels the response behavior became complex due to clusters of a second phase which essentially short the glass. The Fe⁺³ sensors did not respond to Fe⁺², but were affected by the pH of the solution. Since electrodes and membranes are responsive to free Fe⁺³, anions which complexed the Fe⁺³ tend to interfere. Possible cation interferences are limited to those associated with a reversible redox couple. For instance, Fe⁺³ sensors responded to Cu⁺² in the 10⁻⁵ to 10⁻¹ M range, but with 10⁻³ M Fe⁺³ present in solution, the potential was not affected by Cu⁺² concentration up through 10⁻¹ M. Of the cations tested, only Ag⁺ was a major interference. Fe⁺³ sensors used in a continuous monitoring experiment and tested over a 5- to 10-month period decreased in sensitivity by approximately an order of magnitude, but a linear response from < 10⁻⁴ M through 10⁻¹ M Fe⁺³ was observed. Periodic calibration of the sensor was necessary.

The potential responses of doped 1173 glass in both the electrode and membrane configurations support a redox potential mechanism as opposed to a membrane potential or ion exchange mechanism. It has been shown that any sufficiently doped 1173 glass will exhibit a potential response to Fe⁺³, Cu⁺² (in NO₃⁻ medium) and Cu⁺² (in Cl⁻ medium) which is dependent on the Fe⁺³/Fe⁺², Cu⁺²/Cu⁰, and Cu⁺²/Cu⁺¹ redox couples, respectively. Further, it was noted that the electrodes responded only to reversible redox couples in which each ion of the couple is stable in solution. The electrodes appeared not to be inert, but act as reductants which generate the lower oxidation state of the couple and maintain its activity at a constant value in the electrode-solution interface. This agreed with the fact that a response was observed only for the higher oxidation states of the reversible redox couples (e.g., Fe⁺³, Cu⁺², Mn⁺³, S₂O₈⁼, etc.).

Practical ion-selective electrochemical sensors have been fabricated and tested. The active element is composed of doped non-oxide chalcogenide host material. The information and experience gained in performing these investigations indicate that additional sensors can be made by continued investigations, including investigations of new materials. In view of the successes obtained in this initial study, continued investigation of ion-selective electrochemical sensors is warranted.

APPENDIX A
CONVERSION OF MOLES/LITER
TO PARTS PER MILLION
FOR VARIOUS IONS

APPENDIX A
CONVERSION OF MOLES/LITER
TO PARTS PER MILLION
FOR VARIOUS IONS

Ion (ppm)					
Molarity	Fe ⁺³ or Fe ⁺²	Cu ⁺²	Mn ⁺² or Mn ⁺³	Ca ⁺²	Ba ⁺²
10 ⁰	55,847	63,540	54,938	40,080	137,340
10 ⁻¹	5,585	6,354	5,494	4,008	13,734
10 ⁻²	558	634	549	401	1,373
10 ⁻³	55.8	63.4	54.9	40.1	137
10 ⁻⁴	5.58	6.34	5.49	4.01	13.7
10 ⁻⁵	0.558	0.634	0.549	0.401	1.37
10 ⁻⁶	0.056	0.063	0.055	0.040	0.137

Molarity	Mg ⁺²	Cd ⁺²	Hg ⁺²	Ge ⁺⁴	Sn ⁺⁴
10 ⁰	24,312	112,400	200,590	140,120	118,690
10 ⁻¹	2,431	11,240	20,059	14,012	11,869
10 ⁻²	243	1,124	2,006	1,401	1,187
10 ⁻³	24.3	112	201	140	119
10 ⁻⁴	2.43	11.2	20.1	14.0	11.9
10 ⁻⁵	0.243	1.12	2.01	1.40	1.19
10 ⁻⁶	0.024	0.112	0.201	0.140	0.119

Ion (ppm)

Molarity	Zn ⁺²	Na ⁺	K ⁺	Ag ⁺	Cl ⁻
10 ⁰	65,370	22,990	39,102	107,870	35,453
10 ⁻¹	6,537	2,299	3,910	10,787	3,545
10 ⁻²	654	230	391	1,079	354
10 ⁻³	65.4	23.0	39.1	108	35.4
10 ⁻⁴	6.54	2.30	3.91	10.8	3.54
10 ⁻⁵	0.654	0.230	0.391	1.08	0.354
10 ⁻⁶	0.0654	0.023	0.039	0.108	0.035

Molarity	I ⁻	SO ₄ ⁼	S ₂ O ₈ ⁼	PO ₄ ⁼	
10 ⁰	126,904	98,061	196,122	94,976	
10 ⁻¹	12,690	9,806	19,612	9,498	
10 ⁻²	1,269	981	1,961	950	
10 ⁻³	127	98.1	196	95.0	
10 ⁻⁴	12.7	9.81	19.6	9.50	
10 ⁻⁵	1.27	0.981	1.96	0.950	
10 ⁻⁶	0.127	0.098	0.196	0.095	

APPENDIX B

NON-OXIDE GLASSES DOPED WITH IRON OR MANGANESE

by
Rowland E. Johnson, Robert W. Haisty,
and Richard M. Brown

APPENDIX B

NON-OXIDE GLASSES DOPED WITH IRON OR MANGANESE

by

Rowland E. Johnson, Robert W. Haisty and Richard M. Brown

ABSTRACT

A doped non-oxide glass, $\text{Ge}_{28}\text{Sb}_{12}\text{Se}_{60}$, has been used for studies of ion-selective electrochemical sensors. Iron and manganese have been used to modify the basic properties. Addition of dopant up to 1.6% iron or 2.0% manganese gives glasses with a marked increase in electronic conductivity; above these levels, second phases appear in the glasses. Data on conductivity, dielectric constant, loss tangent, and optical absorption versus dopant concentration are presented. The iron-doped samples show greater conductivity at a given dopant concentration, perhaps due to formation of a second glassy phase.

(This work presented at the 135th Meeting of the Electrochemical Society, New York City, May 1969.)

APPENDIX B
NON-OXIDE GLASSES DOPED WITH
IRON OR MANGANESE

Non-Oxide glasses with a wide range of compositions have become available recently. These glasses are often based on one or more chalcogens, S, Se, or Te, with additional elements from Groups IV and V. The small electronegativity differences between atoms and their relatively large polarizability gives almost pure covalent bonds. The glasses are composed of random sized molecules, including chains; electrical conductivity is solely electronic. The glasses can dissolve, to some extent, a very wide range of materials including elements, both metallic and non-metallic, and various compounds. This paper describes some findings on such glasses doped with iron or manganese considered for use as possible ion-selective electrodes.

The glasses have certain advantages as electrochemical sensors. As noted before, they show electronic conduction only, so response should not be limited by ionic movement. There is some possibility of tailoring their electrical conductivity to fit the external measuring circuit. Finally, there is no anionic lattice, as in the case of the oxide glasses. This allows a wider choice of elements to dissolve in the glass to change the electronic properties and to broaden the response to ionic species in solution.

The charge transport processes in non-oxide glasses are still not completely understood. Owen has given a comprehensive review.¹ Electrical conduction has been variously attributed to a hopping mechanism or to a smeared-out conduction band mechanism. Attempts to differentiate between the mechanisms have not succeeded because the glass systems are very complex and the theory of conduction is not fully developed. Almost no work has been done on the effects of impurities on electrical conduction, probably because the effects are small. There seems to be a strong dependence of conduction on localized states in the glass, which may help to explain the lack of impurity contribution. However, there are so few experimental results and the systems are so diverse in properties and composition that a generalized statement on the effects of impurities is impossible.

In our studies, iron or manganese has been used to dope a typical glass, $\text{Ge}_{28}\text{Sb}_{12}\text{Se}_{60}$, designated TI Glass 1173. Large quantities of the glass were available, and the properties (see Table I) have been well characterized. Doped samples were indistinguishable when prepared from 1173 and either the metallic element or the metal selenide. The glass plus dopant were reacted at 1000°C for 16 hours or more in a sealed, evacuated ampoule. After air-quenching to room temperature, the glass sample was annealed at 270° to 300°C for a few minutes and furnace cooled to room temperature. Gold electrodes, when required, were applied by vacuum evaporation. Standard grinding and polishing techniques were used for the optical samples.

1. A. E. Owen, "Electronic Conduction Mechanisms in Glasses," *Glass Ind.* 48, 637 (1967); *Ibid.*, 695.

TABLE I

Physical Characteristics of Glass 1173, $\text{Ge}_{28}\text{Sb}_{12}\text{Se}_{60}$

Softening Point	370°C
Maximum Use Temperature	240°C
Knoop Hardness (50 gram)	150
Modulus of Rupture	1500-3000 psi
Density	4.67 g cm ⁻³
Expansion Coefficient	15 x 10 ⁻⁶ °C ⁻¹
Index of Refraction (10 μm)	2.600

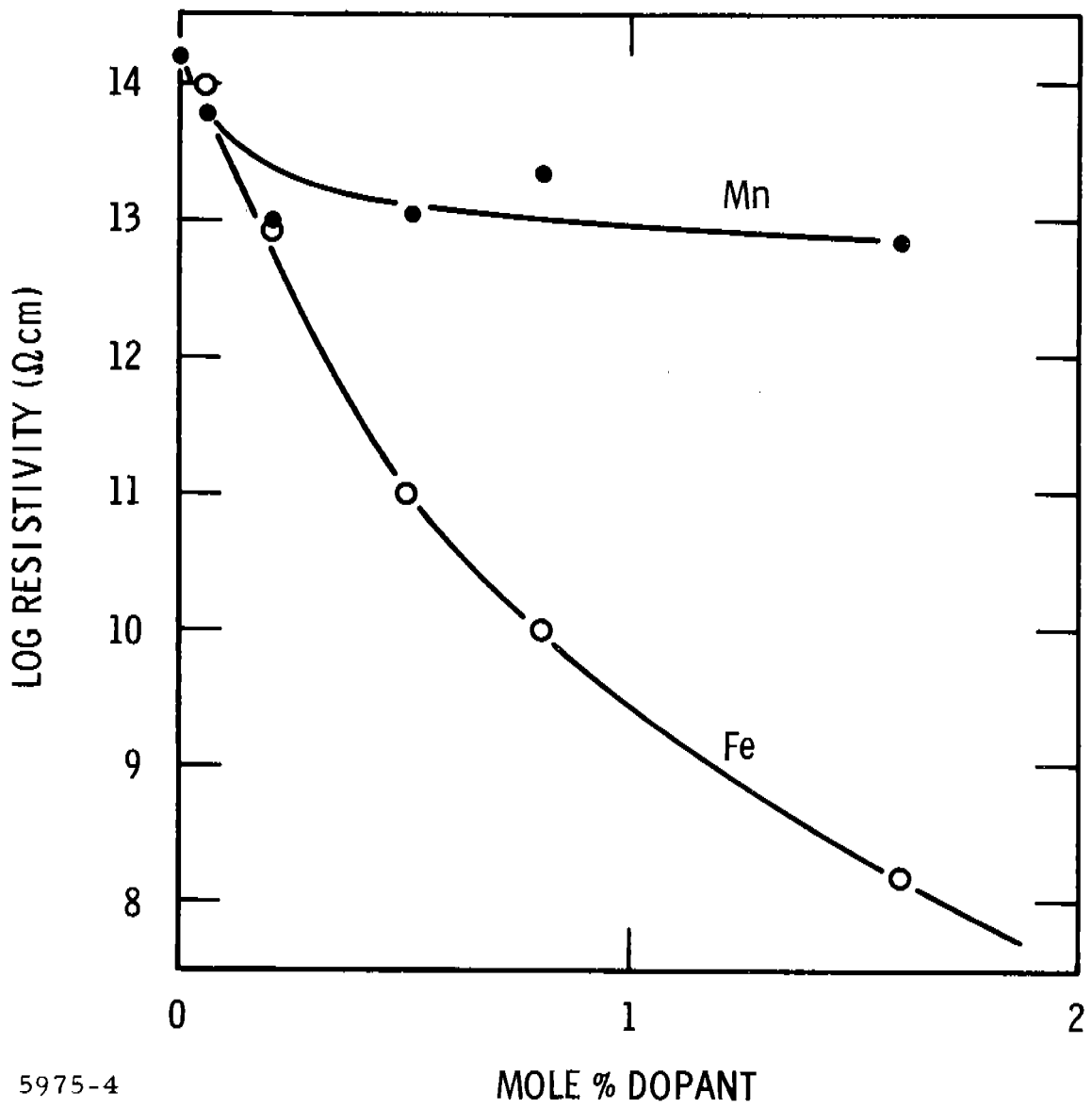
Special care was taken to prepare homogeneous glass samples. Inhomogeneities appeared in a number of different ways:

- (a) Crystallites or scattering centers visible in optical transmission through a polished sample. Examination was by an infrared image converter.
- (b) Irregularities appearing in a microscopic examination of a polished surface. Etching with a strong aqueous base such as KOH helped develop the pattern.
- (c) An electrical conductivity "catastrophe." Samples which showed an unusually high conductivity usually showed crystallite formation by other examination as well.

To some extent, the inhomogeneities could be controlled by extending the reaction time in preparing the doped glass and by more rigorous quenching. We found it impossible to prepare homogeneous iron-doped 1173 above 2.0% (atomic) and manganese-doped 1173 above 2.5% (atomic). All samples reported here are in the homogeneous range.

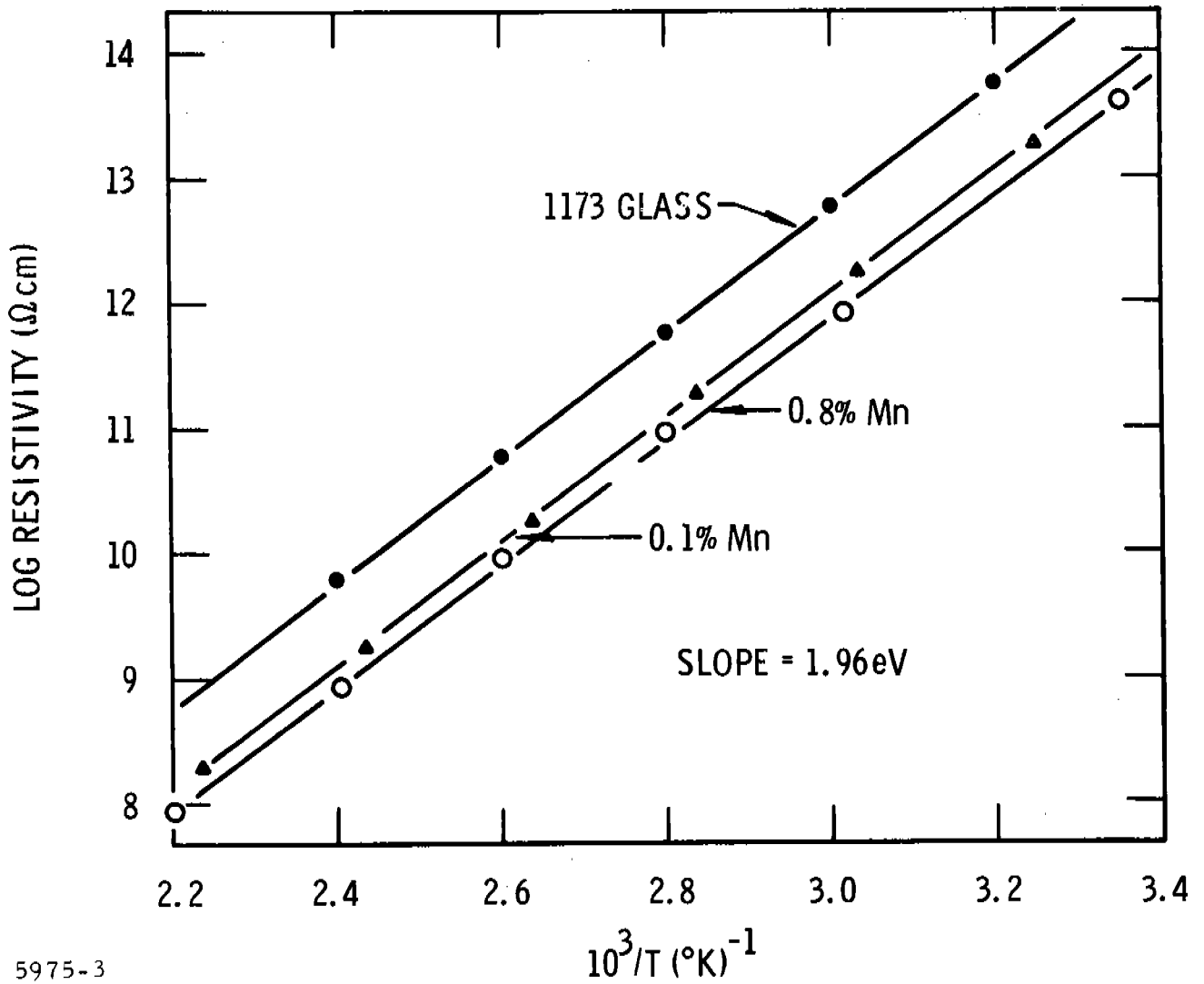
Resistivities of the doped glasses were measured at 25°C with a dc bias and an electrometer to monitor current. Precautions were taken to ensure that all glass samples were in the "switched-off" state, that is, the normal low conductivity state associated with glasses and ceramics. Contacts were evaporated gold, and samples were approximately 0.7 mm thick x 0.5 to 1 cm² in area. Data on resistivities as a function of dopant concentration are shown in Figure B-1. The base glass had a resistivity of 3×10^{14} ohm-cm. Manganese and iron doping show quite different effects on resistivity in this doping range. However, both dopants gave samples with very low resistivity when dopant concentrations were high enough to introduce a second phase. Although sample parameters were variable, crude measurements indicated resistivities as low as 10^2 ohm-cm. No further work was done on these inhomogeneous materials.

The resistivities of selected samples were measured over the temperature range from 25°C to approximately 290°C. Samples were held in a nitrogen ambient to prevent degradation. Figure B-2 shows the data for manganese-doped 1173 with no observable difference of slope between doped and undoped glasses. In contrast, the iron-doped 1173 showed a marked dependence of slope on concentration, as shown in Figure B-3. As the dopant concentration increases, the slopes of the curves at 25°C decrease from the 1.96 eV of the base glass. At higher temperatures, the slopes appear to approach 1.96 eV, similar to the intrinsic behavior of semiconductors as temperature is raised. No homogeneous samples above 1.6% iron could be prepared.



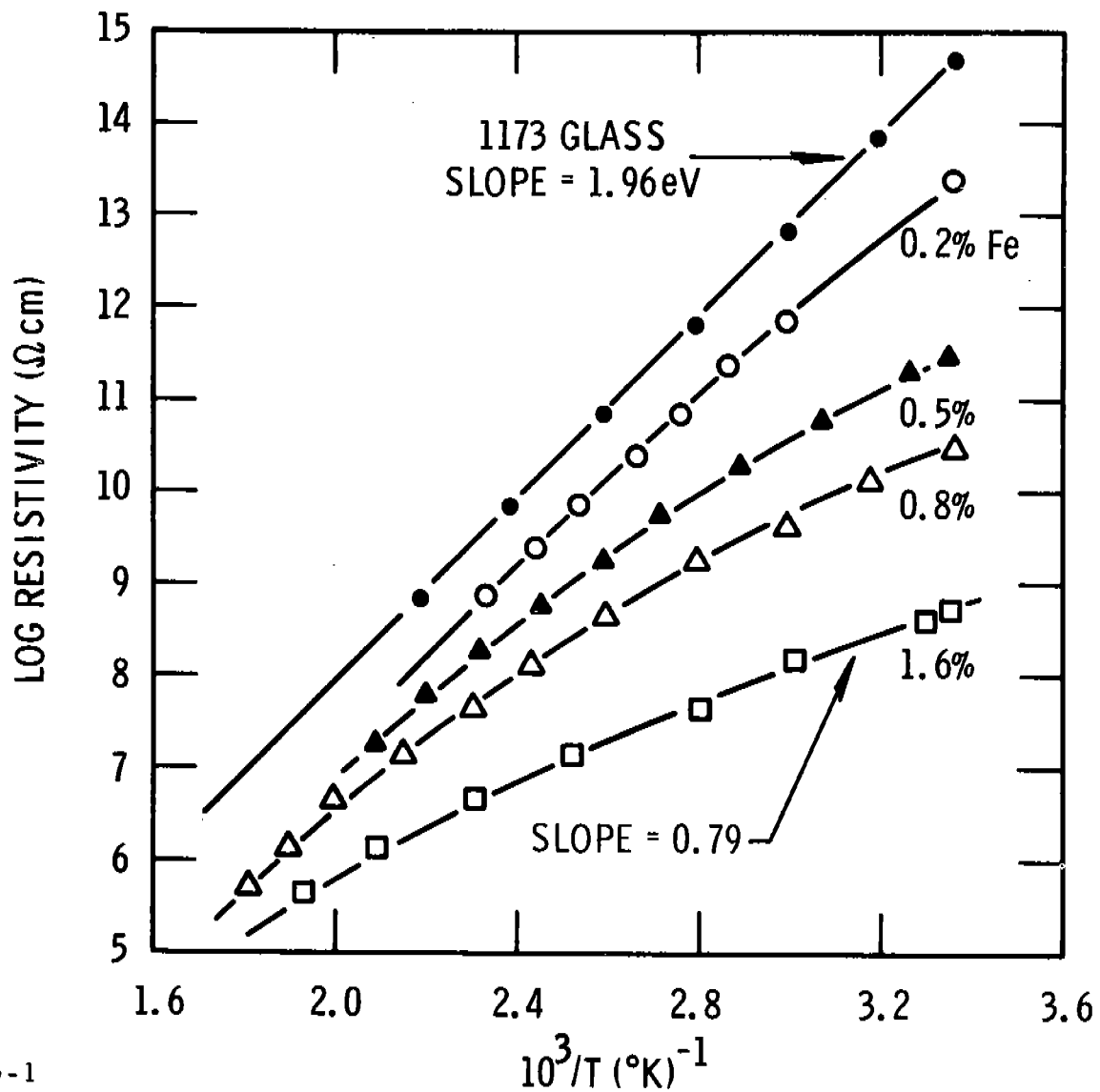
5975-4

Figure B-1 Resistivity of 1173 Glass Doped with Fe or Mn.
Data at 25°C.



5975-3

Figure B-2 Log Resistivity vs 1/T for Mn-Doped 1173 Glass



5975-1

Figure B-3 Log Resistivity vs 1/T for Fe-Doped 1173 Glass

The low frequency (1000 Hz) dielectric constant and loss tangent were measured at 25°C on the same samples used for resistivity measurements. Data are shown in Figure B-4. The manganese-doped samples show practically no change from the base glass; the iron-doped glasses show the expected increase in loss tangent associated with an increased conductivity.

The non-oxide glasses, particularly 1173, show excellent optical transmission in the region from 1 to 15 μm . It is of some interest, therefore, to examine the transmission of the doped glasses for changes due to the iron and manganese doping. The glass samples were roughly 1 mm thick. The index of refraction in the region of interest is 2.6 to 2.7, so the two-surface reflective loss will be approximately 35%.

Figure B-5 shows transmission versus wavelength for manganese-doped 1173. The curves show essentially no difference between the doped and undoped glasses. The estimated short wavelength cut-on is 0.80 μm , or 1.5 eV.

Figure B-6 shows the equivalent data for the iron-doped glasses. These samples show a short wavelength cut-on shifted toward lower energy to about 1.2 eV for 0.8% iron-doped. In addition, there is a broad absorption band centered around 2 μm (0.6 eV). An analysis of this absorption gave a constant absorption coefficient with changing concentration, indicating a concentration dependent species was responsible. Attempts were unsuccessful to fit the absorption edge curves to a linear plot of energy versus a function of the absorption coefficient, either α^2 or $\alpha^{\frac{1}{2}}$. Finally, authentic samples of FeSe and Fe₂Se₃, in a KBr pellet, show no infrared absorption in this wavelength region.

Some tentative conclusions on the doped glasses can be drawn from these data. There is obviously a significant difference in the behavior of manganese and iron over the concentration region where complete solubility exists. The results may be summarized as follows:

- (1) Over this concentration range, the dielectric constant and loss tangent do not appear to be affected, except where the increased conductivity makes a contribution to the loss tangent.
- (2) There seems to be no correlation between the conductivity activation energy and the photoabsorption edge or the absorption band.
- (3) Presumably, the manganese enters substitutionally, for Ge perhaps, with no effect on the electrical conductivity or the optical properties.
- (4) Presumably, iron enters in a number of sites, perhaps in the +2 and +3 oxidation states, perhaps as a second glassy phase. The overall uniform lowering of optical transmission indicates a general absorbing or scattering species with a range of sizes.

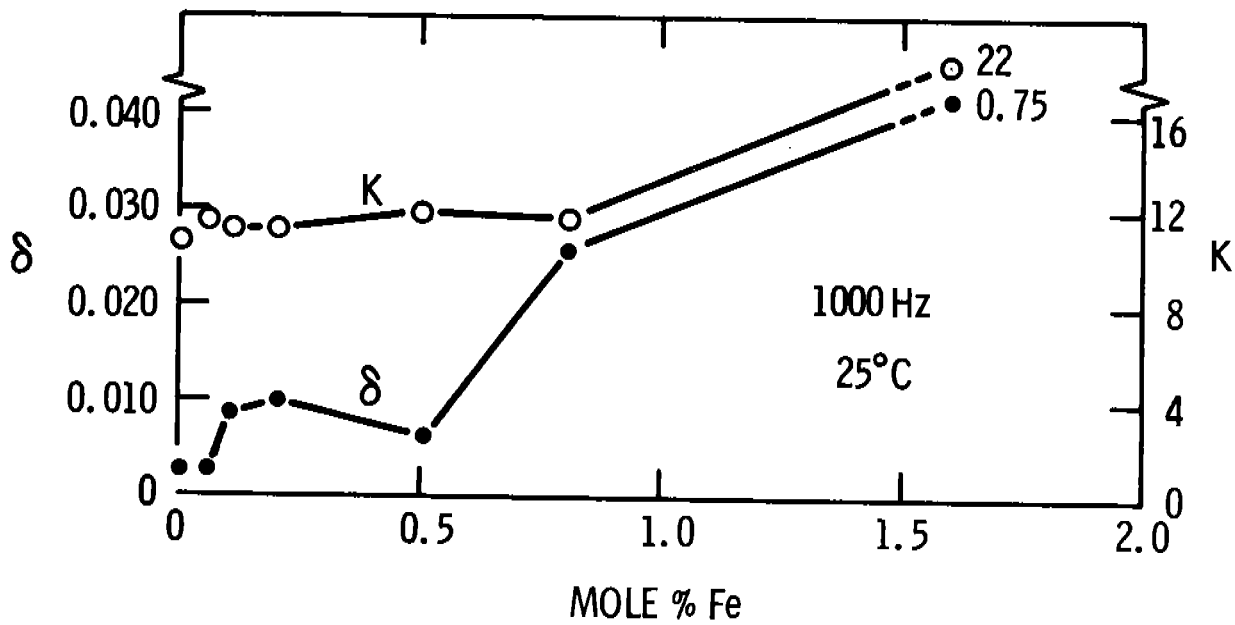
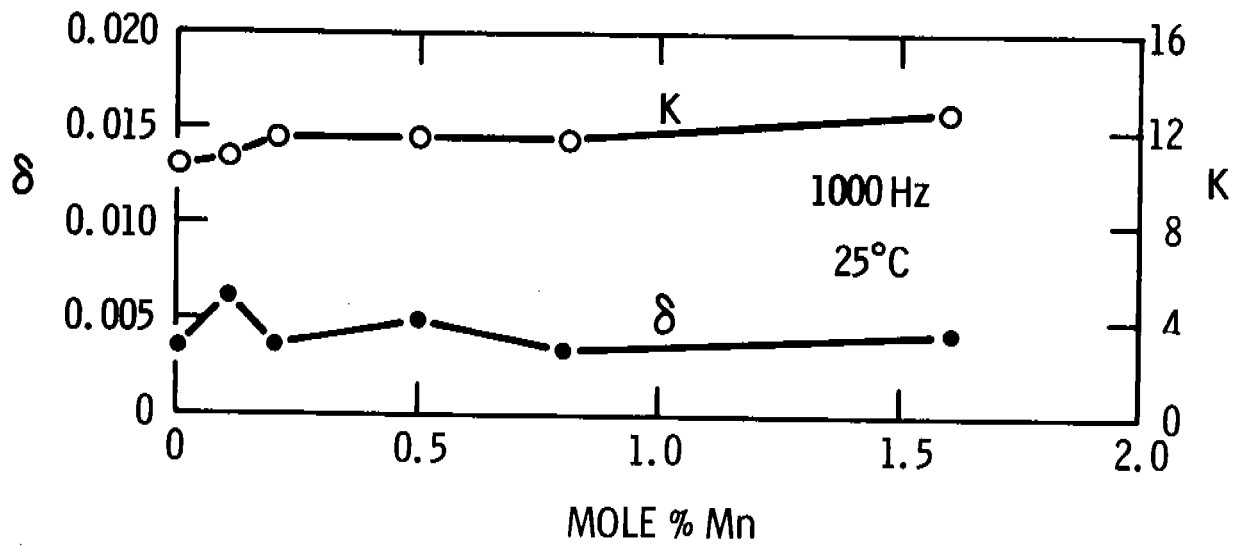


Figure B-4 Dielectric Constant, κ , and Loss Tangent, δ , vs Dopant Concentration for Mn-Doped and Fe-Doped 1173. Data at 25°C.

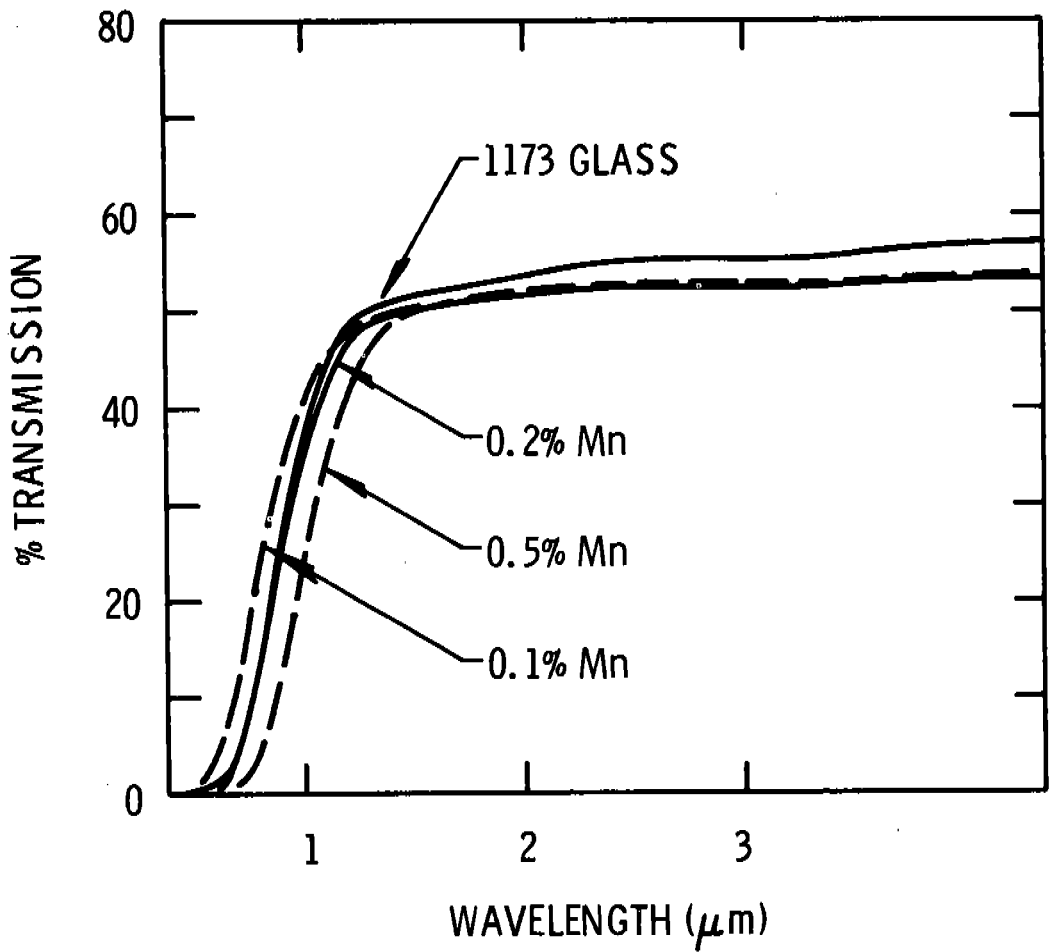
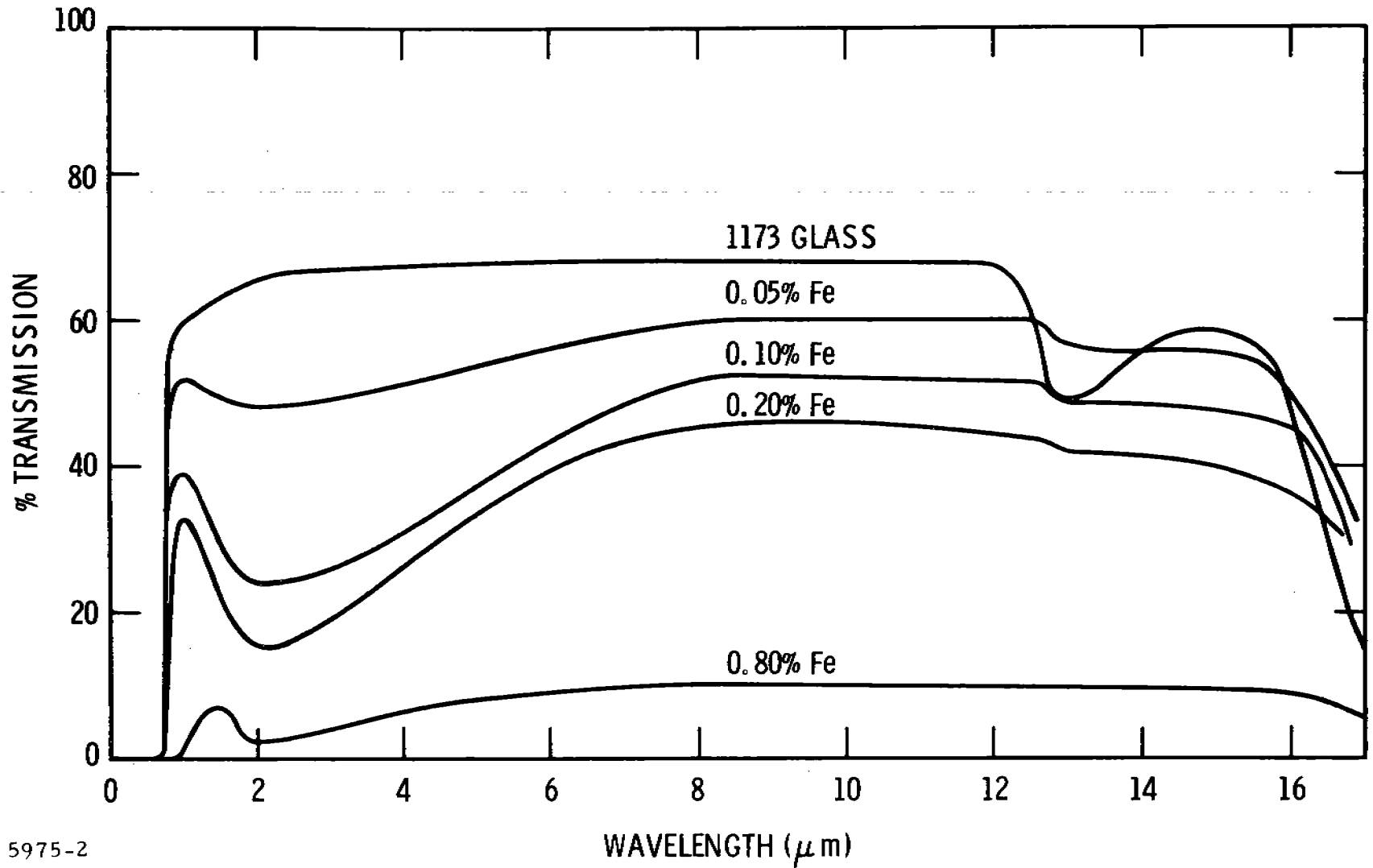


Figure B-5 Optical Transmission vs Wavelength for 1173 Glass Doped with Various Concentrations of Manganese. Long wavelength transmission of the doped samples is essentially that of pure 1173.



5975-2

Figure B-6: Optical Transmission vs Wavelength for 1173 Glass Doped with Various Concentrations of Iron